

https://dspace.org/

A Simulation Model For Use In Testing A Fast-time Predictor Instrument For Benson Boiler Steam Temperature Control

Brandford, David George

2015-01-12
http://hdl.handle.net/10539/16410

Downloaded from a DSpace repository. https://dspace.org/

A SIMULATION MODEL FOR USE IN TESTING A FAST-TIME PREDICTOR INSTRUMENT FOR BENSON BOILER STEAM TEMPERATURE CONTROL

David George Bradford

A Dissertation submitted to the Faculty of Engineering, University of the Witwatersrand, Johannesburg, in part fulfilment of the requirements for the Degree of Master of Science in Engineering.

Johannesburg, February 1985

D E C L A R A T I O N

I declare that this dissertation is my own unaided work. It is being submitted for the degree of Master of Science in Engineering in the University of the Witwatersrand, Johannesburg. It has not been submitted for any degree or examination at any other University.

_____

(D. G. Bradford)

The _____ day of _____, 1985.

To my Parents

A C K N O W L E D G E M E N T S

The author would like to express his appreciation for the assistance received from;

1) The CSIR, the University and the A.M. Jacobs Scholarship funds in providing the necessary financial assistance.

2) C. Williams and B. Pitman, of Escom, in making available the necessary information and in organising contact with Escom Personnel at Duvha Power Station.

3) M. Fell and the staff of units one and three in assisting with on-site learning and data collection exercises.

4) S. McCandlish of Exeter University in formulating the original proposal and for his assistance in the mechanical engineering field during the early stages of this work.

5) Professor I. MacLeod, who took over the supervisory role on the return to Exeter of S. McCandlish, and for his comments on control aspects of this report and the report presentation.

6) My colleagues and father for proof reading the report.

7) My mother for her time and patience for transforming the draft of this report into its final form.

A B S T R A C T

The work reported in this dissertation is aimed at determining a sufficiently accurate model for a section of a power station boiler plant so that at a later time, a fast-time predictor instrument may be designed and tested without interfering with the operation of an on-line boiler unit. The model required for the predictor instrument is a simplification of the simulation model. The instrument enables the operator to predict, in a short time, how an action taken now will affect the boiler unit in the future. It is suggested that such an instrument would enhance the operator's ability to control the boiler thus providing faster response times to system and grid disturbances.

The dissertation includes a review of possible boiler control strategies. A motivation for a fast-time predictor instrument is provided. An analysis of mechanical engineering aspects of the boiler and of simulation techniques enabled a model satisfying the simulation objectives to be developed and justifed. A technique is suggested for determining the parameters for these models.

An attempt was made to identify the model parameters but, due to the limited data available and a suspected violation of the Nyquist sampling theorem, the attempt was not successful. Some recommendations are made for improving the quality of the data logged.

It is concluded that a simulation model for the boiler processes can be obtained and that the parameter estimation technique is feasible, but that the complex task of system identification will require a considerable effort.

C O N T E N T S

CONTENTS

LISTS OF ILLUSTRATIONS

1. INTRODUCTION 1

1.1 THE GENERAL CONTROL PROBLEM 2

1.2 THE PARTICULAR PROBLEM 3

1.3 THE PROPOSED SOLUTION 3

1.3.1 THE GENERAL TECHNIQUE 4

1.3.2 THE SCOPE OF THE WORK UNDERTAKEN 5

1.4 AN OVERVIEW OF THE DISSERTATION 6

2. THE IDEAS BEHIND THE SELECTED APPROACH 7

2.1 AUTOMATIC CLOSED LOOP CONTROL 7

2.1.1 CLASSICAL CONTROL 8

2.1.2 TRANSFER FUNCTION TECHNIQUES 8

2.1.3 STATE-SPACE FEEDBACK CONTROL 9

2.1.4 ADAPTIVE CONTROL 10

2.2 THE MAN IN THE LOOP 12

2.2.1 SIMPLE CLOSED-LOOP CONTROL 12

2.2.2 PREDICTIVE CONTROL 14

2.2.3 THE APPLICATION TO THE PROBLEM OF BOILER CONTROL 16

2.3 THE PLANT SIMULATION 17

3. AN OVERVIEW OF THE BOILER 19

3.1 THE BASIC OPERATION OF THE UNIT 19

3.1.1 THE STEAM CYCLE 19

3.1.1.1 THE FEEDWATER PUMPS 19

3.1.1.2 THE BOILER 22

3.1.1.3 THE TURBINE 22

3.1.1.4 THE CONDENSOR 23

3.1.2 THE ENERGY CYCLE 23

3.1.2.1 THE COAL MILLS 23

3.1.2.2 THE AIR SUPPLY 24

3.1.2.3 THE BOILER 24

3.1.2.4 THE TURBO-GENERATOR 25

3.1.3 THE GENERAL START-UP PROCEDURE 26

3.2 THE CONTROL MODES 30

3.2.1 THE REMOTE OR CO-ORDINATED MODE 30

3.2.2 THE BOILER FOLLOW MODE 30

3.2.3 THE TURBINE FOLLOW MODE 31

3.3 THE BOILER IN MORE DETAIL 31

3.3.1 THE CONVERSION OF WATER TO STEAM 31

3.3.1.1 THE ECONOMISER 31

3.3.1.2 THE DIVISION WALL 35

3.3.1.3 THE SCREW WALL AND THE UPPER PART 35

3.3.1.4 THE STEAM ATTEMPORATOR AND THE RE-CIRCULATION SYSTEM 35

3.3.2 THE TRANSFER OF CHEMICAL ENERGY TO THE STEAM 36

3.4 SUMMARY 39

4. THE TRANSFER FUNCTION AND STATE-SPACE MODELS 40

4.1 INTRODUCTION 40

4.2 A LIST OF NECESSARY PARAMATERS 41

4.3 THE DIVISION OF THE BOILER INTO CELLS 43

4.3.1 THE ENERGY TRANSFER TO THE CELL 46

4.3.1.1 THE ENERGY DUE TO THE SECONDARY AIR FLOW 46

4.3.1.2 THE ENERGY DUE TO THE OIL FLOW 48

4.3.1.2 THE ENERGY DUE TO THE COAL FLOW 48

4.3.1.4 THE ENERGY DUE TO THE CONVECTION AIR FLOW 48

4.3.1.5 THE ENERGY DUE TO THE RE-RADIATED ENERGY 48

4.3.2 THE ENERGY TRANSFER AWAY FROM THE CELL 49

4.3.2.1 THE DIVISION WALL 49

4.3.2.2 THE SCREW WALL AND THE UPPER PART 50

4.3.2.3 THE TUBE BANKS 50

4.3.2.4 THE AIR HEATERS 51

4.3.2.5 THE BOILER EXHAUST GASES 51

4.3.3 SUMMARY 52

4.4 THE STEADY-STATE HEAT TRANSFER EQUATION FOR THE I'TH CELL 52

4.5 THE TRANSFER FUNCTION MODEL 57

4.5.1 THE STATEMENT OF THE MODEL PARAMETERS 57

4.5.2 THE MODEL DEFINITION 59

4.6 THE STATE-SPACE MODEL 64

4.6.1 THE FURNACE STATE-SPACE MODEL 65

4.6.2 THE STEAM TUBE STATE-SPACE MODEL 67

4.6.3 THE CELL STATE-SPACE MODEL 68

4.7 SUMMARY 69

5. REALIZATION OF THE MODEL PARAMETERS 70

5.1 INTRODUCTION 70

5.2 THE STEADY-STATE EQUATIONS 70

5.3 THE TRANSFER FUNCTION MODEL 74

5.3.1 THE CASCADED CELL MODEL 74

5.3.2 THE CELL TRANSFER FUNCTION MODEL 76

5.4 THE STATE-SPACE MODEL 83

5.5 SUMMARY 88

6. A CRITICAL APPRAISAL OF THE ADOPTED APPROACH 90

6.1 INTRODUCTION 90

6.2 THE EARLIER ATTEMPTS 90

6.2.1 THE PHYSICAL MODEL 90

6.2.2 SYSTEM IDENTIFICATION 93

6.2.3 A COMBINATION OF THE PHYSICAL INSIGHT AND SYSTEM IDENTIFICATION TECHNIQUES 94

6.3 THE CHOSEN MODE 97

6.4 THE METHOD FOR DETERMINING THE MODEL PARAMETERS 100

6.4.1 THE MAXIMUM LIKELIHOOD MODEL 100

6.4.2 THE CELL TRANSFER FUNCTION MODELS 105

6.4.3 THE STATE-SPACE MODELS 105

6.5 SUMMARY 106

7. CONCLUSION AND RECOMM[illegible]S 107

7.1 CONCLUSION 107

7.2 RECOMMENDATION 107

REFERENCES

APPENDIX A : TWO METHODS FOR LINEARIZATION OF THE HEAT RADIATION EQUATION

APPENDIX B : DERIVATION OF THE CASCADED CELL MODEL FROM THE SINGLE CELL MODEL

APPENDIX C : THE LIST OF POINTS USED FROM THE LOGGED DATA

APPENDIX D : THE IMSL ROUTINES

APPENDIX E : THE DATA FILES AND THEIR CONTENTS

APPENDIX F : THE MULTIPLICATION OF SPECIFIC MATRIX FORMS

APPENDIX G : DETERMINING THE MATRIX K_{598}

APPENDIX H : DETERMINING THE MATRIX H_5

APPENDIX I : DETERMINING THE MATRIX K_{57}

APPENDIX J : DETERMINING THE MATRIX F_5

APPENDIX K : GRAPHS OF THE INPUTS AND OUTPUTS CONSIDERED IN SECTION 5.3.1

L I S T O F I L L U S T R A T I O N S

2.1	THE BLOCK DIAGRAM FOR AN ADAPTIVE CONTROLLER	10
2.2	THE ROLE OF EXPERT SYSTEMS IN ADAPTIVE CONTROL	12
2.3	THE ROLE OF THE FAST-TIME PREDICTOR INSTRUMENT	15
2.4	OPERATOR REACTION TO POTENTIALLY CRITICAL TEMPERATURE RISES	16
3.1	BLOCK DIAGRAM REPRESENTATION OF MAJOR ELEMENTS IN THE UNIT	20
3.2	ENERGY FLOW DIAGRAM OF GENERATING UNIT	21
3.3	EFFICIENCY OF ELECTRICITY GENERATING PLANT	21
3.4	CURVES OF SELECTED BOILER PARAMETERS DURING A COLD START-UP	27
3.5	CURVES OF SELECTED BOILER PARAMETERS DURING A WARM START-UP	28
3.6	SCHEMATIC REPRESENTATION OF THE BOILER HEAT TRANSFER SURFACES	32
3.7	PLAN VIEW OF BOILER FROM ABOVE 'A' LEVEL BURNERS	33
3.8	BLOCK DIAGRAM REPRESENTATION OF WATER AND STEAM CIRCUITS BEFORE THE SUPERHEATER TUBES	34
4.1	THE BOILER UNIT SHOWING THE SUB-UNITS OF INTEREST	43
4.2	THE PHYSICAL DIVISION OF BOILER INTO CELLS	44
4.3	THE BLOCK DIAGRAM OF THE MODEL FOR THE I'TH CELL	46
4.4	THE BLOCK DIAGRAMS OF THE MODELS FOR THE EVAPORATOR AND DIVISION WALL	57
4.5	BLOCK DIAGRAM REPRESENTATION OF CASCADED MODELS	58
5.1	TABLE OF PARAMETER VALUES FOR ALL CELLS AS DEFINED BY EQUATION 4.16 IN SECTION 4.4	74

CHAPTER 1 INTRODUCTION

The increasing demand for electrical energy ensures the existance of the Electricity Supplier for the foreseeable future. Modern technology in the First World, and the industrialisation of Third World countries has dictated a steady growth rate in the industry since the major strides taken so long ago by Michael Faraday and James Watt. Today's 600 MW and even rarer 900 MW boilers are indeed very different from early drum boilers; the original kettle included!

The demand for more energy has been matched only by man's incorrigible greed for profits, and these combine to form the much quoted theories on Economies of Scale. To maintain the growth rate, the demand for greater efficiency has necessitated a considerable investment in research and development. Before progressing to larger more efficient units present units must be well enough understood. The technology must exist for satisfactory control. Taking a step up the ladder of boiler size would be sheer folly without the supporting technology. The increase in efficiency is often only marginal and any unforeseen problems could thwart the rules of Economies of Scale until such time as the technology again exists.

One such advance has been the development of the single-pass boiler unit. Far less water is in the boiler at any instant. The water present only cycles once through the tube banks being converted directly from water to superheated steam. Such units have a far more rapid response time. It should therefore be possible to provide a better response to system disturbances and hence an improved service to the consumer. This response time results in a plant inherently more difficult to control. The time available within which the operator must perform adequate control is much reduced. Conditions can and occasionally do develop too swiftly for meaningful operator intervention. This difficulty is further compounded by the human controller's inability to satisfactorily perform more than second order control. The operator can comprehend 2nd order simple harmonic motion, but

4th order harmonic motion is considerably more complex (Sheridan, 1974).

1.1 THE GENERAL CONTROL PROBLEM

The increased speed of the unit response time, resulting in reducing starting costs, can only be beneficial if the control exists to adequately cope with the problems resulting from faster response times. Complete automation of the unit is not yet considered a viable proposition. Confidence in such a system is not yet adequate. The social implications of such a development also require serious deliberation. The operator must therefore remain an essential element of the feedback loop. Additional information or assistance must be made available, to the operator, to improve unit controllability. An instrument providing this support should enhance the operator's ability to control the unit.

A modern 600 MW Benson once-through boiler unit of the type in operation at Duvha Power Station in the Eastern Transvaal has a designed cold start to full load start-up time of eight hours (FIGURE 3.4). The consequences of a boiler unit trip results in many lost generating hours. All fire must be removed and all fuel purged from the system. If repairs are required the system must be cooled enough to allow access for the maintenance crew. If no damage has occurred the boiler must be allowed to reach conditions from which the unit may be restarted.

To avoid complications, operators prefer to start up the boiler at a much slower rate than intended. This ensures that stresses in metals, due to thermal effects, remain at a minimum. The more typical start-up time is then twenty four hours. Due to maintenance problems and failure of sub-systems even this figure is optimistic, as consecutive start-ups are aborted, resulting in delays of a couple of days. During this time vast quantities of oil and coal are consumed with no power being generated.

The excessive start-up time considerably complicates maintenance scheduling and the provision of a satisfactory service to the end user. Synchronisation time, when the generator is linked to the national grid, may be delayed by forty eight hours or more.

1.2 THE PARTICULAR PROBLEM

One particular problem of the type discussed above is that of the steam temperature control at the inlet to the first steam attemporator (FIGURE 3.8). The attemporators add spray water to the system to control the steam temperature. The attemporated steam is then superheated and attemporated further in a number of stages before driving the turbine. The first attemporator inlet temperature must remain within controllable bounds to ensure that later heating and spray water stages are able to produce steam of the right quality for use by the turbine. Should this temperature be too high the addition of spraywater may be insufficient to maintain control of the steam temperature at the inlet to the turbine. An excessive temperature will also produce high metal stresses which may result in a boiler trip. This temperature has a tendancy to change very rapidly, compared to the system response times, preventing the operator from taking satisfactory control action. The transfer function relating the steam temperature to the disturbance is thought to include real poles close to the origin. The operator is not capable of adequately closing the loop in this case. In an attempt to prevent the rate of tube expansion exceeding its maximum, the operator's reaction may cause an oscillatory response which may result in a unit trip due to the maximum rate of contraction being exceeded. This may result in damage to the unit in which case the boiler would need to be cooled sufficiently to allow repair work to take place. At the very least a purge cycle will be required and a warm start initiated.

1.3 THE PROPOSED SOLUTION

The purpose of the project described in this report is to investigate a way of providing the operator with additional information enabling him to take satisfactory control action. The operator should remain an essential element of the control loop making use of information that has been suitably processed and displayed by the proposed instrument. He would be able to try new techniques for control purposes without catastrophic delays. The instrument could also be used as an on line training aid enabling operators to use different mills and firing rates to maintain the steam attemporator inlet temperature.

The remainder of this section discusses the strategy and approach, to the above problems, that have been adopted in the present study.

1.3.1 THE GENERAL TECHNIQUE

A fairly simple mathematical model for the plant, in this case the boiler, is obtained. Given certain inputs this model can be used to predict what the output should be in the future. Ideally, the execution time of the prediction model must be many times faster than the time constants of the real plant. This enables the operator to see, in a few minutes, what effect an action taken now, is likely to have on the plant in a few hours time. Should action taken now result in an unsatisfactory prediction then the action can be cancelled or altered immediately.

Because of the nature of Escom's generating plant it is not possible to run tests directly on the boiler. In order to verify that the fast-time predictor instrument does indeed work therefore requires an additional more sophisticated model to simulate the boiler plant. This enables the predictor instrument to be tested against the simulation. It would also

be possible to determine whether a meaningful improvement in controllability is apparent with the predictor instrument in operation. Once the necessary confidence is obtained, a hardware implementation of the fast-time predictor instrument could be undertaken. Again verification would take place against the boiler simulation. The final stage would then be to transfer the instrument to the plant and test its effectiveness in actual operation.

1.3.2 THE SCOPE OF THE WORK UNDERTAKEN

A mathematical model for sections of the boiler unit is required to form the basis of the detailed simulation described above. The scope of this thesis is limited to the development of such a model. The model must be of sufficient accuracy such that at a later stage it can be used to verify and evaluate the fast-time predictor instrument.

The nature of the problem precludes several modelling techniques. It is not practical to perform step tests on the power station units. The large number of unknown parameters requires considerable numerical processing capability. Off-line modelling techniques are therefore required to determine these parameters. The chosen method for realisation of the model follows.

Data from the plant was logged from the relevant data points at a sampling rate of one sample every five minutes. The most suitable data set was determined from the data logged. Enthalpies from measured temperature and pressure points were obtained for the steam and flue gases. A maximum likelihood parameter estimation technique was employed to develop a multi-input multi-output auto-regressive moving average model from available data. Algebraic manipulation of the resulting transfer functions yields the cell transfer function model. Finally a state-space cell model was obtained from the cell transfer function model.

This complicated procedure is made necessary by the unavailability of information concerning intermediate mills supplying the furnace.

1.4 AN OVERVIEW OF THE DISSERTATION

This report discusses in detail the methodology behind the adopted approach. This is covered in Chapter 2. Considerable space is allocated in Chapter 3 to providing the necessary mechanical engineering background material that is required to appreciate the complexity of the generation unit and in particular the boiler. The model is discussed in Chapter 4 and Chapter 5. The first of these chapters is devoted to the physical definition of the model while the latter is concerned with actually obtaining quantitative data on the model parameters. The success of the model is discussed in Chapter 6 along with a brief section on other attempted modelling techniques. Finally, Chapter 7 suggests some future work for the continuation of the project as well as some important conclusions.

CHAPTER 2 THE IDEAS BEHIND THE SELECTED APPROACH

To improve the plant efficiency and to ensure that certain parameters remain bounded requires some form of additional control. Mention of control immediately brings to mind open and closed-loop systems. Open-loop systems have their inputs derived only from a control law and no consideration is made of the process output. The relationship between input and output must be well defined and time invarient to ensure a bounded output. These truly open-loop systems are rare since the operation of the unit observed is seldom well defined. The output is therefore usually monitored and the input adjusted accordingly, hence the term closed-loop control.

Many plants make use of fully automatic closed-loop control. The control of these plants is transparent to the operator or higher-level controller. An example is water level in a tank, or fluid flow regulated by a valve. Once the requirements have been established automatic control ensures that these requirements are satisfied. An alternative form of closed-loop control involves manual control. In many systems it is the operator who observes the output and through his experience of the plant manipulates the inputs to achieve desired results. The human operator is slow to react, is more unreliable, is easily bored but has one saving grace, his reasoning ability. What then are the advantages and disadvantages of these two forms of control?

2.1 AUTOMATIC CLOSED-LOOP CONTROL

Closing the loop with automatic control enables the human operator to be removed. Many design techniques for automatic control may be employed These include:

a) Classical Single Input Single Output Control (SISO)
b) Transfer Function Techniques
c) State-Space Feedback Control
d) Adaptive Control

CHAPTER 2 THE IDEAS BEHIND THE SELECTED APPROACH

In the following sections, the various available techniques for automatic control will be reviewed. For the purpose of this report automatic control specifically excludes all forms of manual control.

2.1.1 CLASSICAL CONTROL

The techniques of SISO control (Dorf, 1980) do not readily apply themselves to complex systems. The use of PID controllers in individual feedback paths is rarely satisfactory if attempted in isolation. Interaction terms in a system make the PID controllers extremely difficult to adjust for optimal performance. The effects of system non-linearities are transmitted through all loops via interaction terms. The system must be well known for effective control. That is, enough knowledge about the plant must be available to allow systematic tuning of the PID controllers. The PID controllers would be tuned so as to reduce interaction to a minimum. In a large system the use of PID controllers in all loops makes this approach costly.

2.1.2 TRANSFER FUNCTION TECHNIQUES

The matrix multivariable form of this technique allows considerably more freedom than classical control. Popular design techniques include non-interacting control, decomposing into dyadic matrix form, characteristic loci, Nyguist array and the inverse Nyguist array (Owens, 1978). These techniques are aimed at either eliminating, or reducing the interaction terms to an acceptable level. Extensive use is made of eigenvalue and eigenvector methods. In the first three techniques mentioned this can involve complicated controller matrices and indeed these matrices may include non-linear or irrational functions of the Laplace operator 's'.

For all these transfer function techniques methods exist for determining system stability. The effects

of non-linearities on the system can be determined within acceptable bounds using describing function techniques. Transfer function design techniques are more effective than SISO Control since interaction is largely limited. They are also more robust to parameter changes unless the order of the system is large.

2.1.3 STATE-SPACE FEEDBACK CONTROL

Classical control and transfer function techniques do not easily adjust to system changes. These changes may result from alterations in the required plant perfomance or could be a result of a system reconfiguration. These two methods would usually require total revision of controllers. This task is considerably simpler if state-space techniques are used. The manner in which cascaded systems are represented in matrix form allows each sub-system to retain its own identity within the matrices representing the system. Should a section of the model change or operate about a new steady-state value then the transfer function controller or PID controllers must be recalculated or retuned. This is not the case in a cascaded state-space model where only the relevant sub-matrices need be altered.

A suitably chosen controller enables the poles and zeros of the system to be placed where required. The multivariable equivalent for PI control may also be used (Owens, 1981). The techniques for determining the stability of the state-space approach, as well as non-linear effects, are not as easily applied as those defined for the transfer function techniques. As with the transfer function techniques, the robustness of the method reduces considerably as the order is increased. Variations in the actual system variables could greatly affect the intended control action. In extreme cases this may be unstable.

2.1.4 ADAPTIVE CONTROL

An approach most suited to problems where parameters are known to vary is one of adaptive control (Astrom, 1973 and Astrom, 1977). The particular downfall of all the above techniques is their lack of robustness or the sensitivity of the output to changes in parameters. Disturbances in the form of noise or unmeasurable input parameters may considerably affect the ability to control the plant. A technique for tracking these parameters could then be used to continually re-define the control law ensuring that the required effect is obtained at the output. Figure 2.1 shows how the inputs, outputs and internal states could be used in a parameter estimation algorithm. The most recent parameters could then be used to determine the parameters required in the feedback loop to obtain the desired control. The most popular of these algorithms is the recursive least squares technique. For a high order system the computation involved in determining first the plant model parameters and secondly the controller parameters may be excessive.

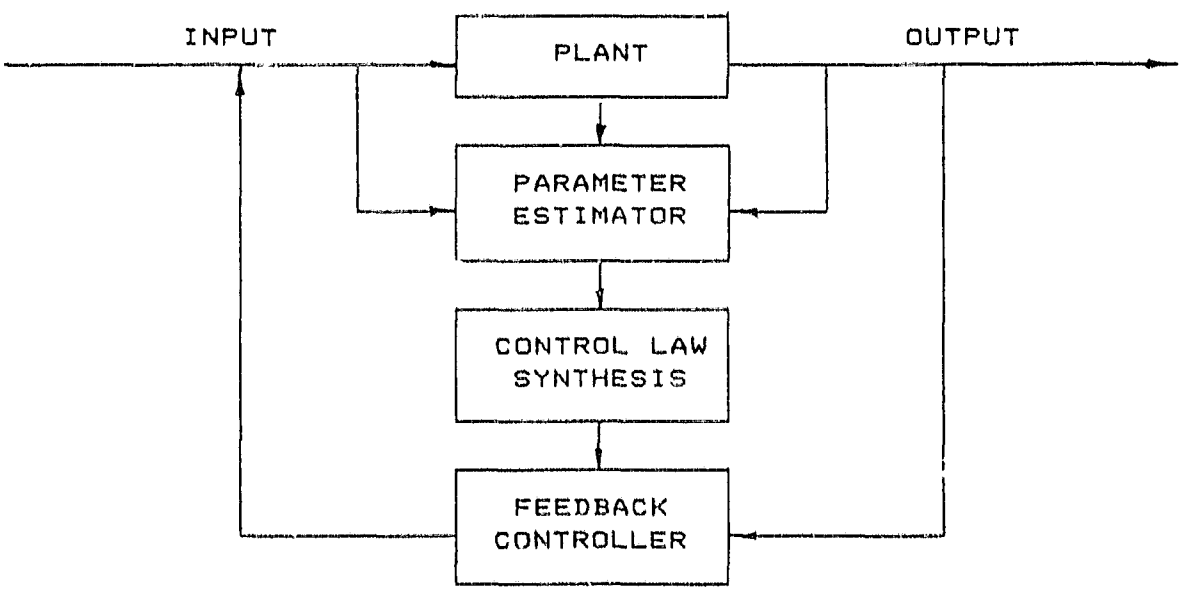


FIGURE 2.1: THE BLOCK DIAGRAM FOR AN ADAPTIVE CONTROLLER

CHAPTER 2 THE IDEAS BEHIND THE SELECTED APPROACH

The adaptive controller above is the only automatic closed-loop control strategy capable of performing the complex task of power station control. Adaptive controllers are still in their infancy and often require considerable processing power to be effective. Powerful techniques coupled to the necessary processing power would enable such a system to correctly respond to non-linearities and disturbances for most of its operating time. The risk does exist that the disturbance may be sufficiently great to cause the controller to converge to a new non-optimum or unstable state. The robustness of the controller cannot be guaranteed over a sufficiently wide range of inputs. The confidence in the strategy is not yet sufficiently high to allow adaptive controllers total control of sensitive highly complex systems.

The human operator is better suited for dealing with unusual or unexpected inputs. His knowledge, after countless years of power station control, cannot be ignored. The concept of expert systems (Duda, 1981 and Merry, 1987) would have to be introduced to the control strategy before the operator could be freed for higher level control tasks. An expert system attempts to form a vast core of knowledge assembled from many relevant sources. These sources would include information from the system designers, the manufacturers, the system engineers and the operator. The correctly collated information would make available to the controller the same decision making powers previously executed by the operator. The expert system would finally have a major role to play in determining what state the plant is presently in and hence which control law should be implemented (FIGURE 2.2). Only with the aid of such an expert system, would the adaptive controller be capable of informed meaningful control action.

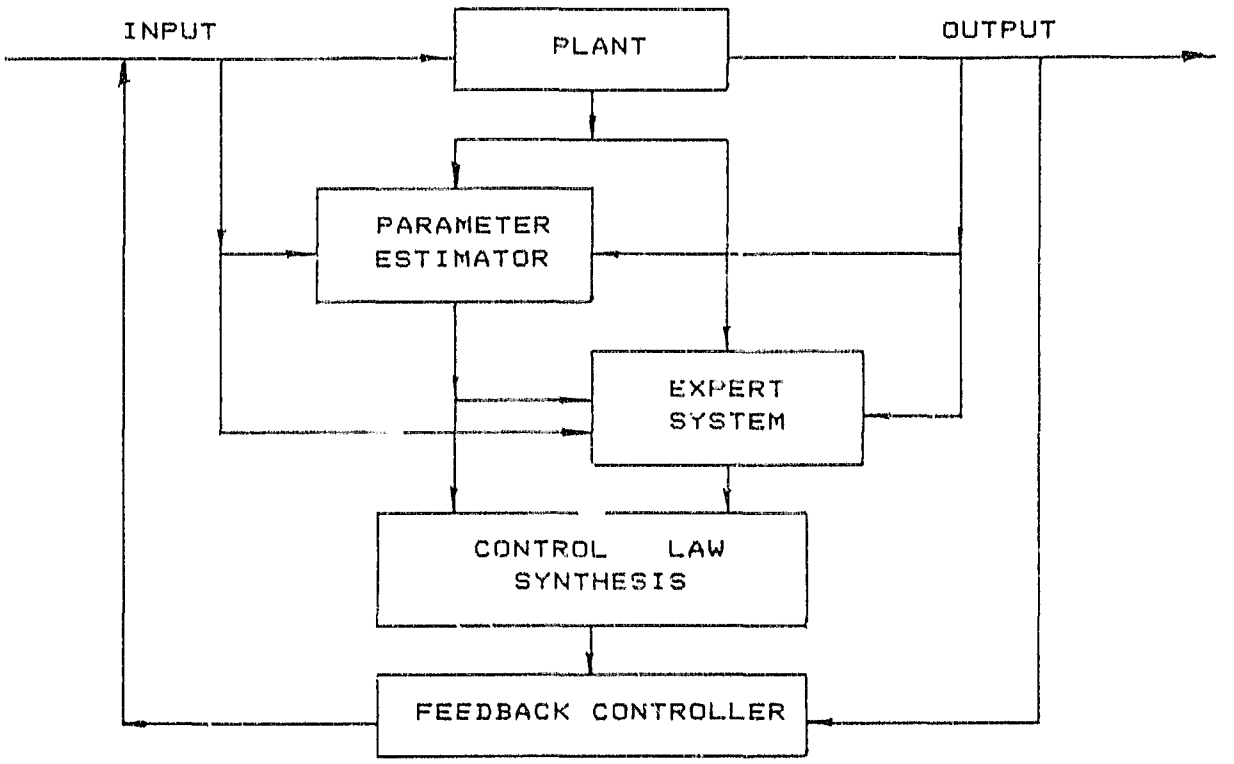


FIGURE 2.2: THE ROLE OF EXPERT SYSTEMS IN ADAPTIVE CONTROL

2.2 THE MAN IN THE LOOP

The previous section discussed some of the techniques available for automatic control. While many of these techniques would be quite satisfactory for low level control, none of the techniques warrants sufficient confidence for use at the much higher level of the unit control room.

The human operator still has an important role to play in closing the loop. Today's role of the operator in the feedback loop is discussed followed by an alternative approach to this role.

2.2.1 SIMPLE CLOSED-LOOP CONTROL

The technology exists to reliably control a large number of minor power station functions. These include low level regulatory and sequencing control such as small motor and pump starting and lubrication controls, positional control of valves, velocity

control of conveyers and speed control of the turbine. Higher level control may include flow rates, firing rates and steam temperature. Experience has shown that the low level functions have good reliability. The operator is then justified in allowing automatic control of these loops. Should these loops foil or loose control, monitoring equipment informs the operator who then tales the necessary action. The disturbance caused by the failure of an automatic control loop is usually minor.

Higher level automatic control loops have alarms. These allow the operator to assume that the automatic controller is performing satisfactorily. The operator-set alarms warn him of any problems that may develop enabling him to take corrective action. Control can be returned to the automatic controller once the operator has returned the system to a suitable state.

At a still higher level the operator will himself spend time monitoring parameters and taking action thus closing the control loop (FIGURE 2.3a)). As technology improves, low level control loops could have redundancy. High level loops will run with sufficient reliability and control capability to reduce the requirement for operator intervention to extreme cases. Loops presently requiring the full time monitoring of an operator will be closed with low levels of reliability. They will still require attention but at an alarm level. This will free the operator for still higher control strategies.

A drawback of the supervisory role of the human operator, at some levels of control, (steam temperatures, etc.) and the full time monitoring by the operator, in order to close still higher level loops, is that all these control strategies cannot run faster than real-time. The operator can only know the effects of changes in the input after the

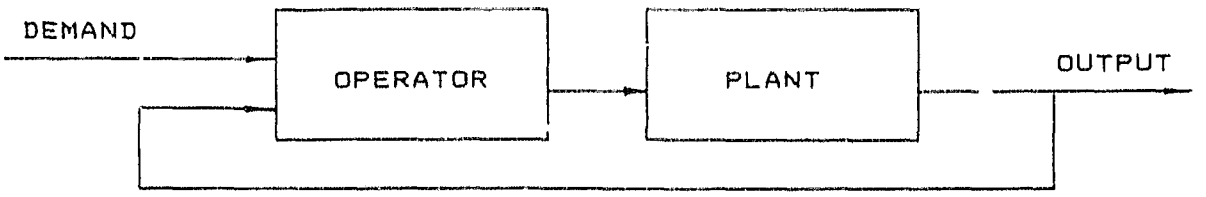
system has responded. This response time is in certain cases considerably longer than response times of sub-systems relying on the same outputs. Control of these sub-systems is then very difficult and indeed marginally unstable.

2.2.2 PREDICTIVE CONTROL

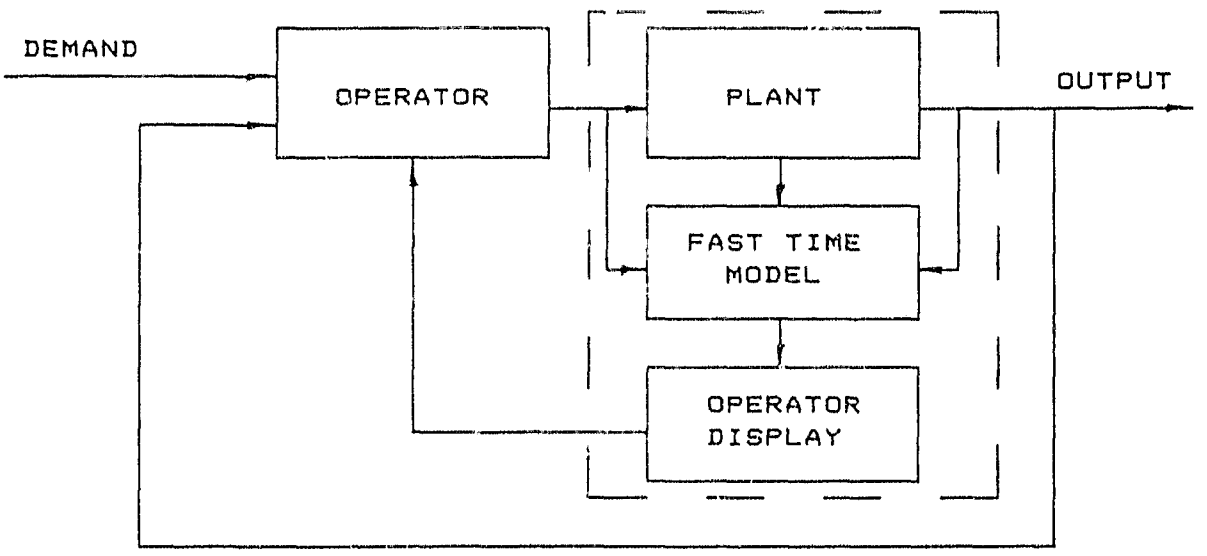
An alternative method for relieving some of the pressure on the operator is to introduce some assistance in the form of a predictor instrument. (Sheridon, 1974 and McCormick, 1964) A predictive control strategy enables the operator to see the effects of changing inputs, not in real-time but in a fraction of real-time. If the change in input does not produce the expected output given by the predictor instrument, the operator may then re-adjust the inputs until satisfactory output is achieved. The operator can then be reasonably confident that suitable control action has been taken without having to wait for the plant to respond. The final plant response may not be exactly as predicted but should be fairly close. Experience would eventually enable the operator to control the output using the predictor instrument as a guideline as well as using his own knowledge of the predictor and plant behaviour.

Consider the configuration shown in FIGURE 2.3a). In order for the operator to achieve a first order response at the output he must be capable of adjusting the plant input in such a way that the plant, which in this case has a 4th order transfer function, behaves like a 1st order system. In FIGURE 2.3b) the same plant has a predictor instrument linked to it. This has the effect of providing some feedback around the original plant (Kelley, 1958). The characteristics of the original plant are modified accordingly. The effective plant now controlled by the operator is enclosed in the dashed line. To force the plant to behave like a

1st order system the operator now only needs to control a 3rd or even 2nd order effective plant. This task is more easily within his grasp than that of controlling the 4th order system.



a) PLANT CONTROLLED ONLY BY OPERATOR



b) PLANT CONTROLLED BY OPERATOR WITH AID OF PREDICTOR INSTRUMENT

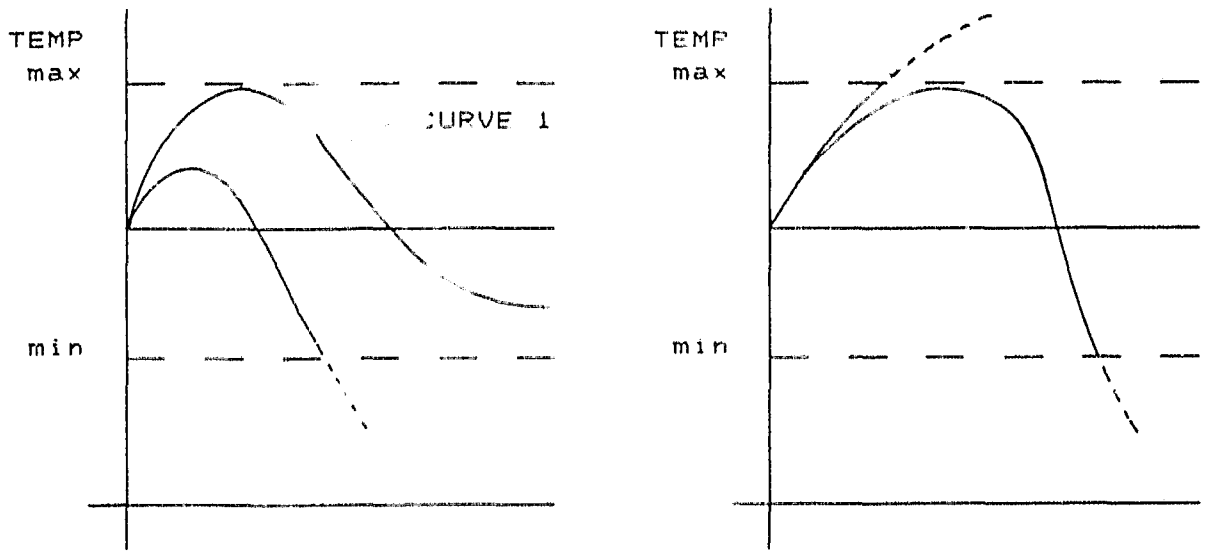
FIGURE 2.3: THE ROLE OF THE FAST-TIME PREDICTOR INSTRUMENT

The benefits of a predictor instrument are that; it allows the operator to try new techniques for more effective control without undesirable consequences since the operator may alter any dubious decision long before the plant responds and it reduces the complexity of the plant being controlled. The technique was first suggested for use in an analogue system for assisting operators in maintaining the trim on a submarine. This plant has multiple poles

close to the origin (Kelley, 1958 and Kelley, 1962). A more recent use has been in the aircraft industry (Riepe, 1983) for assisting with landing approach paths.

2.2.3 THE APPLICATION TO THE PROBLEM OF BOILER CONTROL

An initial investigation indicated that operators experience considerable difficulty in controlling the first attemporator inlet steam temperature. It becomes extremely hard to regain control of this temperature once it begins to fluctuate. Since the temperature rise is very swift, a quick response is essential. A consequence of these temperature fluctuations is excessive metal differential temperatures which may result in high stress areas. Failure of these areas is not desirable and attempts to prevent the critical condition being reached, after the temperature rise starts, often results in the boiler unit tripping. Usually this is a result of the operator over-reacting.



a) ACTION TAKEN AT AN EARLY STAGE

b) ACTION TAKEN TOO LATE

FIGURE 2.4: OPERATOR REACTION TO POTENTIALLY CRITICAL TEMPERATURE RISES

Consider FIGURE 2.4a). The operator sees the temperature straying beyond the controllable range of the attemporating water and initiates excessive control action resulting in this temperature cooling to such an extent that excessive contraction of the metal occurs and the unit trips. A less excessive action would have kept the temperature within the required bounds. Another cause of tripping occurs when the temperature rise has progressed to an advanced state (FIGURE 2.4b)) and desperate action by the operator causes the temperature to swing rapidly towards the lower limit and a trip due to excessive contraction occurs. A final case occurs when action taken is insufficient or too late to prevent the maximum differential temperature from being exceeded. The only acceptable control is that of curve 1. To achieve this additional information is required to give the operator an idea of how much action will be required to maintain satisfactory control.

A fast-time predictor instrument is well suited to such a problem. To control the attemperator steam temperature of FIGURE 2.4 the operator may adjust the feedwater flow, the firing rate or the choice of burners to be taken out of, or placed in service. The advantages of moving fire around the combustion chamber enables the flame temperature at the outlet of the furnace to be reduced. Increasing the overall firing rate increase the steam temperature at the outlet of the upper part. These combined actions serve to decrease the temperature gradient across the metal walls. The feedwater rate need not then be altered, and as long as the control action taken is subtle no disruption of the steam supply is necessary.

2.3 THE PLANT SIMULATION

The fast-time predictor instrument has the effect of reducing the complexity of the plant that the operator has to control. The predictor model need not be

accurate for significant reduction in system complexity to be achieved (FIGURE 2.3). Verifing these statements would ultimately require that the fast-time predictor instrument be linked to the real plant. Due to the nature of the plant, a high degree of confidence must exist in the equipment before tests can be run on the boiler unit. All attempts must be made to ensure that the data provided to the operator by the fast-time predictor instrument is as accurate as possible.

A simulation is therefore required to enable the technique suggested to be verified and later demonstrated. From the simulation model a simplified fast-time model can then be created.

The range of techniques available for determining the model is severely limited. Input and output information is easily measured. No measurements are possible for the assumed or suggested state-space variables. Step responses cannot be used since it is not possible to perform step inputs to the coal mills. This is, however, possible for oil firing. Intermediate burner levels are often not used during a start-up and the effect of these burners cannot then be determined by using input and output information.

A technique to determine these intermediate transfer functions is discussed in Chapter 4. Chapter 3 provides the necessary background on the boiler.

CHAPTER 3 AN OVERVIEW OF THE BOILER

The condensor, boiler, turbine and generator together form a single unit within a power station. In order to understand the operation of any single process within the unit it is necessary to have an appreciation of the combined processes. This will enable high level control strategies as well as aspects on steam and energy flow to be discussed.

This chapter discusses the complete energy generating unit and some control strategies before considering, in more detail the operation of the boiler. In turn, this will pave the way for a greater appreciation of the complexities facing the operator and engineer in controlling the vital steam temperature that this dissertation is primarily concerned with, namely the first attemporator inlet steam temperature.

3.1 THE BASIC OPERATION OF THE UNIT

The explanation of the basic unit operation is facilitated by considering three aspects of unit operation, namely, the steam cycle, the energy cycle and the start-up procedure (Babcock, 1955; Central, 1971; ESCOM, (8 and 9); Hollis, 1982). The following sections refer to FIGURES 3.1 and 3.2.

3.1.1 THE STEAM CYCLE

3.1.1.1 THE FEEDWATER PUMPS

Treated water is forced through the steam circuit by the feedwater pumps. These supply high pressure water (up to 20 MPa) to the boiler unit. The water at this stage has a strictly controlled purity which is essential to prevent scaling taking place in the boiler tubes. Scaling results in a degradation of the heat transfer characteristics within the boiler. These deposits also cause hot spots on the heat transfer surfaces which result in excessive metal stresses and possible tube failure.

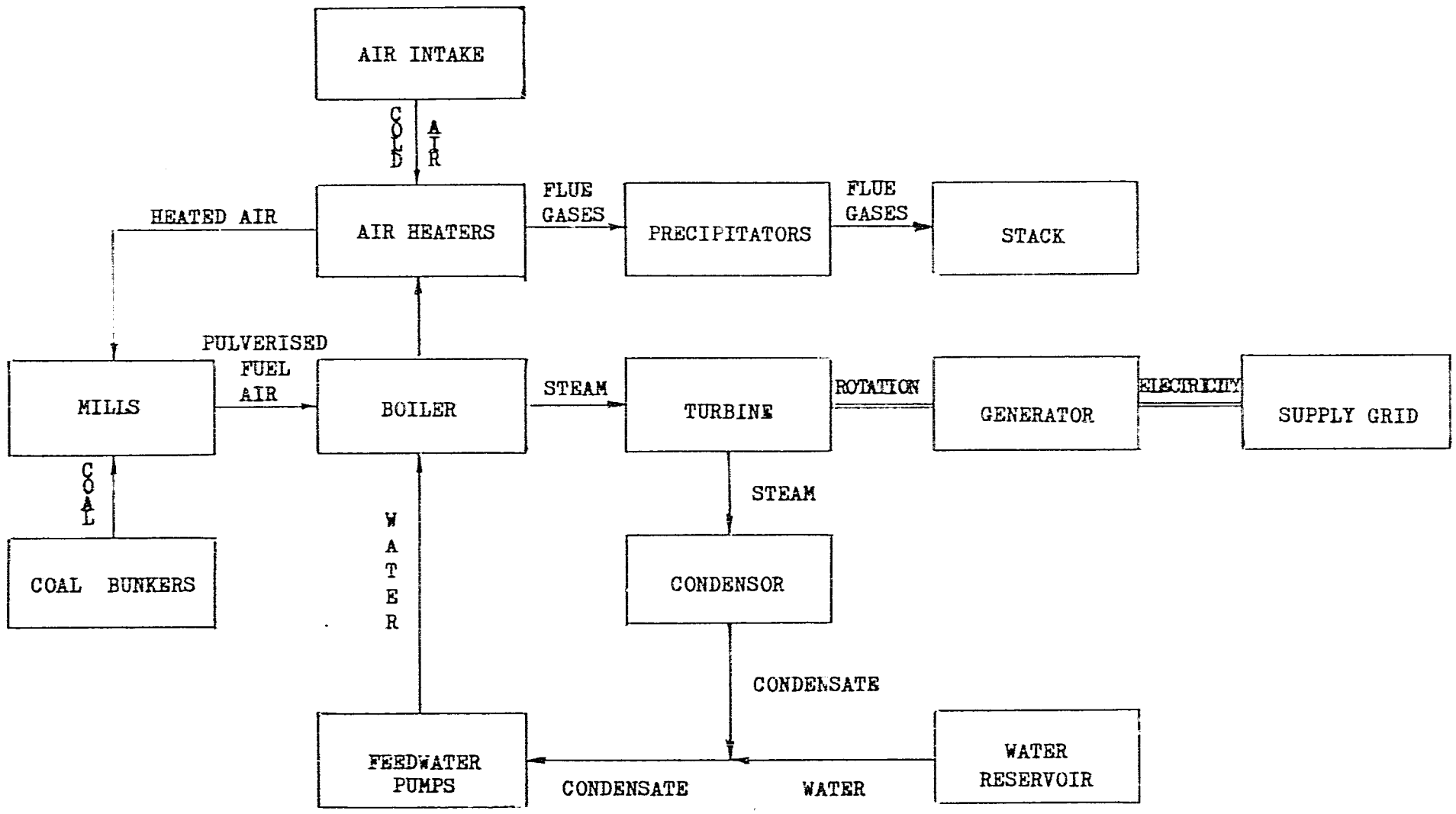


FIGURE 3.1 BLOCK DIAGRAM REPRESENTATION OF MAJOR ELEMENTS IN THE UNIT

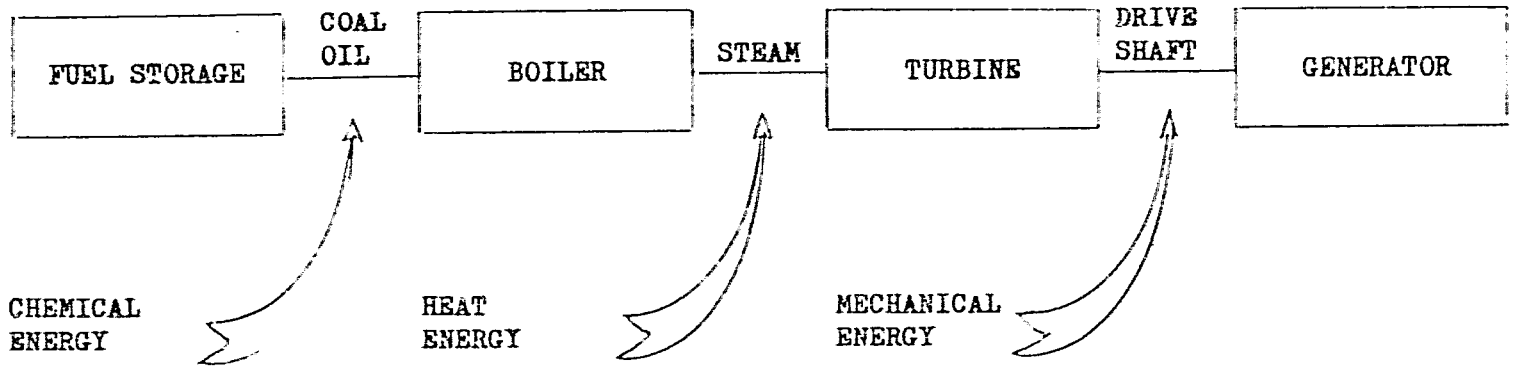


FIGURE 3.2 ENERGY FLOW DIAGRAM OF GENERATING UNIT

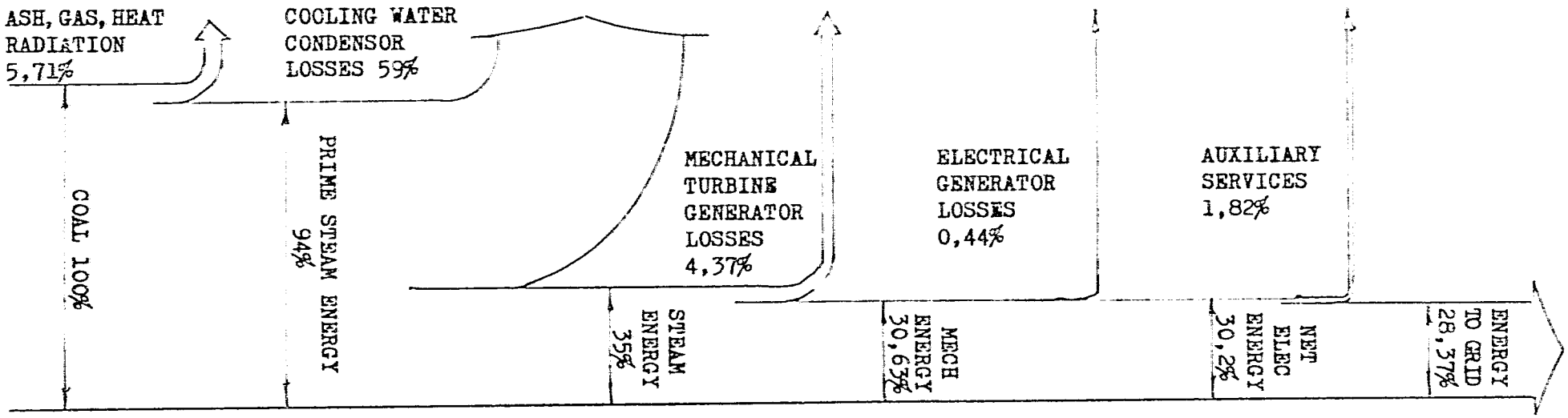


FIGURE 3.3 EFFICIENCY OF ELECTRICITY GENERATING PLANT

3.1.1.2 THE BOILER

The boiler unit heats this highly pressurised water from roughly 40^{o}C to 500^{o}C . The mass flow rate of steam through the boiler must necessarily be of the same order at the input and output. The ability of the boiler to supply power to the following stages is measured by two parameters, pressure and enthalpy. Pressure is a measure of the quantity of steam available, while enthalpy measures the quality of the steam available. The boiler must supply enough steam of sufficient quality to match the load requirements of the turbine-generator.

A secondary function fulfilled by the boiler is the reheating of steam exhausted from the high pressure turbine for use in further turbine stages.

3.1.1.3 THE TURBINE

The turbine converts the available steam energy from the boiler to rotational energy as efficiently as possible. The turbine unit consists of a number of stages, each designed to use steam of a different pressure. High pressure steam from the superheaters of the boiler unit is fed to a high pressure turbine. This exhaust steam is reheated by the boiler before passing through an intermediate pressure steam turbine. The final stage is a low pressure turbine which extracts further energy from the exhaust steam of the intermediate pressure section.

It is essential that only steam of sufficient quality is supplied to the turbine. Only superheated steam is permissible since water vapour in saturated steam could condense in the supply tubes, or in the turbine itself, causing contraction and corrosion which may result in

extensive damage. During the start-up procedure steam bypasses the turbine until satisfactory steam conditions exist.

3.1.1.4 THE CONDENSOR

For an acceptable cycle efficiency to be achieved the exhaust from the turbine low pressure section must be maintai ed at a sufficiently low pressure. The cc densor cools the steam output causing condensation which provides the necessary vacuum for the turbine. Incondensible gases are removed by a vacuum pump. FIGURE 3.3 shows quite clearly that this is the primary source of heat loss in the generating cycle. The ability of the turbine to convert heat to mechanical energy must therefore be viewed against the necessary condensor plant making such a system feasible.

The condensate is then returned to the water flow (FIGURE 3.1) at the inlet to the feedwater pumps. Constant monitoring of the water ensures that the quality of the water is maintained; in particular the oxygen level or aeration of the water must be monitored. The condensate continues to circulate in the steam cycle with any losses being made up from the water treatment plant.

3.1.2 THE ENERGY CYCLE

3.1.2.1 THE COAL MILLS

Coal from the Duvha open cast mine stock pile is transported by conveyor belt to hoppers for each unit which in turn, feed the the coal mills. There are six mills per unit each supplying fuel to different levels within the furnace. The mills crush the coal and mix it with heated air. This primary air carries the pulverised fuel, in suspension, to the furnace where it is mixed with

secondary air to ensure that sufficient oxygen is available for complete combustion of the coal to take place.

3.1.2.2 THE AIR SUPPLY

The air inlet is situated near the top of the boiler house. This slightly warmer air is drawn into the system by forced draught fans. It is heated by the flue gases in the airheater. Two air flows are evident at this stage, the primary and secondary air flows. The primary air flow is fed to the mills where it removes moisture from the coal and carries the pulverised fuel to the boiler in suspension. The secondary air is heated to prevent flame chilling from occuring as well as improving the thermal efficiency.

3.1.2.3 THE BOILER

On entering the boiler the airborne coal is well mixed, by swirl vanes, with secondary air. Sufficient air must be supplied to ensure that all the fuel is burnt. The oxygen content of the flue gases is monitored to provide an indication of the combustion process. No oxygen detected in the flue gases means that unburnt coal is leaving the furnace. Too much oxygen indicates that too much air is being supplied. Less air is then fed to the furnace enabling the dry flue gas losses to be reduced.

The flame is carefully controlled to ensure that combusion only occurs in the fire chamber. Burning coal (sparklers) or burning gases present in the convection section of the boiler could cause klinker formation or excessive metal surface temperatures. A similar problem arises when large droplets of oil are carried into the convection area. The flashpoint of the oil may be reached at a later time causing unwanted

fire. (Oil is burnt to promote flame stability under transient conditions.)

Heat radiated from the furnace and heat carried by convection currents is absorbed by the side walls and the tube banks of the boiler. The point at which the water is converted to superheated steam occurs in the furnace side walls. Further heating takes place in superheater and reheat tubes in the convection section of the furnace. A vital part of the boiler plant is the steam attemporators which add water to the superheated steam thus controlling its temperature.

The flue gas leaving the furnace is drawn through an airheater and through precipitators where 99.8% of all airborne ash is removed before the gases are vented to atmosphere. Soot blowing with high pressure steam is undertaken twice daily in an attempt to prevent particles settling on heat transfer surfaces and degrading system performance.

3.1.2.4 THE TURBO-GENERATOR

The turbine was discussed in SECTION 3.1.1.3. It is worth repeating the importance of avoiding condensation in the turbine. Metals in the turbine are machined to very fine tolerances and expansion or contraction by only a small amount is all that is required for surfaces to touch. The turbine casing is seven times heavier than the turbine shaft and hence different rates of expansion are present in each. Barring gear continually rotates the turbine-generator shaft to prevent deformation, even when the unit is not loaded.

The load angle of the generator determines the power supplied to the national grid and hence the

turbine steam demand. The generators are capable of delivering 660 MVA at 22kV. The generator conductors are water cooled while the stator and rotor are encapsulated in hydrogen. A boiler trip should result in the turbine-generator set tripping. If this does not occur the load angle of the generator will slowly reverse until the generator draws current, from the national grid, in order to drive the turbine.

As is evident from FIGURE 3.3 only 28% of the available coal energy is finally consumed by the national grid.

3.1.3 THE GENERAL START-UP PROCEDURE

The typical cold start and warm start curves are shown in FIGURES 3.4 and 3.5.

The first stage in the start-up process is to establish satisfactory conditions for air flow. The induced draught and forced draught fans are started. All secondary air dampers are opened and the boiler is purged.

The oil burners may be ignited after it has been verified that water is present in the evaporator tubes. At this stage it is essential that the dry superheater steam surfaces are not subjected to temperatures above 600^{o}C. The circulation pump should now be moving water through the economiser, division wall and evaporator tube sections. As the temperature in the system is raised by the oil burners evaporation begins to take place. The blowdown vessel level controller attempts to maintain the water in the system at a constant level, hence the feedwater pump starts making up the level in the blow down vessel as the circulating water component is reduced. During this time steam is allowed to circulate in the superheater and reheater tube banks. This steam bypasses the turbine and its pressure

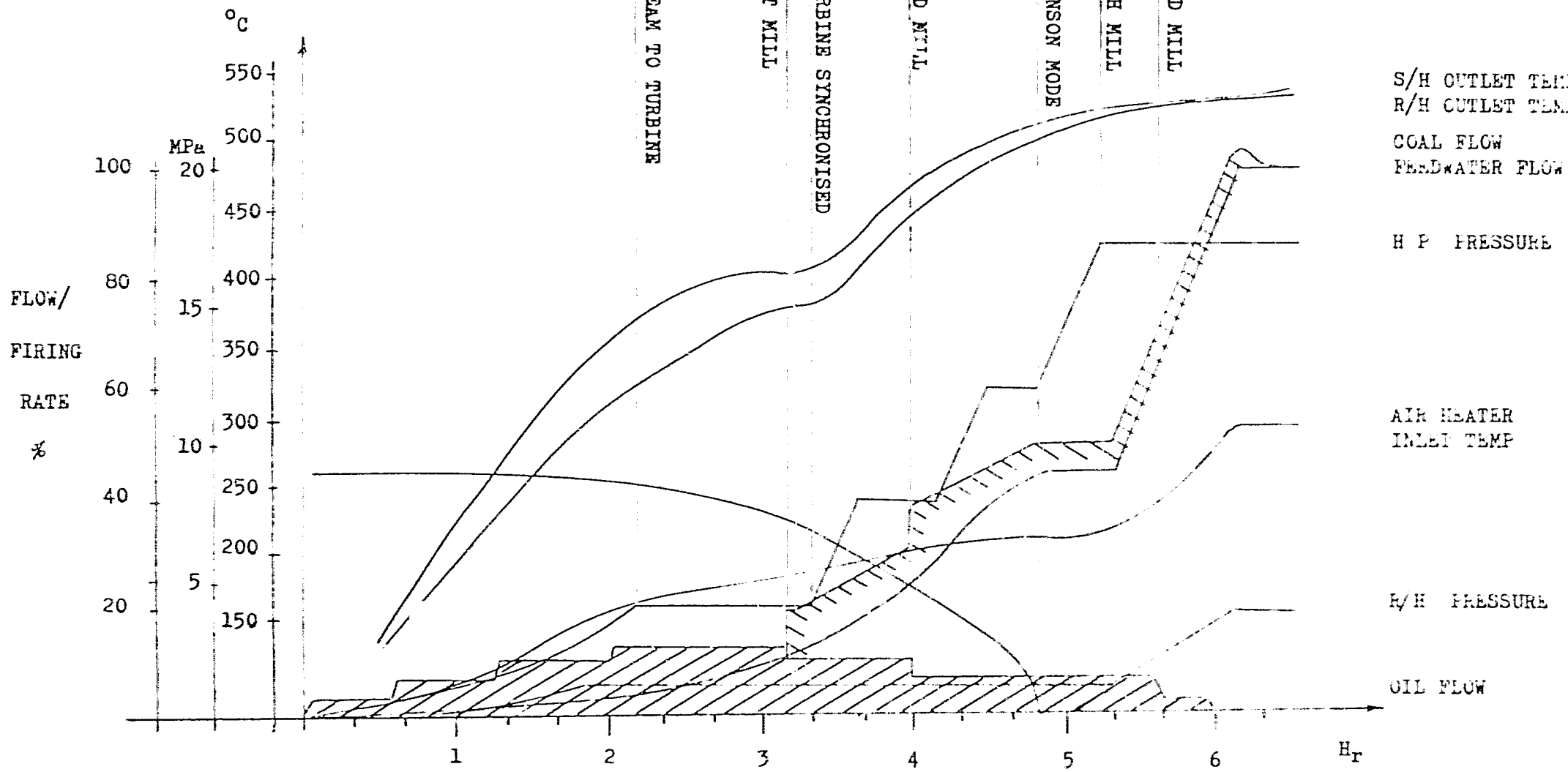


FIGURE 3.4 CURVES OF SELECTED BOILER PARAMETERS DURING A COLD START-UP

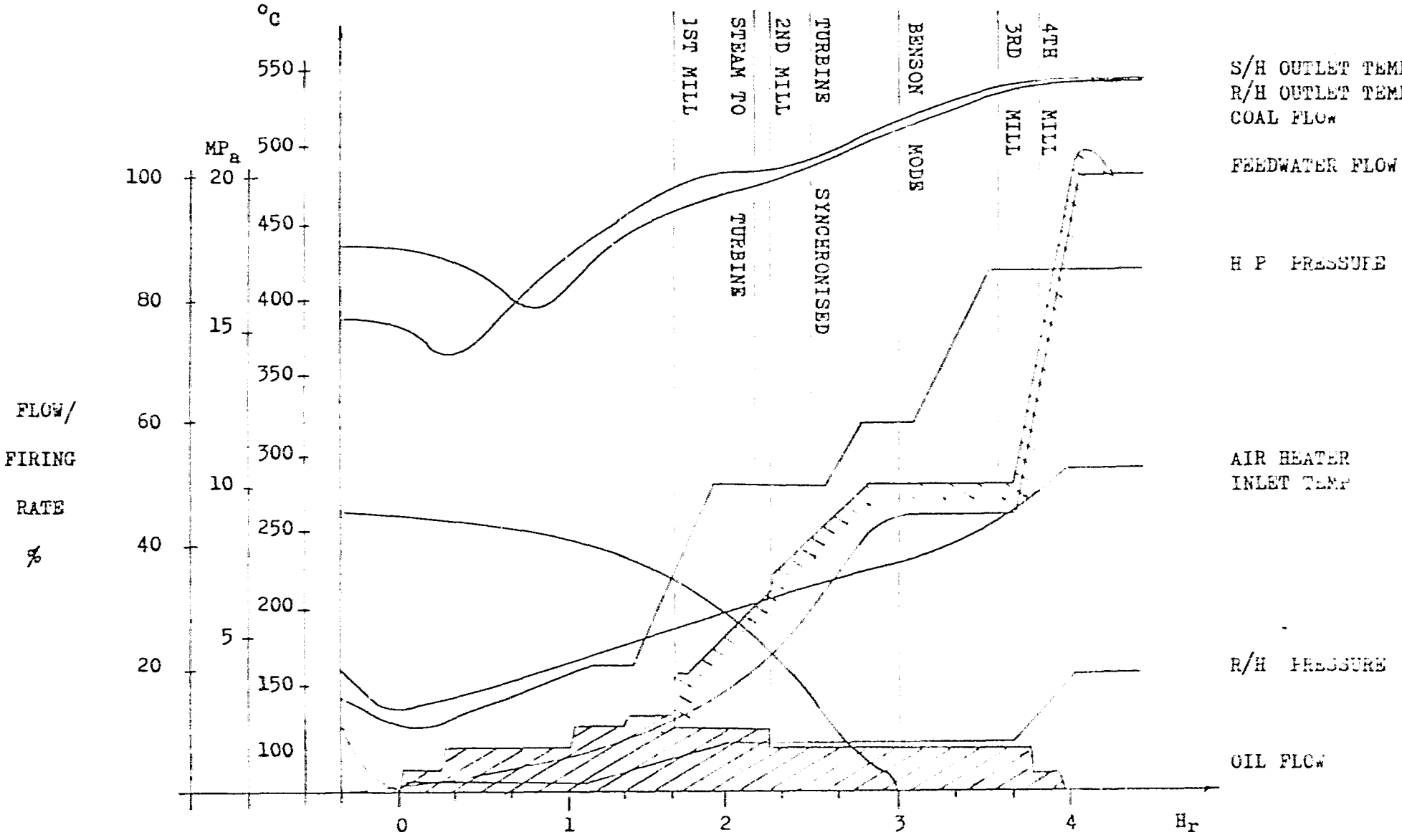


FIGURE 3.5 CURVES OF SELECTED BOILER PARAMETERS DURING A WARM START-UP

is controlled by the high pressure and intermediate pressure reducing plant of the turbine. When suitable steam conditions exist steam may be fed to the turbine.

Once suitable steam condition exists in the superheater tubes the first of the coal mills may be started. This causes a significant rise in feedwater temperature at the economiser inlet. Shortly after the first mill has been started satisfactory steam conditions should exist tr bring the turbine up to synchronous speed. Oil burners are removed as the mills are loaded reducing the firing rate slightly. This must be done to prevent the maximum temperature rise of $6^{o}C$ per minute being exceeded on the heat transfer surfaces. Synchronous speed can be reached once the boiler is generating 30% of full load. At roughly 45% of full load sufficient heat is available to convert all the water to steam in the evaporator screw wall. The circulating pumps are removed from service and the level in the collecting vessels is allowed to fall away completely. Total evaporation now occurs in the evaporator. The boiler is said to have entered its Benson mode of operation. The water now only passes once through the system as no recirculation occurs. Up until this stage the boiler had the multipass characteristics of a drum boiler.

The firing rate is adjusted to maintain a steady 3^{o} C per minute temperature increase in the superheater (S/H) and reheater (R/H) tubes. After the steam temperature reaches $\pm$ $400^{o}C$ conditions exist to allow the unit load to be increased more rapidly. In preparation for this, extra coal mills are started. Finally the firing and feedwater rates are raised, thus increasing the steam pressure and the capability of the unit to do work.

It is critically important for reasons of flame stability that the oil burners corresponding to a

particular burner level are ignited before the mills are started.

3.2 THE CONTROL MODES

3.2.1 THE REMOTE OR CO-ORDINATED MODE

It is possible to control the unit remotely. This requires a signal to be supplied to both the boiler unit and the turbine. The boiler controller ensures that sufficient fuel and water is fed to the boiler for the required steam enthalpy and steam pressure to be achieved. The turbine controller ensures that the differences between the desired output and the obtained output is r uced by altering the generating angle. Up until synchronisation time occurs the turbine will match the speed of the turbo-generator to the quality and quantity of the available steam.

Co-ordinated control may be initiated from the control desk. It may also be remotely controlled from Escom's centralised control centre at Simmer Pan, Germiston.

3.2.2 THE BOILER FOLLOW MODE

Should problems occur with the turbine plant then the turbo-generator can be manually controlled. The boiler could then be set to a following mode in which the firing rate and feedwater flow rate are automatically adjusted to match the demand from the turbo-generator. This also enables the boiler unit to maintain a steam reserve should there be problems with the turbine or generator. The boiler can discharge 35% of its full load steam to the condensor. If the emergency is known to be temporary then the boiler unit will not have to reduce all of its load. Hence it can match the turbine's requirements more quickly when the turbine load is again increased.

3.2.3 THE TURBINE FOLLOW MODE

The more common source of trouble is the boiler unit. In this case the turbine can be made to follow the steam output of the boiler unit. This form of control can be used during a boiler start-up when the turbine adjusts its speed to use the available steam. Once synchronisation has occurred the turbo-generator adjusts the generating angle to match the available steam output.

3.3 THE BOILER IN MORE DETAIL

The cross-sectional and plan views of the boiler are shown in FIGURES 3.6 and 3.7. The steam flow through the relevant heating surfaces is discussed (FIGURE 3.8.) as well as how the air and fuel enters the combustion chambers, radiates energy to the side wall heating surfaces, transfers heat to the heater tube banks and finally leaves the boiler as flue gases.

3.3.1 THE CONVERSION OF WATER TO STEAM

3.3.1.1 THE ECONOMISER

It has already been mentioned that the water fed to the economiser is recycled condensate from the boiler. These tubes are preheated by other steam systems before start-up. The initial temperature at the economiser inlet is 80^{o}C. This rises to 225^{o}C at full load. The water, under pressures of up to 20 MPa, is warmed by flue gas convection flow over the economiser tubes. The majority of the heat available in the flue gases has already been extracted by lower tube banks. The heated water leaves the economiser after passing through a header allowing temperature mixing and pressure equalization. The water is still in liquid form at this stage.

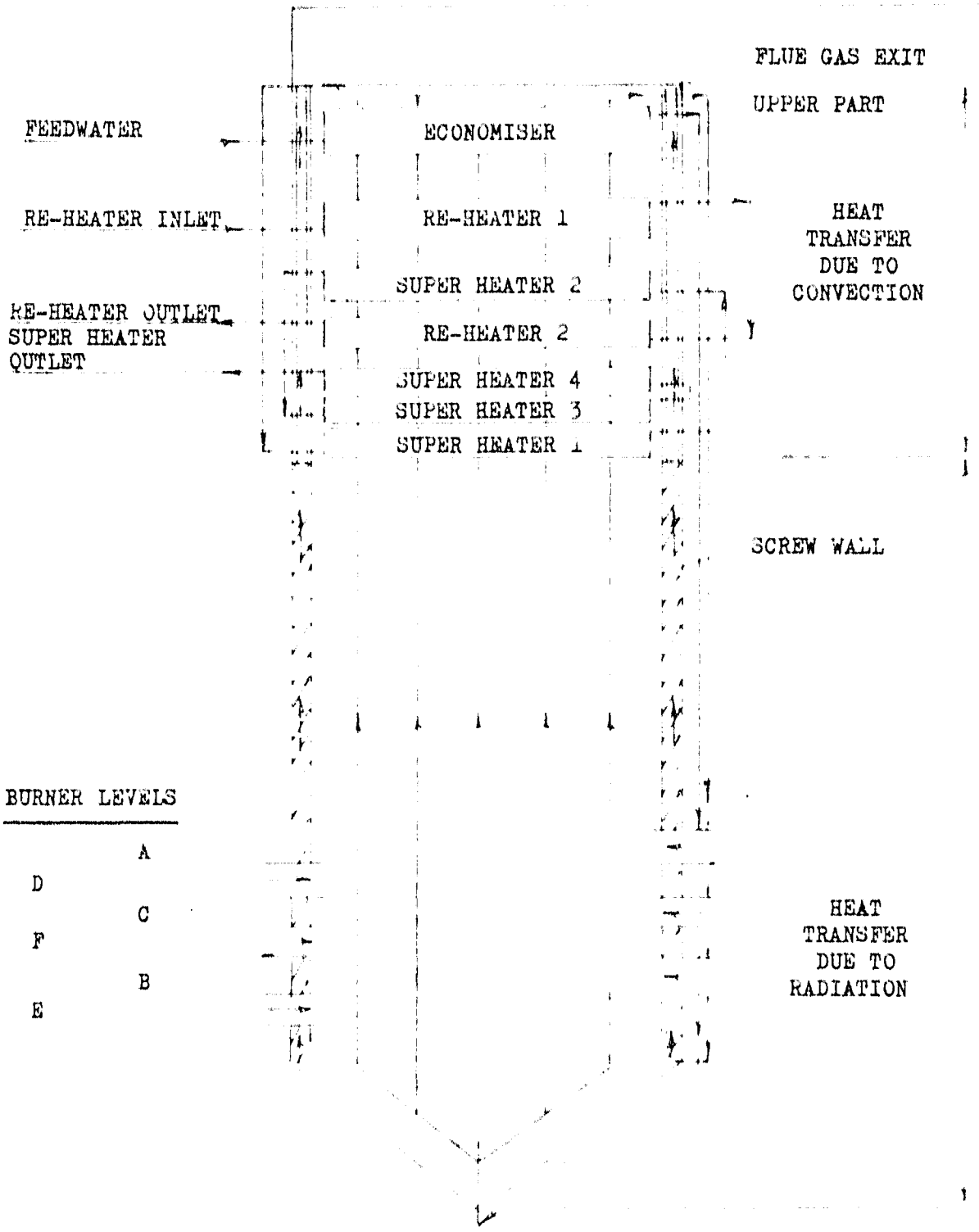


FIGURE 3.6 SCHEMATIC REPRESENTATION OF THE BOILER HEAT TRANSFER SURFACES

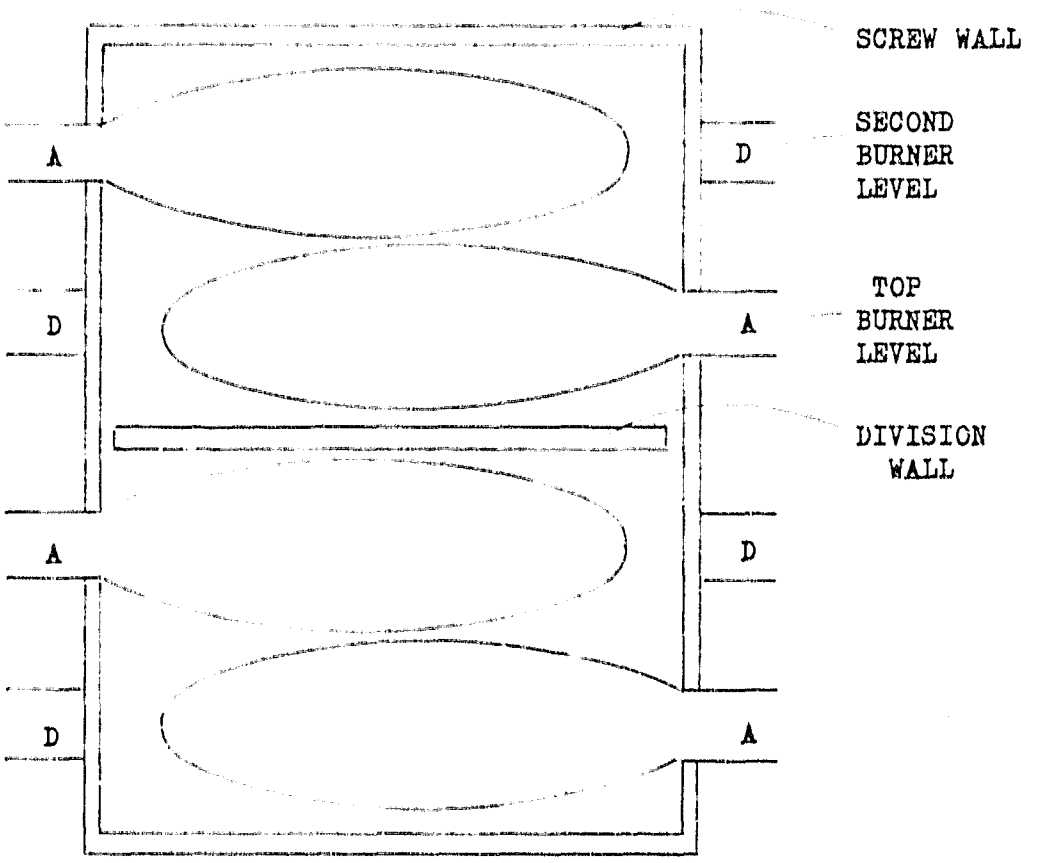


FIGURE 3.7 PLAN VIEW OF BOILER FROM ABOVE 'A' LEVEL BURNERS

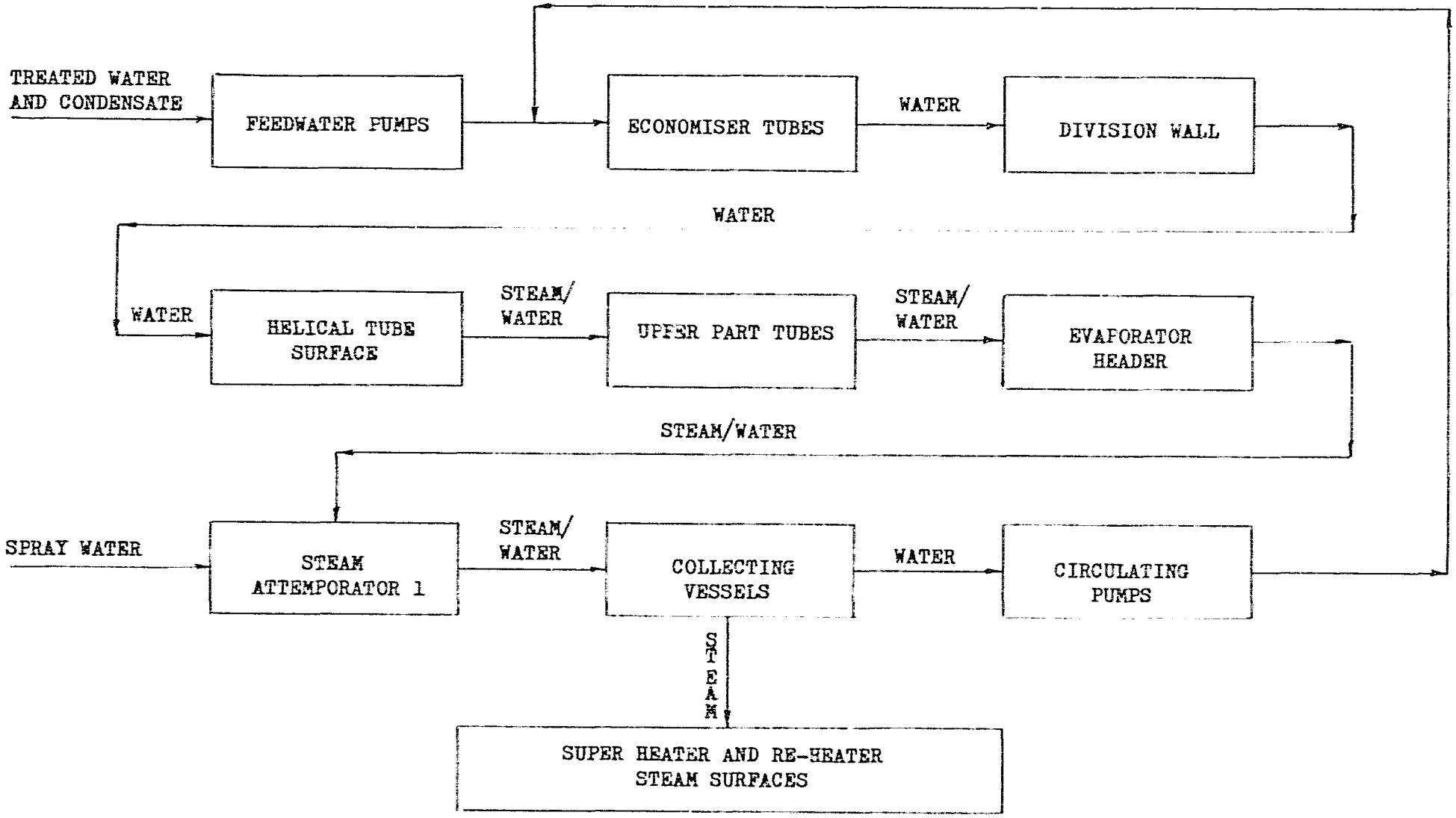


FIGURE 3.8 BLOCK DIAGRAM REPRESENTATION OF WATER AND STEAM CIRCUITS BEFORE THE SUPER HEATER TUBES

3.3.1.2 THE DIVISION WALL

The division wall consists of many parallel vertical tubes which carry water. The panel is suspended from the top of the combustion chamber. The panel divides the combustion chamber into two equal halves and receives radiated energy from both halves of the furnace (FIGURE 3.7). Water fed to the division wall in liquid form leaves the division wall as water but at a much higher temperature.

3.3.1.3 THE SCREW WALL AND THE UPPER PART

The water from the division wall feeds the evaporator heating surfaces. The evaporator is divided into two sections, the screw wall and the upper part. The screw wall consists of helical tubes rising around the walls of the furnace. At the top of the combustion chamber these spiralling tubes feed into a header tube. The water is then led upwards through the convection section of the boiler in vertically rising tubes. During start-up, the water is in its liquid phase in the screw wall and upper part. Once the circulating pumps have been removed from service the point of evaporation moves into the screw wall and upper part. At full load, direct conversion from water to unsaturated steam occurs in the screw wall.

3.3.1.4 THE STEAM ATTEMPORATOR AND THE RE-CIRCULATION SYSTEM

The upper part tubes feed another header which contains water jets. When steam is being produced at the upper part outlet these jets are used to control the temperature of that steam. At this stage, any steam generated along with any water is carried to the collecting vessels. Here the attemporated steam component continues

to further heating stages. The water component is fed back to the feedwater pumps and economiser inlet by the re-circulating pumps. This accounts for increases in the economiser inlet temperature. As more and more water is converted to steam the feedwater rate increases to maintain the collector tank level. A stage is reached where the feedwater rate no longer consists of circulating water. It is no longer necessary to remove water from the collecting vessels to maintain a specific level. At this stage all feedwater is condensate. The water level controller in the collecting tanks is then removed from service, the circulating pumps shut down and the water level is allowed to fall away as the rate of evaporation increases.

3.3.2 THE TRANSFER OF CHEMICAL ENERGY TO THE STEAM

Air and coal are thoroughly mixed on entering the boiler ensuring even combustion. The combustion chamber is fed by six levels of burners. There are four burners per level (FIGURE 3.7). The chamber itself is divided into two sections each half of which is fed by twelve burners. Unburnt coal and ash is either carried upwards by convection or falls downward to be removed by sluice water in the bottom of the furnace. Combustion of the coal must be confined to the furnace. Unburnt coal or "sparklers" carried onto the tube banks above the combustion chamber directly results in high metal temperatures and may result in slag forming on the tube banks or on the side walls. Thermal efficiency is reduced, hot spots occur and falling klinker may do damage to surfaces below.

The flame requires careful control if the necessary results are to be achieved without damage occurring. The three main parameters affecting the flame condition are:-

i) the time taken for particles to burn
ii) the flame temperature
iii) the turbulance of the air/coal mixture.

These parameters depend on another list of factors:-

1) The flow rate of the fuel entering the furnace:

This determines how close to the nozzle combustion takes place. Low velocities can cause nozzle damage. It is not always possible to simply reduce flow rates of all mills in operation if individual flow rates drop too low.

2) The volatile content of the fuel:

Fuel of a low volatile content, results in a long time required for combusion and hence a longer duller flame. Fuel of a high volatile content requires less combustion time and has a short bright flame.

3) The fineness of the fuel:

Should the mill feed rate be too low excessively fine powder results. This increases the chances of explosions in the feed pipes and in the mill. Too coarse a fuel results in "sparklers" within the furnace being carried upwards into the convection zone by the flue gases.

4) Insufficient secondary air pressure:

Too little air results in not enough oxygen being supplied to allow the coal to burn to completion. Too much oxygen results in large dry flue gas heat loses. Fluctuations in the secondary air pressure directly affect the air/fuel ratio (point 7).

5) Incorrect swirl vane settings:

If insufficient turbulance exists to mix the secondary air and the pulverised fuel mixture then incomplete combustion may result. Too much turbulance produces a very ragged flame. Either condition can lead to instability of the flame.

stion air temperature:

To ow a combustion temperature caused by cool secondary air, or too small a fire, results in flame chilling. The flames have ragged edges and unburnt particles are carried away by the flue gases. To prevent this, oil burners should be reignited if the flame temperature drops too low.

7) The Air/fuel ratio:

A rich fuel to air ratio causes puffing in the furnace or uneven combustion. This is strongly linked to swirl vane settings and secondary air pressure. Too weak a mixture results in flame chilling and high flue gas losses.

Most of the parameters mentioned above are those that usually fall within the operator's control. Certain factors do however change on a daily basis. These include volatile content, moisture, ash content and total calorific value of the supplied coal. A daily "proximate" analysis of the coal is done by the station chemist. This information is available to the operators. These parameters assist the operator in determining what the full load fuel flow rates will be and how to modify his control of the plant to deal with fluctuations in coal quality.

3.4 SUMMARY

The information presented in this chapter serves to form the background information necessary for latter chapters. The quantity of information about global aspects of unit operation is vast and earlier sections have attempted to provide the minimum necessary information. Further information is available in Babcock, (1955) and Central, (1971). More detailed information on the specific plant, in this case the Duvha Power Station boilers, can be found in ESCOM,(8); ESCOM, (9) and Hollis, (1982).

A second objective has been to emphasize the difficulty of determining firing effects, expecially as discussed in SECTION 3.3.2. This is the largest difficulty in determining system parameters and serves to verify the arguments for predictive control laid out in Chapter 2.

CHAPTER 4 THE TRANSFER FUNCTION AND STATE-SPACE MODELS

4.1 INTRODUCTION

In order to adequately predict changes in the first attemporator steam condition, an accurate mathematical model for the combustion chamber and heat transfer surfaces must be obtained. This work is particularly concerned with the effect of individual furnaces on the attemporator steam condition. For this reason it is essential to consider the energy available at each level within the furnace rather than considering the more macroscopic case of total energy inflow against total energy outflow. The latter approach is more usually considered. The energy supplied at each level of the boiler forms the most complicated aspect of this work. This aspect is further compounded by little published work being available on the effects of the individual burners on the boiler characteristics. The science of combustion is largely a black art and simple models for flames and the resulting radiation do not exist.

The uncertainty associated with the flames has been avoided by rather considering the energy transfers across the cell boundaries. All inputs, outputs and state variables were therefore chosen in terms of energy flow rates (J/s). The exception is the flue gas temperatures. The pressure of the flue gas remains close to 1 atmosphere. The temperatures may then be related to the energy flow rate with the use of gas tables (Keenan, 1983). All heat transfer from flue gases to side walls results from radiation and convection. Conduction is not considered as a significant heat transfer mechanism.

Steady-state equations for the heat transfer are shown in later sections of this Chapter. Radiation effects result in highly non-linear temperature relationships. These may be linearized using a Taylor series expansion. An alternative approach which uses least squared interpolating technique is suggested in Appendix A.

CHAPTER 4 THE TRANSFER FUNCTION AND STATE-SPACE MODELS

The sources of energy available at each level can be listed as energy due to:

i) Secondary airflow
ii) Coal flow rate
iii) Convection airflow
iv) Re-radiation of energy back to furnace from side walls.

This energy is then available for heat transfer to:

i) The division wall
ii) The screw wall and upper part
iii) The tube banks, economiser, superheaters and reheaters.
iv) The airheaters
v) The boiler exhaust gases

This chapter is concerned with energy transferred to the division wall, screw wall and upper part. The other energy absorbing surfaces are not considered since they occur after the first attemporator in the steam cycle.

Two models for the combustion chamber and heat transfer surfaces are to be obtained. These are:

i) The transfer function model
ii) The state-space model

The chapter continues by defining the basis for these models. The steady-state energy transfer equation is investigated. This assists in the understanding of the two models which are described later in the Chapter. Chapter 5 explains how the model paramaters may be obtained.

4.2 A LIST OF NECESSARY PARAMETERS

F_{ci} : i = 2 to 7 ;	The mass flow rate of coal for all 4 burners in the i'th cell	;	kg/s
F_{oi} : i = 2 to 7 ;	The mass flow rate of the oil in the i'th cell	;	kg/s
A/f :	A ratio of the air to fuel (volumetric)	;	-

T_s :	; The secondary air duct temperature which is assumed the same for all levels	;	^oC
A_{si} : i = 1 to 9	; The surface area of the screw wall and upper part heat transfer surfaces in the i'th cell. Note that A_{s2} to A_{s7} are equal	;	m^2
A_{di} : i = 1 to 9	; The surface area of the division wall heat transfer surfaces in the i'th cell. Again A_{d2} to A_{d7} are equal	;	m^2
H_i : i = 1 to 9	; The total energy flow rate at the centre of the i'th cell	;	J/s
Q_{si} : i = 1 to 9	; The energy absorbed by the i'th cell evaporator surface per second	;	J/s
Q_{di} : i = 1 to 9	; The energy absorbed by the i'th cell division wall surface per second	;	J/s
Q_{ai} ; i = 1 to 9	; The energy carried away from the i'th cell by convection air flow per second	;	J/s
E_{si} : i = 1 to 9	; The energy re-radiated from the i'th cell wall of the evaporartor per second	;	J/s
E_{di} : i = 1 to 9	; The energy re-radiated from the i'th cell wall of the division wall per second	;	J/s
T_i : i = 1 to 9	; The temperature at the core of the i'th cell	;	^oC
θ_{si} : i = 1 to 9	; The surface temperature of the evaporator absorbing surface of the i'th cell	;	^oC
θ_{di} : i = 1 to 9	; The surface temperature of the division wall absorbing surface of the i'th cell	;	^oC
c_c :	; Calorific value of coal	;	J/kg
c_o :	; Calorific value of oil	;	J/kg
c_a :	; Specific heat of secondary air assuming constant pressure	;	$J/kg.K^{-1}$
p_a :	; Density of secondary air	;	kg/m^3
p_c :	; Density of coal	;	kg/m^3

T_s :	; The secondary air duct temperature which is assumed the same for all levels	;	^{o}C
A_{si} : i = 1 to 9	; The surface area of the screw wall and upper part heat transfer surfaces in the i'th cell. Note that A_{s2} to A_{s7} are equal	;	m^2
A_{di} : i = 1 to 9	; The surface area of the division wall heat transfer surfaces in the i'th cell. Again A_{d2} to A_{d7} are equal	;	m^2
H_i : i = 1 to 9	; The total energy flow rate at the centre of the i'th cell	;	J/s
Q_{si} : i = 1 to 9	; The energy absorbed by the i'th cell evaporator surface per second	;	J/s
Q_{di} : i = 1 to 9	; The energy absorbed by the i'th cell division wall surface per second	;	J/s
Q_{ai} ; i = 1 to 9	; The energy carried away from the i'th cell by convection air flow per second	;	J/s
E_{si} : i = 1 to 9	; The energy re-radiated from the i'th cell wall of the evaporartor per second	;	J/s
E_{di} : i = 1 to 9	; The energy re-radiated from the i'th cell wall of the division wall per second	;	J/s
T_i : i = 1 to 9	; The temperature at the core of the i'th cell	;	^{o}C
θ_{si} : i = 1 to 9	; The surface temperature of the evaporator absorbing surface of the i'th cell	;	^{o}C
θ_{di} : i = 1 to 9	; The surface temperature of the division wall absorbing surface of the i'th cell	;	^{o}C
c_c :	; Calorific value of coal	;	J/kg
c_o :	; Calorific value of oil	;	J/kg
c_a :	; Specific heat of secondary air assuming constant pressure	;	$J/kg.K^{-1}$
ρ_a :	; Density of secondary air	;	kg/m^3
ρ_c :	; Density of coal	;	kg/m^3

S_{si}	: i = 1 to 9 ;	Steam/water enthalpy flow rate at the output of i'th evaporator cell	; J/s
S_{so}	: ;	Enthalpy flow rate at the input to the first evaporator cell	; J/s
S_{di}	: i = 1 to 9 ;	Water enthalpy flow rate at output of i'th division wall cell	; J/s
S_{do}	: ;	Enthalpy flow rate at the input to the first division wall cell	; J/s
	: ;	Stefan-Boltzmann Constant for heat equation	; $Js^{-1}m^{-2}K^{-4}$
H_{ri}	: i = 1 to 9 ;	Energy available in the i'th cell for absorbtion after heating the air flow per second	; J/s
U_{si}	: ;	Temperature of the evaporator steam in the i'th cell	; ^{o}C
U_{di}	: ;	Temperature of the divisic wall steam in the i'th cell	; ^{o}C

4.3 THE DIVISION OF THE BOILER INTO CELLS

The flow diagram for the boiler unit considered is given in FIGURE 4.1.

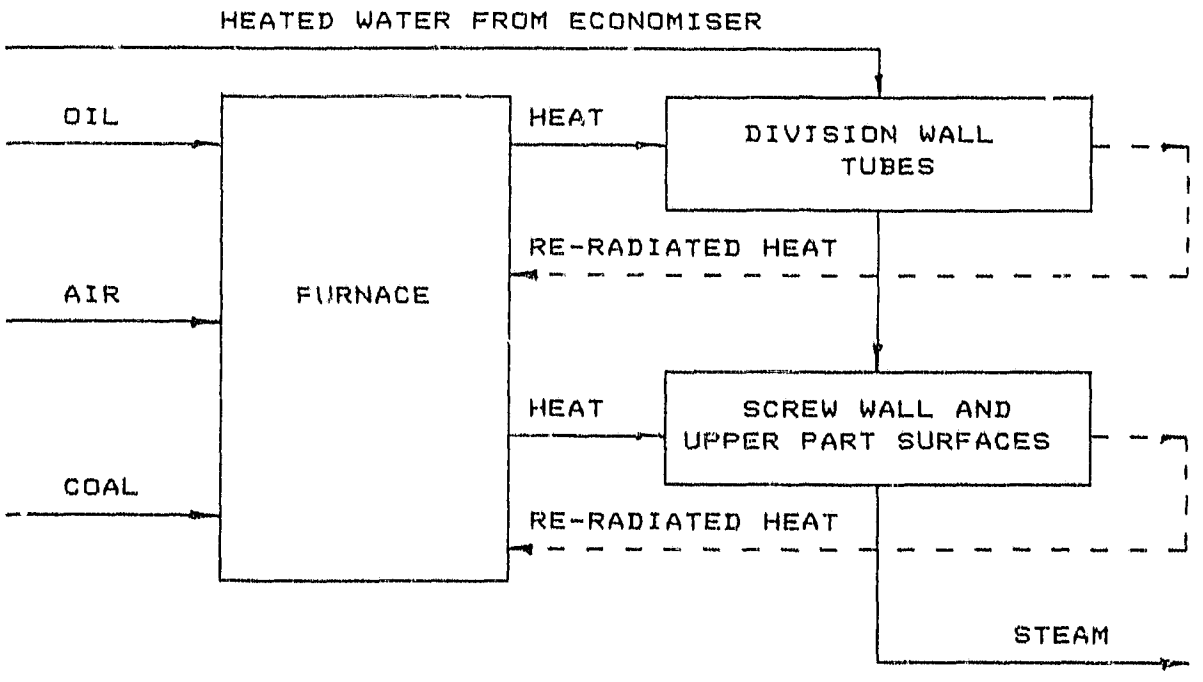


FIGURE 4.1: THE BOILER UNIT SHOWING THE SUB-UNITS OF INTEREST

The success of this model (FIGURE 4.1) depends on the number of cells making up the division wall and evaporator units. A single heat output from the furnace to the heat absorbing surfaces ignores a great deal of information. It does not consider the effect of different firing rates at different levels on the output. Instead an evenly distributed firing rate is assumed.

In the single output furnace model two extreme cases may be noted. Fire may be applied near the top of the furnace. This will result in the steam output responding with virtually no delay. Fire applied at the bottom of the furnace will result in a far greater delay since the steam affected must first rise through the sidewall. Changes in steam condition are detected at the outlet. Since the total heat available is transferred as a single entity, in the model of FIGURE 4.1, this detail is lost.

Dividing the division wall and screw wall into sections leads to the logical continuation shown in FIGURE 4.2. Here the whole boiler is divided into cells. This must obviously include division of the furnace into corresponding cells. For convenience nine cells are used. Eight of these are within the combustion chamber. This was thought to be a fair cell division since eighty per cent of the available energy is radiated in the combustion chamber.

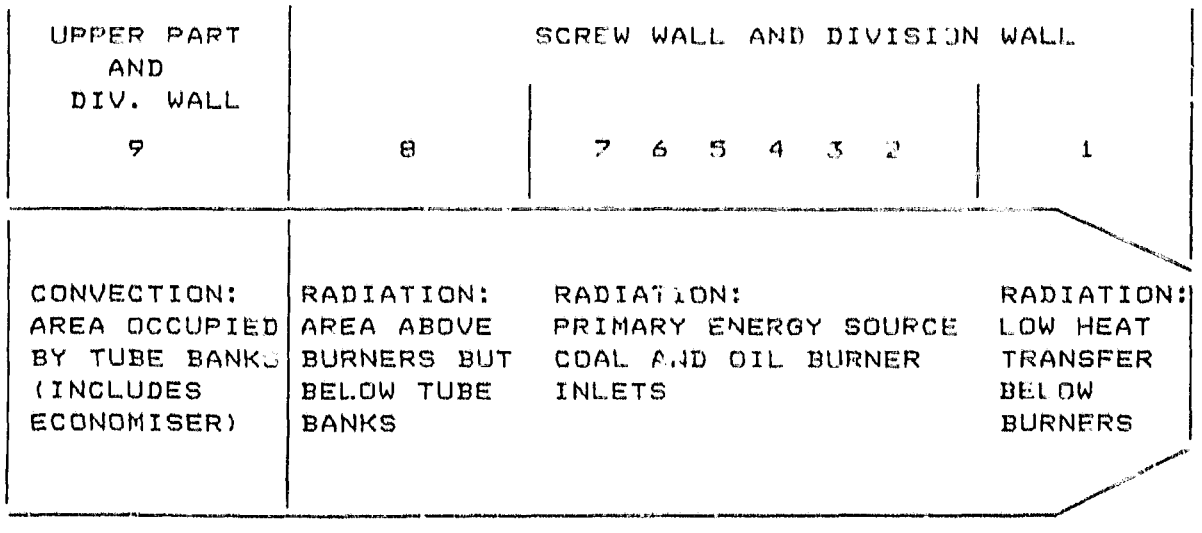


FIGURE 4.2: THE PHYSICAL DIVISION OF THE BOILER INTO CELLS

Six of these eight levels correspond to burner levels. The area above the burners, cell 8, is likely to receive a fair amount of radiation from the top burner level as well as heating effects from convection flow. Cell 1 below the lowest burner only receives radiation. The heat absorbed by this cell may be sufficiently small to allow it to be combined with cell 2 or ignored.

Cells 1 through to 9 contain both evaporator and division wall heating surfaces. The ratio of the radiated energy absorbed by the division wall and the evaporator is assumed to be in direct proportion to their respective areas.

$$\frac{Q_{di}\text{(Division wall)}}{Q_{si}\text{(Evaporator)}} = \frac{A_{di}\text{(Division wall)}}{A_{si}\text{(Evaporator)}} \quad \text{(4.1)}$$

for i = 1 to 9.

From the geometry of the boilers installed at Duvha Power Station the assumption can be made that:

$$\frac{A_{di}\text{(Division wall)}}{A_{si}\text{(Evaporator)}} = \frac{\sum_{i=1}^{9} A_{di}\text{(Total division wall area)}}{\sum_{i=1}^{9} A_{si}\text{(Total evaporator area)}}$$

$$= \frac{2207m^2}{5482m^2} = 0,4026 \quad \text{(4.2)}$$

Equation 4.1 uses the total radiated energy for both halves of the furnace and the total absorbing surface area for both halves of the furnace. Each half of the furnace is assumed to behave identically at any moment in time.

Each of the nine cells defined may be further broken down into constituent models. The form for each cell model is shown in FIGURE 4.3. This model has the same basis for all cells but will not have all the inputs at all levels.

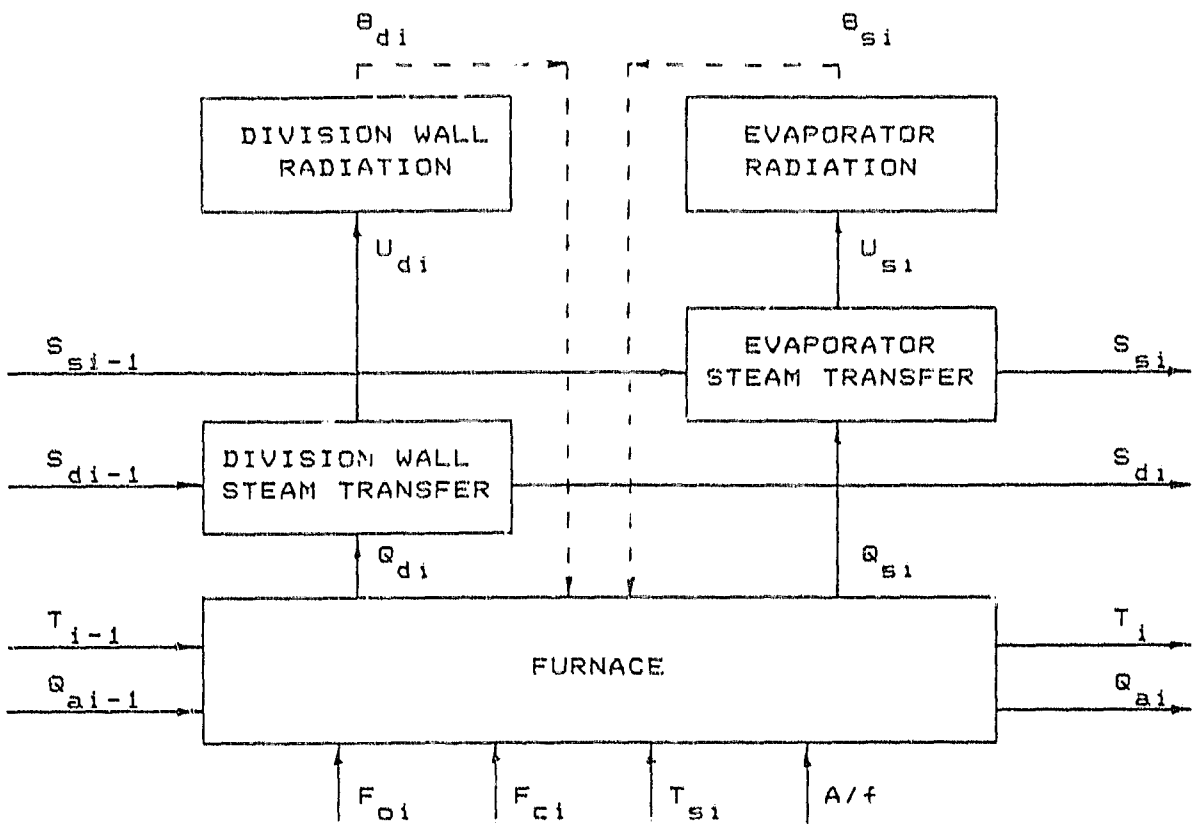


FIGURE 4.3: THE BLOCK DIAGRAM OF THE MODEL FOR THE I'TH CELL

4.3.1 THE ENERGY TRANSFER TO THE CELL

The cell model (FIGURE 4.3) attempts to represent all the energy transfers across the physical boundaries of each cell. A typical cell is considered. Energy to this cell is available from sources already listed in SECTION 4.1. The actual parameters may now be explained.

4.3.1.1 THE ENERGY DUE TO THE SECONDARY AIR FLOW

The energy available is a function of the coal flow rate F_{ci}, the air temperatures and the air fuel ratio A/f. The mass flow rate of the air is obtained from knowledge of the volumetric air/fuel ratio as well as the coal mass flow rate. Three assumptions are made in connection with the secondary air flow.

a) $\dot{m}_o$, the oil flow rate has not been included in the calculation for air flow. If no coal

is being fed to the furnace then no air is assumed to flow. The justification for this assumption is that when only oil burners are in operation the secondary air temperature will be low.

The air has not been well heated since the air heater bypass is open during early firing stages. It is assumed that this low temperature results in little energy fed to the boiler by secondary air flow. A more significant implication is that there is no air available for convection flow and convection heat transfer. All energy is assumed to be radiated to the side walls.

b) Bias controls allow the operators to adjust the air to fuel mixtures at each level according to conditions existing at that level. Worn mill parts or a coarser coal mixture require a higher air to fuel ratio. This model assumes that the air/fuel ratio is the same at all levels. This is considered a fair assumption since bias controls cause only small deviations from the average. The combined effect of the bias controls must also yield the average air to fuel ratio.

c) Primary air supplied to the mill is normally heated to 400^{o}C. The pulverised fuel mixture of roughly 1 part coal to 1.4 parts air has a temperature ranging from 50^{o}C to 150^{o}C. The hot primary air removes moisture from the coal. The final air to fuel ratio contains approximately five times more air than is accounted for by the primary air flow. This is made up of secondary air with a temperature ranging from 150^{o}C to 350 ^{o}C. The assumption is made that all air, secondary and primary, is supplied at the secondary air temperature T_s . The energy

excess resulting from this assumption is 12% at full load.

4.3.1.2 THE ENERGY DUE TO THE OIL FLOW

The total flow rate per burner level is 1,02 ton per hour. The mass rate of oil flow F_{oi} has one of three settings, zero, 60% of full power and full power. Oil firing at all of the six levels is equivalent to ± 10% of the firing rate.

4.3.1.3 THE ENERGY DUE TO THE COAL FLOW

The mass flow rate of the coal is assumed to be directly proportional to the energy produced by burning. The constants of proportionality do however change with differences in moisture and ash content. The maximum fuel mass flow rate is therefore a function of the coal quality. The maximum flow rate corresponds to 600 MW divided by the number of mills in use at full load (4 or 5).

4.3.1.4 THE ENERGY DUE TO THE CONVECTION AIR FLOW

The energy in the rising air stream is Q_{ai-1}. This is a function of the total amount of air flowing into the furnace at all levels below the i'th level and of the previous cells core temperature. If a fire exists at the i'th level energy from the flame will have to be supplied to heat the rising flue gases thus increasing the convection flow energy. The rising air temperature T_{i-1} must be known to calculate how much energy the convection air removes and therefore how much energy remains for radiation.

4.3.1.5 THE ENERGY DUE TO THE RE-RADIATED ENERGY

Some levels in the furnace do not have fuel supplied to them. In particular level 9 in the

convection section of the furnace may have a sufficiently low temperature to make it necessary to consider re-radiation. If the water/steam in the division wall and evaporator is hot enough the side wall surfaces may radiate energy to the convection air flow. The typical temperatures at the top of the division wall and the evaporator are 330^{o}C and 390^{o}C respectively under full load conditions. The flue gas temperature at the exit from the furnace is 390^{o}C at ful' load. The temperature differences are small and hence the re-radiation of energy is considered a minor effect Omission of this source of energy flow within the cell allows the division wall and evaporator models to be considered separately.

4.3.2 ENERGY TRANSFER AWAY FROM THE CELL

The boiler unit itself is a remarkably efficient heat machine converting 94% of the available energy described above into steam energy. The heat absorbing surfaces making use of this available energy were listed in SECTION 4.1. Further information is provided below.

4.3.2.1 THE DIVISION WALL

FIGURE 3.7 shows how the division wall divides the boiler into two halves. These vertically rising tubes receive radiation from both halves of the combustion chamber. The purpose of the division wall is to raise the water temperature sufficiently to allow total evaporation to occur in the evaporator. The total surface area available for heat absorbtion is 220? m.^{2} The wall is designed to absorb 141,4 kJ/m^{2}s or 312 MJ/s at full load. Under these conditions the steam temperature is raised to 330^{o}C from 305^{o}C at full load.

The division wall surface is of considerable importance to the chosen model. It accounts for about 30% of the energy absorbed by the model shown in FIGURE 4.1. For the purpose of this model cells 2 to 7, as defined in FIGURE 4.2, are assumed to have identical heat absorbing properties.

4.3.2.2 THE SCREW WALL AND THE UPPER PART

In the combustion chamber the steam tubes are arranged in a helical spiral, called the screw wall, which provides an effective surface area of 3621 m^2. These spiralling tubes feed into the vertically rising tubes of the upper part (1861 m^2) which is in the convection zone of the boiler. The combined surfaces make up the evaporator (5482 m^2). They are capable of absorbing 513 MJ/s at full load and heat the water from 330 ^{o}C to 390 ^{o}C. The purpose of these surfaces is to raise the enthalpy of the water such that total evaporation of the water occurs. The majority of the available energy is used in the direct conversion of water to superheated steam. At lower loads direct conversion does not occur. The steam at the top of the evaporator may then be saturated.

The evaporator accounts for the remaining 70% of energy absorbed by the considered model. It is the output or the steam condition at the top of the evaporator that is of interest since this is the critical steam temperature at the inlet to the first steam attemperator (FIGURES 3.6 and 3.8; SECTION 2.2.3). As with the division wall cells 2 to 7 are assumed to have identical heat absorbing properties.

4.3.2.3 THE TUBE BANKS

The first of four superheater banks receives radiation from the combustion chamber. All the other tube banks extract energy from the flue

gases flowing over their surface. This occurs in the convection area of the furnace. Steam reheating for the intermediate turbine stages occurs in this region as does pre-warming of the water fed to the division wall.

All the above mentioned heat transfer surfaces remove energy from the flue gases and hence have an effect on the 9th and uppermost cell in the model. The model does not consider this heat absorbtion. A compromise is made by considering the temperature measured below the economiser instead of considering the temperature measured above the economiser. This higher temperature attempts to offset the energy absorbed by the tube banks (SECTION 6.4.1). Some justification can be found in the fact that 80% of the energy available in the furnace is radiated. Only 20% is transferred by convection.

4.3.2.4 THE AIR HEATERS

After the flue gas has passed through the convection section of the boiler it is drawn through the airheater which heats the primary and secondary air flows. The primary air is heated to 350 ^{O}C. This air is used to carry pulverised coal to the furnace. The secondary air is heated to 285^{O}C and provides sufficient oxygen to the furnace to ensure that combustion occurs to completion. The energy transfer of the airheater is not considered in the model. The secondary air temperature is considered but this is measured directly.

4.3.2.5 THE BOILER EXHAUST GASES

The balance of the energy is lost to the precipitators and to the stack. This is not considered worth recovering and amounts to 6% of the available energy. Hot ash carried by the

flue gas is removed by electrostatic plates and the 'clean air' is vented to the atmosphere. Further heat extraction is not desirable due to sulphuric acid forming in the air heaters if the flue gas temperature falls below a critical temperature.

4.3.3 SUMMARY

A division of the boiler sections of concern has been suggested. The variables and constants to be used have been listed. The energy flow across cell boundaries has been discussed with reference to the selected variables. It is now possible to consider various ways in which the variables may be related. A steady-state analysis can be performed based on the energy flows discussed after which transfer function and state-space models are suggested.

4.4 THE STEADY STATE HEAT TRANSFER EQUATION FOR THE I'TH CELL

The total energy flow rate at the centre of the i'th cell, H_i, is the sum of energy resulting from

i) the coal flow rate ; F_{ci}

ii) the oil flow rate ; F_{oi}

iii) the secondary air temperature ; T_s

iv) the convection heat energy flow rate from the previous level ; Q_{ai-1}

v) the re-radiated heat flow rate from the evaporator surfaces ; E_{si}

vi) the re-radiated heat flow rate from the division wall surfaces ; E_{di}

An equation for H_i in terms of these variables can now be derived (Holman, 1980 and Pitts, 1977 were used to provide the necessary thermodynamic and heat transfer background). The assumption is made that the energy supplied from air, which is necessary when only the oil burners are in operation, is negligible. This

assumption is valid since the secondary air temperature T_s is sufficiently low and only starts to rise once the air heaters are brought into operation.

$$H_1 = F_{c1}\ c_c + F_{d1}\ T_{d1} + \frac{A/f\ F_{c1}\ p_a\ c_a\ T_s}{p_c} + Q_{ai-1} + E_{s1} + E_{d1} \qquad (4.3)$$

The 3rd term of H_1 contains a non-linear function of A/f, F_{c1} and T_s. A Taylor linearization of this term yields:

$$A/f\ F_{c1}\ T_s = \hat{A/f}\ \hat{F}_{c1}\ \hat{T}_s + \hat{F}_{c1}\ \hat{T}_s\ (A/f - \hat{A/f}) + \hat{A/f}\ \hat{T}_s\ (F_{c1} - \hat{F}_{c1}) + \hat{A/f}\ \hat{F}_{c1}\ (T_s - \hat{T}_s) \qquad (4.4)$$

The variables with a tilde refer to the point about which the linearization takes place.

A hat on the variable refers to the difference between the actual variable and its tilde value ($\hat{T}_s = T_s - \tilde{T}_s$).

The 4th, 5th and 6th terms of equation (4.3) can be defined further.

$$Q_{ai-1} = \frac{A/f\ p_a\ c_a\ (F_{c1} + F_{c2} \ldots + F_{c1-1})\ T_{i-1}}{p_c} \qquad (4.5)$$

Equation (4.5) can also be linearized in the same way as equation (4.4).

$$Q_{ai-1} = \frac{p_a\ c_a}{p_c}\{\tilde{A/f}(\tilde{F}_{c1}+\tilde{F}_{c2}+\tilde{F}_{c1-1})\tilde{T}_{i-1} + (\hat{F}_{c1}+\hat{F}_{c2}+\hat{F}_{c1-1})\tilde{T}_{i-1}\hat{A/F} + \tilde{A/f}\ \tilde{T}_{i-1}(\hat{F}_{c1}+\hat{F}_{c2}\ldots+\hat{F}_{c1-1}) + \tilde{A/f}(\hat{F}_{c1}+\hat{F}_{c2}\ldots\hat{F}_{c1-1})\hat{T}_{i-1}\} \qquad (4.6)$$

$$E_{si} = A_{si}\ \sigma\ \theta_{si}^4 \qquad (4.7)$$

$$E_{di} = A_{di}\ \sigma\ \theta_{di}^4 \qquad (4.8)$$

Black body radiation has been assumed in equations (4.7) and (4.8). Linearization of θ_s and θ_d over the range θ_{s1} to θ_{s2} and θ_{d1} to θ_{d2} is performed using method two in Appendix A. This yields:

$$E_{si} = A_{si}\,\sigma(m_s\theta_{si} + c_s) \qquad (4.9)$$

$$E_{di} = A_{di}\,\sigma(m_d\theta_{di} + c_d) \qquad (4.10)$$

If the variables F_{ci}, F_{oi}, θ_{si} and θ_{di} are transferred to their difference values $\hat{F}_{ci}$, $\hat{F}_{oi}$, $\hat{\theta}_{si}$ and $\hat{\theta}_{di}$ then the following equation for H_i is obtained:

$$H_i = K_{1i}' + K_{2i}'\,\hat{F}_{ci} + K_{3i}'\,(\hat{F}_{ci-1} + \ldots\hat{F}_{c2} + \hat{F}_{c1}) + K_{4i}'\,\hat{F}_{oi} + K_{5i}'\,\hat{A/f} + K_{6i}'\,\hat{T}_s + K_{7i}'\,\hat{T}_{i-1} + K_{8i}'\,\hat{\theta}_{si} + K_{9i}'\,\hat{\theta}_{di} \qquad (4.11)$$

Where

$$K_{1i}' = \tilde{F}_{ci}c_c + \tilde{F}_{oi}c_o + \frac{p_a c_a \tilde{A/f}}{p_c}\{(\tilde{F}_{c1}+\tilde{F}_{c2}\ldots+\tilde{F}_{ci-1})\tilde{T}_{i-1} + \tilde{F}_{ci}\,\tilde{T}_s\} + A_{si}\,\sigma(m_s\tilde{\theta}_{si} + c_s) + A_{di}\,\sigma(m_d\tilde{\theta}_{di} + c_d)$$

$$K_{2i}' = c_c + \frac{p_a c_a}{p_c}\tilde{A/f}\,\tilde{T}_s$$

$$K_{3i}' = \frac{p_a c_a}{p_c}\tilde{A/f}\,\tilde{T}_{i-1}$$

$$K_{4i}' = c_o$$

$$K_{5i}' = \frac{p_a c_a}{p_c}(\tilde{F}_{c1} + \tilde{F}_{c2} + \ldots\tilde{F}_{ci-1})\,\tilde{T}_{i-1} + \tilde{F}_{ci}\,\tilde{T}_s)$$

$$K_{6i}' = \frac{p_a c_a}{p_c}\tilde{A/f}\,\tilde{F}_{ci}$$

$$K_{7i}' = \frac{p_a c_a}{p_c} A\tilde{/}f \; (\tilde{F}_{c1} + \hat{F}_{c2} + .. \tilde{F}_{c1-1})$$

$$K_{8i}' = A_{s1} \sigma \; m_s$$

$$K_{9}' = A_{d1} \sigma \; m_d$$

The total heat available, at the cell core, for heat exchange must equal the radiated energy, and the convection air energy.

$$H_1 = Q_{d1} + Q_{s1} + Q_{a1} \qquad (4.12)$$

Since Q_{d1} and Q_{s1} represent absorbed radiated energy the heat radiation equation could be applied. This is no considered because of the lack of knowledge concerning combustion and because of the continual variation of the coal quality. These two uncertainties make it very difficult to determine the effective radiating surface area of the flame and the ef ective radiating temperature of the coal. Instead it is preferable to re-arrange equation (4.12) bearing in mind equation (4.1).

$$Q_{d1} = \left\{1 + \frac{A_{s1}}{A_{d1}}\right\}^{-1} (H_1 - Q_{a1}) \qquad (4.13)$$

$$Q_{s1} = \left\{1 + \frac{A_{d1}}{A_{s1}}\right\}^{-1} (H_1 - Q_{a1}) \qquad (4.14)$$

Q_{a1} is obtained directly from equation (4.6)

$$Q_{a1} = \frac{p_a c_a}{p_c} \left(A\tilde{/}f \; \tilde{T}_1 \sum_{j=1}^{1} \tilde{F}_{cj} + \hat{T}_1 \sum_{j=1}^{1} \hat{F}_{cj} \; A\hat{/}f \right.$$

$$\left. + A\tilde{/}f \; \tilde{T}_1 \sum_{j=1}^{1} \hat{F}_{cj} \; A\tilde{/}f \sum_{j=1}^{1} \tilde{F}_{cj} \; \hat{T}_1 \right) \qquad (4.15)$$

The expressions (4.13) and (4.14) may be simplified by combining (4.11) and (4.15) to give H_{ri} the net energy

available for radiation after the convection air flow has been heated. At this stage E_{d1} and E_{s1} are dropped from the steady-state equations (SECTION 4.3.1.5).

$$H_{ri} = H_i - Q_{ai}$$

$$H_{ri} = K_{1i}'' + K_{2i}'' \hat{F}_{ci} + K_{3i}'' \sum_{j=1}^{i-1} \hat{F}_{cj} + K_{4i}'' \hat{F}_{oi} + K_{5i}'' A\tilde{f} + K_{6i}'' \hat{T}_s + K_{7i}'' \hat{T}_{i-1} + K_{8i}'' \hat{T}_i \qquad (4.16)$$

where

$$K_{1i}'' = \hat{F}_{ci} c_c + F_{oi} c_o + \frac{p_a c_a}{p_c} A\tilde{f} \left(\sum_{j=1}^{i} \hat{F}_{cj} (\hat{T}_{i-1} - \hat{T}_i) + \tilde{F}_{ci} (\hat{T}_s - \hat{T}_{i-1}) \right)$$

$$K_{2i}'' = c_c + \frac{p_a c_a}{p_c} A\tilde{f} (\tilde{T}_s - \hat{T}_i)$$

$$K_{3i}'' = \frac{p_a c_a}{p_c} A\tilde{f} (\hat{T}_{i-1} - \tilde{T}_i)$$

$$K_{4i}'' = c_o$$

$$K_{5i}'' = \frac{p_a c_a}{p_c} \left(\sum_{j=1}^{i} \tilde{F}_{cj} (\tilde{T}_{i-1} - \tilde{T}_i) + \hat{F}_{ci} (\tilde{T}_s - \tilde{T}_{i-1}) \right)$$

$$K_{6i}'' = \frac{p_a c_a}{p_c} A\tilde{f} \tilde{F}_{ci}$$

$$K_{7i}'' = \frac{p_a c_a}{p_c} A\tilde{f} \left(\sum_{j=1}^{i-1} \tilde{F}_{cj} \right)$$

$$K_{8i}'' = -\frac{p_a c_a}{p_c} A\tilde{f} \left(\sum_{j=1}^{i} \tilde{F}_{cj} \right)$$

The steady-state equation for the steam/water tube heat-transfer for the evaporator and division wall is now easily obtained. The change in enthalpy from input to

output may be related to the energy absorbed and the energy radiated (Re-radiated energy is not considered.).

$$S_{si} - S_{si-1} = Q_{si} \qquad (4.17)$$

$$S_{di} - S_{di-1} = Q_{di} \qquad (4.18)$$

The steady-state analysis of this section has enabled equation (4.16) to be derived. This equation relates the inputs, outputs and internal states of the i'th cell under steady-state conditions. The equation was derived from consideration of the heat balance within the i'th celland provides a means of verifying the models that are developed in the following two sections of this Chapter.

4.5 THE TRANSFER FUNCTION MODEL

4.5.1 THE STATEMENT OF THE MODEL PARAMETERS

Consider again the model shown in FIGURE 4.3. Justification for omitting the effects of re-radiation was given in SECTION 4.3.1.5. Two separate models may then be obtained, one for the division wall and the other for the evaporator. These are shown in FIGURE 4.4 a) and b).

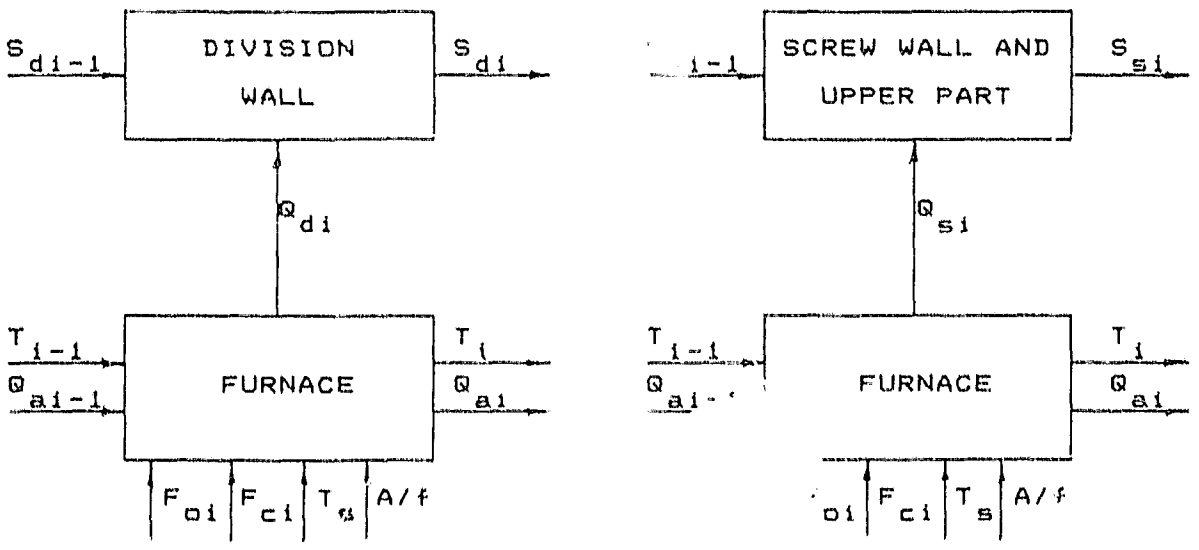
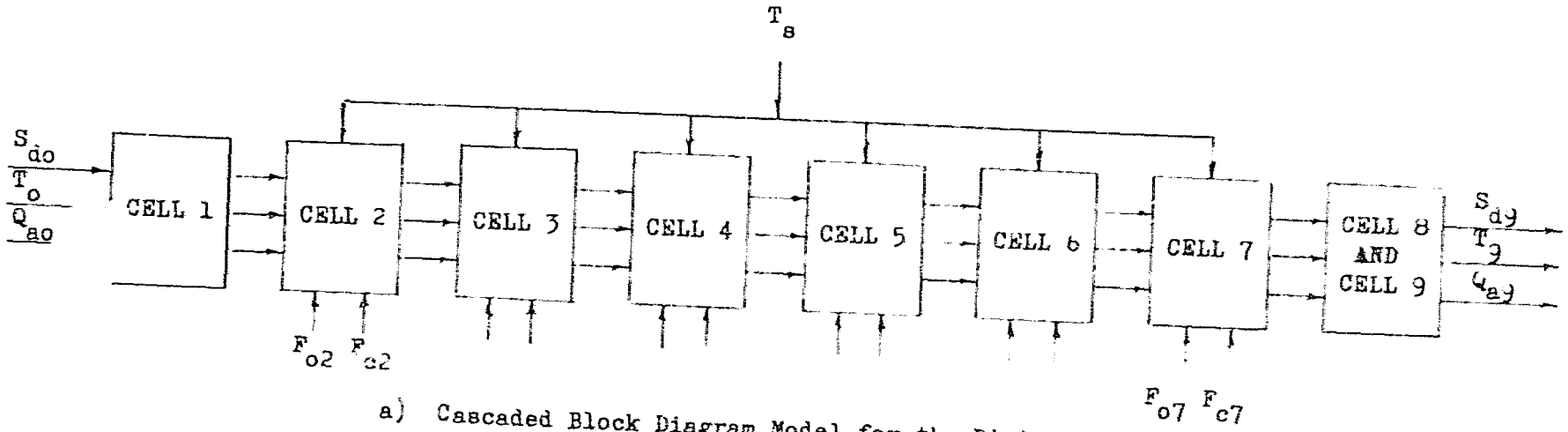
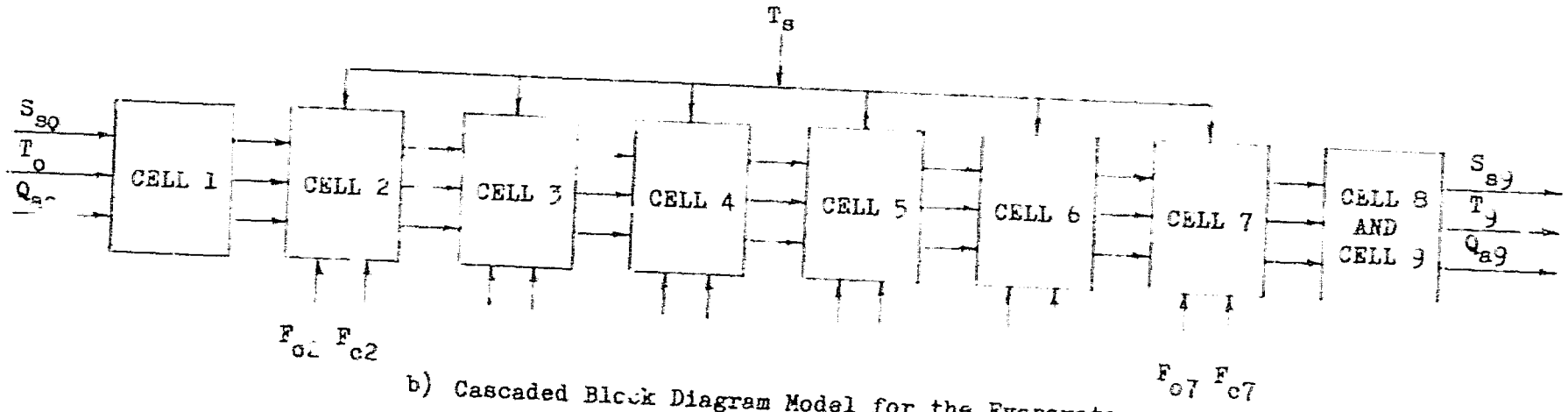


FIGURE 4.4: THE BLOCK DIAGRAM OF THE MODELS FOR THE EVAPORATOR AND THE DIVISION WALL



a) Cascaded Block Diagram Model for the Division Wall



b) Cascaded Block Diagram Model for the Evaporator

FIGURE 4.5 BLOCK DIAGRAM REPRESENTATION OF CASCADED MODELS

The cell models may be cascaded to form the unit input/output transfer function model. The cascaded model is shown in FIGURE 4.5 with all the relevant inputs and outputs. It is not possible to distinguish between cells 8 and 9 from the available data. They are therefore combined in this model. (FIGURE 4.5)

4.5.2 THE MODEL DEFINITION

The model for each cell has been defined in terms of its inputs and its outputs. Each input and output may be related by a transfer function. Since all the data is sampled the use of 'z' transform theory is necessary.

An initial global view of the cascaded cell model may be taken. Consider the outputs Q_{a9}, T_9, S_{s9}, S_{d9}. These are related to the inputs $F_{o2}..F_{o7}$, $F_{c2}..F_{c7}$, T_s, S_{so} and S_{do} as follows:-

$$Q_{a9} = G_a [F_{o2}...F_{o7}, F_{c2}...F_{c7}, T_s]^T \quad (4.19)$$

$$T_9 = G_t [F_{o2}...F_{o7}, F_{c2}...F_{c7}, T_s]^T \quad (4.20)$$

$$S_{s9} = G_s [F_{o2}...F_{o7}, F_{c2}...F_{c7}, T_s, S_{so}]^T \quad (4.21)$$

$$S_{d9} = G_d [F_{o2}...F_{o7}, F_{c2}...F_{c7}, T_s, S_{do}]^T \quad (4.22)$$

where

$G_a = (G_{a1}..... G_{a13})$ (1 x 13)

$G_t = (G_{t1}..... G_{t13})$ (1 x 13)

$G_s = (G_{s1}..... G_{s14})$ (1 x 14)

$G_d = (G_{d1}..... G_{d14})$ (1 x 14)

(Each element in G_a, G_t, G_s, G_d represents a single transfer function).

Data collected from the plant does not include the point S_{so} or S_{d9}. The complete model must then be obtained without reference to S_{so} or S_{d9}. This means

that Q_{a9}, T_9, S_{s9} must be found in terms of $F_{o2}\cdots F_{o7}$, $F_{c2}\cdots F_{c7}$, T_s and S_{do}.

Only S_{s9} is dependant on S_{so}. Equation (4.21) may be re-written as

$$S_{s9} = (G_{s1}\cdots G_{s13})\,(F_{o2}\cdots F_{o7}, F_{c2}\cdots F_{c7}, T_s)^T + G_{s14}\{(G_{d1}\cdots G_{d13}\,(F_{o2}\cdots F_{o7}, F_{c2}\cdots F_{c7}, T_s)^T + G_{d14}\,S_{do}\}$$

$$S_{s9} = \{(G_{s1}\cdots G_{s13}) + G_{s14}\,(G_{d1}\cdots G_{d13})\}\,(F_{o2}\cdots F_{o7}, F_{c2}\cdots F_{c7}, T_s)^T + G_{s14}\,G_{d14}\,S_{so}$$

$$= \{(G_{s1} + G_{s14}\,G_{d1}), (G_{s2} + G_{s14}\,G_{d2}) \cdots\cdots (G_{s14} + G_{s14}\,G_{d14})\}\,\{F_{o2}\cdots F_{o7}, F_{c2}\cdots F_{c7}, T_s, S_{do}\}^T \qquad (4.23)$$

Combining Q_{a9}, T_9 and S_{s9} gives:-

$$\begin{Bmatrix} Q_{a9} \\ T_9 \\ S_{s9} \end{Bmatrix} = \begin{bmatrix} G_{a1} & \cdots\cdots & G_{a13} & 0 \\ G_{t1} & \cdots\cdots & G_{t13} & 0 \\ (G_{s1} + G_{s14}\,G_{d1}) & \cdots\cdots & (G_{s13} + G_{s14}\,G_{d13}) & (G_{s14} + G_{s14}\,G_{d14}) \end{bmatrix} \begin{Bmatrix} F_{o2} \\ \vdots \\ F_{o7} \\ F_{c2} \\ \vdots \\ F_{c7} \\ T_s \\ S_{do} \end{Bmatrix} \qquad (4.24)$$

Similarly a matrix can be formed relating Q_{a7}, T_7 and S_{s7} to the same inputs

$$\begin{Bmatrix} Q_{a7} \\ T_7 \\ S_{s7} \end{Bmatrix} = \begin{bmatrix} G'_{a1} & \cdots\cdots & G'_{a13} & 0 \\ G'_{t1} & \cdots\cdots & G'_{t13} & 0 \\ (G'_{s1} + G'_{s14}\,G_{d1}) & \cdots\cdots & (G'_{s13} + G'_{s14}\,G_{d13}) & (G'_{s14} + G'_{s14}\,G_{d14}) \end{bmatrix} \begin{Bmatrix} F_{o2} \\ \vdots \\ F_{o7} \\ F_{c2} \\ \vdots \\ F_{c7} \\ T_s \\ S_{do} \end{Bmatrix} \qquad (4.25)$$

In a similar manner the [illegible] outputs of each cell can be related by a transfer function model

$$W_{ai} = f_{ai}(\ldots, F_{oi}, F_{ci}, Q_{ai-1}, T_{i-1}) \quad (4.26)$$

$$T_i = f_{ti}(\ldots, F_{oi}, F_{ci}, Q_{ai-1}, T_{i-1}) \quad (4.27)$$

$$S_{si} = f_{si}(\ldots, F_{oi}, F_{ci}, Q_{ai-1}, T_{i-1}, S_{si-1}) \quad (4.28)$$

$$S_{di} = f_{di}(\ldots, F_{oi}, F_{ci}, Q_{ai-1}, T_{i-1}, S_{di-1}) \quad (4.29)$$

where:

$$g_{ai} = (g_{ai1} \ldots\ldots\ldots g_{ai5}) \quad (1 \times 5)$$

$$g_{ti} = (g_{ti1} \ldots\ldots\ldots g_{ti5}) \quad (1 \times 5)$$

$$g_{si} = (g_{si1} \ldots\ldots\ldots g_{si6}) \quad (1 \times 6)$$

$$g_{di} = (g_{di1} \ldots\ldots\ldots g_{di6}) \quad (1 \times 6)$$

Each element in g_{ai}, g_{ti}, g_{si} and g_{di} represents a single transfer function.

It is more convenient to express the cell model in the following form:

The division wall cell model:

$$\begin{Bmatrix} Q_{ai} \\ T_i \\ S_{di} \end{Bmatrix} = \begin{Bmatrix} g_{ai1} \\ g_{ti1} \\ g_{di1} \end{Bmatrix} T_s + \begin{Bmatrix} g_{ai2} & g_{ai3} \\ g_{ti2} & g_{ti3} \\ g_{di2} & g_{di3} \end{Bmatrix} \begin{Bmatrix} F_{oi} \\ F_{ci} \end{Bmatrix} + \begin{Bmatrix} g_{ai4} & g_{ai5} & 0 \\ g_{ti4} & g_{ti5} & 0 \\ g_{di4} & g_{di5} & g_{ti6} \end{Bmatrix} \begin{Bmatrix} Q_{ai-1} \\ T_{ai-1} \\ S_{di-1} \end{Bmatrix} \quad (4.30)$$

The evaporator cell model:

$$\begin{Bmatrix} Q_{ai} \\ T_i \\ S_{si} \end{Bmatrix} = \begin{Bmatrix} g_{ai1} \\ g_{ti1} \\ g_{si1} \end{Bmatrix} T_s + \begin{Bmatrix} g_{ai2} & g_{ai3} \\ g_{ti2} & g_{ti3} \\ g_{si2} & g_{si3} \end{Bmatrix} \begin{Bmatrix} F_{oi} \\ F_{ci} \end{Bmatrix} + \begin{Bmatrix} g_{ai4} & g_{ai5} & 0 \\ g_{ti4} & g_{ti5} & 0 \\ g_{si4} & g_{si5} & g_{si6} \end{Bmatrix} \begin{Bmatrix} Q_{ai-1} \\ T_{ai-1} \\ S_{di-1} \end{Bmatrix} \quad (4.31)$$

A new notation is now introduced to simplify equations (4.30) and (4.31). The new equations are:

The division wall cell model:

$$X_{di} = K_{di}\, X_{di-1} + H_{di}\, Y_i + F_{di}\, T_s \qquad (4.32)$$

The evaporator cell model:

$$X_{si} = K_{si}\, X_{si-1} + H_{si}\, Y_i + F_{si}\, T_s \qquad (4.34)$$

Where

$$X_{di} = (Q_{ai}, T_i, S_{di})^T \qquad X_{si} = (Q_{ai}, T_i, S_{si})^T$$

$$K_{di} = \begin{Bmatrix} g_{ai4} & g_{ai5} & 0 \\ g_{ti4} & g_{ti5} & 0 \\ g_{di4} & g_{di5} & g_{di6} \end{Bmatrix} \qquad K_{si} = \begin{Bmatrix} g_{ai4} & g_{ai5} & 0 \\ g_{ti4} & g_{ti5} & 0 \\ g_{si4} & g_{si5} & g_{si6} \end{Bmatrix}$$

$$H_{di} = \begin{Bmatrix} g_{ai2} & g_{ai3} \\ g_{ti2} & g_{ti3} \\ g_{di2} & g_{di3} \end{Bmatrix} \qquad H_{si} = \begin{Bmatrix} g_{ai2} & g_{ai3} \\ g_{ti2} & g_{ti3} \\ g_{si2} & g_{si3} \end{Bmatrix}$$

$$F_{di} = \begin{Bmatrix} g_{ai1} \\ g_{ti1} \\ g_{di1} \end{Bmatrix} \qquad F_{si} = \begin{Bmatrix} g_{ai1} \\ g_{ti1} \\ g_{si1} \end{Bmatrix}$$

$$Y_i = \begin{Bmatrix} F_{oi} \\ F_{ci} \end{Bmatrix}$$

At this stage it is worth recalling that

1) $F_{oi} = 0$ for $i < 2$ or $i > 7$

   $F_{ci} = 0$ for $i < 2$ or $i > 7$

2) cells 2 to 7 are assumed identical hence

   $K_{di} = K_{d7}$ for $i = 2$ to 7

   $K_{si} = K_{s7}$ for $i = 2$ to 7

   $H_{di} = H_d$ for $i = 2$ to 7

   $H_{si} = H_s$ for $i = 2$ to 7

   $F_{di} = F_d$ for $i = 2$ to 7

   $F_{si} = F_s$ for $i = 2$ to 7

3) the ratio of energy absorbed by the steam passing through the division wall and the evaporator, resulting from the inputs T_s, F_{oi} and F_{ci}, must equal the ratio of the division wall area to the evaporator area.

   $g_{di1} = \lambda\, g_{si1}$

   $g_{di2} = \lambda\, g_{si2}$

$$g_{di3} = \lambda\, g_{si3}$$

$$\lambda = 0.4 \quad \text{(Equation 4.2)}$$

4) $S_{so} = S_{d9}$. The steamenthalpy flow rate at the outlet from the division wall must equal the steam enthalpy flow rate at the input to the evaporator (FIGURE 3.8).

Cascading the division wall and evaporator cell models yields the following equations incorporating the above simplifications.

The division wall cascaded model:

$$X_{d9} = K_{d9}\, K_{d8} \left\{ K_{d7}^{6}\; K_{d1}\; X_{do} + \sum_{i=5}^{0} K_{d7}^{i}\; H_d\, Y_{7-i} \right.$$

$$\left. + (I - K_{d7}^{5})\,(I - K_{d7})^{-1}\; F_d\, T_s \right\} \qquad (4.35)$$

The evaporator cascaded model:

$$X_{s9} = K_{s9}\, K_{s8} \left\{ K_{s7}^{6}\, K_{s1}\, X_{so} + \sum_{i=5}^{0} K_{s7}^{i}\; H_s Y_{7-i} \right.$$

$$\left. +(I - K_{s7}^{5})\,(I - K_{s7})^{-1}\, F_s\, T_s \right\} \qquad (4.36)$$

Again since S_{so} is not available $S_{so} = S_{d9}$ must be eliminated from the equations.

This yields:

$$X_{s9} = K_{s98} \left\{ K_{s7}^{6}(M_{s1} + N_{s1}\, k_{d98}\, K_{d7}^{6}\, M_{d1}) \begin{Bmatrix} Q_{ao} \\ T_o \end{Bmatrix} \right.$$

$$+ K_{s7}^{6}\, N_{s1}\, k_{d98}\, K_{d7}^{6}\, N_{d1}\, S_{do}$$

$$+ (K_{s7}^{6}\, N_{s1}\, k_{d98} \sum_{i=5}^{0} K_{d7}^{i} H_d + \sum_{i=5}^{0} K_{s7}^{i} H_s)\; Y_{7-i}$$

$$+ (K_{s7}^{6}\, N_{s1}\, k_{d98}\, (I - K_{d7}^{5})\, (I - K_{d7})^{-1} F_d$$

$$\left. + (I - K_{s7}^{5})(I - K^{-1} F_s)\, T_s \right\} \qquad (4.37)$$

The outputs at the 7th level can similarly be related to the available inputs.

$$X_{s7} = K_{s7}^{6}\,(M_{s1} + N_{s1}\,k_{d98}\,K_{d7}^{6}\,M_{d1})\begin{Bmatrix} Q_{ao} \\ T_{o} \end{Bmatrix}$$

$$+ K_{s7}^{6}\,N_{s1}\,k_{d98}\,K_{d7}^{6}\,N_{d1}\,S_{do}$$

$$+ (K_{s7}^{6}\,N_{s1}\,k_{d98}\sum_{i=5}^{0} K_{d7}^{i}H_{d} + \sum_{i=5}^{0} K_{s7}^{i}{}_{s})\,Y_{7-i}$$

$$+ (K_{s7}^{6}\,N_{s1}\,k_{d98}\,(I-K_{d7}^{5})\,(I-K_{d7})^{-1}F_{d}$$

$$+ (I-K_{s7}^{5})(I-K_{s7})^{-1}F_{s})\,T_{s} \qquad (4.38)$$

The intermediate steps in obtaining equations (4.37) and (4.38) are shown in Appendix B.

The model of the plant is now available in two transfer function forms. The form given by equations (4.24) and (4.25) relates the measurable inputs and outputs. Each of these transfer functions must then be directly related to the cell transfer function model. This relationship is provided by the cascaded cell model of equations (4.37) and (4.38). Equating coefficients in these two models yields the cell transfer function models. Once these are available it only remains to relate the cell transfer function models to the cell state-space models.

4.6 THE STATE-SPACE MODEL

The cell transfer function model has been found (Equations 4.37 and 4.38). From this the state-space model can be obtained. Figure 4.4 describes the state-space model inputs and outputs as for the transfer function model. Two state-space models may be defined. One describes the furnace dynamics and the second describes the steam tube dynamics. The steady-state equations of SECTION 4.4 are used to justify certain matrix formats. The furnace and steam tube dynamics may

then be combined to form the combined state-space cell models.

4.6.1 THE FURNACE STATE-SPACE MODEL

The suggested state-space model for the furnace is

$$x_i(k+1) = A_i x_i(k) + B_{ai} Q_{ai-1}(k) + B_{ti} T_{i-1}(k) + B_{oi} F_{oi}(k) + B_{ci} F_{ci}(k) + B_{si} T_s(k) \quad \text{---(4.39)}$$

where

$$W_{di}(k) = C_{di}\, x_i(k) \qquad W_{si}(k) = C_{si}\, x_i(k)$$

$$Q_{ai}(k) = C_{ai}\, x_i(k) + D_{ai}(Q_{ai-1}(k), T_{i-1}(k), F_{ci}(k))^T$$

$$T_i(k) = C_{ti}\, x_i(k) + D_{ti}(Q_{ai-1}(k), T_{i-1}(k), F_{ci}(k))^T$$

For a second order system in controllable canonical form the matrices and vectors have the following form:

$$A_i = \begin{Bmatrix} 0 & 1 \\ -a_{1i} & -a_{2i} \end{Bmatrix} : B_{ai} = \begin{Bmatrix} 0 \\ b_{ai} \end{Bmatrix} : B_{ti} = \begin{Bmatrix} 0 \\ b_{ti} \end{Bmatrix}$$

$$B_{oi} = \begin{Bmatrix} 0 \\ b_{oi} \end{Bmatrix} : B_{ci} = \begin{Bmatrix} 0 \\ b_{ci} \end{Bmatrix} : B_{si} = \begin{Bmatrix} 0 \\ b_{si} \end{Bmatrix}$$

$$C_{di} = \{\, 0 \; c_{di} \} : C_{si} = \{\, 0 \; c_{si} \}$$

$$C_{ai} = \{\, 0 \; c_{ai} \} : C_{ti} = \{\, 0 \; c_{ti} \}$$

$$D_{ai} = \{d_{a1i}, d_{a2i}, d_{a3i}\} : D_{ti} = \{d_{t1i}, d_{t2i}, d_{t3i}\}$$

$$x_i(k) = \begin{Bmatrix} z_i(k-1) \\ z_i(k) \end{Bmatrix}$$

The state variable $z_i(k)$ represents the energy available within the cell for radiation to the side walls at any time interval.

No justification for the form of matrices A_i, B_{ai}, B_{ti} B_{oi}, B_{ci}, and B_{si} is required. These matrices satisfy the controllable canonical form. The matrix forms of $C_{di}, C_{si}, C_{ai}, C_{ti}, D_{ai}$ and D_{ti} should be justified.

$W_{di}(k)$ and $W_{si}(k)$ represent the energy radiated to the division wall and evaporator surfaces. These are directly proportional to $H_{ri}(k)$ (Equations 4.13 and 4.14) and so $z_i(k-1)$ need not be considered in C_{di} and C_{si}. The time constants involved in the time taken for changes in the gas temperature and the flue gas energy flow rate to occur are assumed to be negligible. These two variables are therefore not dependant on $z_i(k-1)$ which explains the form of C_{ai} and C_{ti}. This direct relationship with $H_i(k)$ is not sufficient to define the outputs $Q_{ai}(k)$ and $T_i(k)$ and therefore extra information about the air flow rates is required. This is available from the variables $Q_{ai-1}(k)$, $T_{i-1}(k)$ and $F_{ci}(k)$.

The model described in equation (4.39) can be rewritten as follows:-

$$x_i(k+1) = A_i\, x_i(k) + B_i\, u_i(k) \qquad (4.40)$$
$$v_{di}(k) = C_{di}\, x_i(k) + H_i\, r_i(k)$$
$$v_{si}(k) = C_{si}\, x_i(k) + H_i\, r_i(k)$$

where

$$x_i(k) = (z_i(k-1), z_i(k))^T$$
$$u_i(k) = (Q_{ai-1}(k), T_{i-1}(k), F_{oi}(k), F_{ci}(k), T_s(k))^T$$
$$v_{di}(k) = (Q_{ai}(k), T_i(k), W_{di}(k))^T$$
$$v_{si}(k) = (Q_{ai}(k), T_i(k), W_{si}(k))^T$$
$$r_i(k) = (Q_{ai-1}(k), T_{i-1}(k), F_{ci}(k))^T$$

$$A_i = \begin{Bmatrix} 0 & 1 \\ -a_{1i} & -a_{2i} \end{Bmatrix} \quad : \quad B_i = \begin{Bmatrix} 0 & 0 & 0 & 0 \\ b_{ai} & b_{ti} & b_{oi} & b_{ci} & b_{si} \end{Bmatrix}$$

$$C_{di} = \begin{Bmatrix} 0 & c_{ai} \\ 0 & c_{ti} \\ 0 & c_{di} \end{Bmatrix} \quad : \quad C_{si} = \begin{Bmatrix} 0 & c_{ai} \\ 0 & c_{ti} \\ 0 & c_{si} \end{Bmatrix}$$

$$H_i = \begin{Bmatrix} d_{a1i} & d_{a2i} & d_{a3i} \\ d_{t1i} & d_{t2i} & d_{t3i} \\ 0 & 0 & 0 \end{Bmatrix}$$

This new model can be simplified for cell 1, 8 and 9. As for SECTION 4.5, the transfer function model, cells 8 and 9 are combined to form one model. For these cells $F_{oi} = F_{ci} = T_{si} = 0$. Equation (4.40) then becomes:-

$$x_i(k+1) = A_i\, x_i(k) + B_i\, u_i(k) \qquad (4.41)$$

$$v_{di}(k) = C_{di}\, x_i(k) + H_i\, r_i(k)$$

$$v_{si}(k) = C_{si}\, x_i(k) + H_i\, r_i(k)$$

where

$$x_i(k) = (z_i(k-1), z_i(k))^T$$

$$u_i(k) = (Q_{ai-1}(k), T_{i-1}(k))^T$$

$$v_{di}(k) = (Q_{ai}(k), T_i(k), W_{di}(k))^T$$

$$v_{si}(k) = (Q_{ai}(k), T_i(k), W_{si}(k))^T$$

$$r_i(k) = (Q_{ai-1}(k), T_{i-1}(k))^T$$

$$A_i = \begin{Bmatrix} 0 & 1 \\ -a_{1i} & -a_{2i} \end{Bmatrix} \quad : \quad B_i = \begin{Bmatrix} 0 & 0 \\ b_{ai} & b_{ti} \end{Bmatrix}$$

$$C_{di} = \begin{Bmatrix} 0 & c_{ai} \\ 0 & c_{ti} \\ 0 & c_{di} \end{Bmatrix} \quad : \quad C_{si} = \begin{Bmatrix} 0 & c_{ai} \\ 0 & c_{ti} \\ 0 & c_{si} \end{Bmatrix}$$

$$H_i = \begin{Bmatrix} d_{a1i} & d_{a2i} \\ d_{t1i} & d_{t2i} \\ 0 & 0 \end{Bmatrix}$$

It is worth remembering that for cells 2 to 7

$$A_i = A_7 : \quad B_i = B_7 : \quad C_{di} = C_{d7} : \quad C_{si} = C_{s7}$$

and $H_i = H_7$.

4.6.2 THE STEAM TUBE SPACE-STATE MODEL

The chosen state-space models for the steam tube surfaces have the form

The division wall state-space model:

$$y_{di}(k+1) = j_{di}\, y_{di}(k) + l_{di}\, S_{di-1}(k) + m_{di}\, W_{di}(k) \qquad (4.42)$$

$$S_{di}(k) = n_{di}\, y_{di}(k)$$

The evaporator state-space model:

$$y_{si}(k+1) = j_{si} Y_{si}(k) + l_{si} S_{si-1}(k) + m_{si} W_{si}(k) \quad (4.43)$$

$$S_{si}(k) = n_{si}\, y_{si}(k)$$

Both these models represent 1st order systems. The state variables y_{di} and y_{si} represent the rate of energy flow leaving each steam tube section. Hence $S_{di} = y_{di}$ and $S_{si} = y_{si}$. The units of S_{si}, S_{si-1} W_{di} and W_{si} are all the same. The model should satisfy equations (4.17) and (4.18). For this to be the case $l_{si} = l_{di} = m_{si} = m_{di}$ (SECTION 5.4)

4.6.3 THE CELL STATE-SPACE MODEL

A state-space model for the furnace and the division wall may now be obtained by combining equations (4.40) and (4.42). A similar model is obtained by combining the furnace and evaporator state-space models. (Equations (4.41) and (4.43))

The combined division wall space-state model:

$$x'_{di}(k+1) = A'_{di} x'_{di}(k) + B'_{di}\, u'_{di}(k) \quad (4.44)$$

$$v'_{di}(k) = C'_{di} x'_{di}(k) + D_i r'_i(k)$$

where

$$x'_{di} = (z_i(k-1), z_i(k), y_{di}(k))^T$$

$$u'_{di} = (Q_{ai-1}, T_{i-1}(k), F_{oi}(k), F_{ci}(k), T_s(k), S_{di-1}(k)))^T$$

$$v'_{di} = (Q_{ai}(k), T_i(k), S_{di}(k))^T$$

$$r'_i = (Q_{ai-1}(k), T_{i-1}(k), F_{ci}(k))^T$$

$$A'_{di} = \begin{Bmatrix} 0 & 1 & 0 \\ -a_{1i} & -a_{2i} & \\ 0 & c_{di} & j_{di} \end{Bmatrix}$$

$$B'_{di} = \begin{Bmatrix} 0 & 0 & 0 & 0 & 0 & 0 \\ b_{ai} & b_{ti} & b_{oi} & b_{ci} & b_{si} & 0 \\ 0 & 0 & 0 & 0 & 0 & l_{di} \end{Bmatrix}$$

$$C'_{di} = \begin{Bmatrix} 0 & c_{ai} & 0 \\ 0 & c_{ti} & 0 \\ 0 & 0 & 1 \end{Bmatrix} \quad : \quad D_i = \begin{Bmatrix} d_{a1i} & d_{a2i} & d_{a3i} \\ d_{t1i} & d_{t2i} & d_{t3i} \\ 0 & 0 & 0 \end{Bmatrix}$$

The combined evaporator state-space model:

$$x'_{si}(k+1) = A'_{si}x'_{si}(k) + B'_{si}u'_{si}(k) \qquad (4.45)$$
$$y'_{si}(k) = C'_{si}x'_{si}(k) + D_i r'_i(k)$$

where

$$x'_{si} = (z_i(k-1), z_i(k), y_{si}(k))^T$$

$$u'_{si} = (Q_{ai-1}, T_{i-1}(k), F_{oi}(k), F_{ci}(k), T_{si}(k), S_{si-1}(k)))^T$$

$$y'_{si} = (Q_{ai}(k), T_i(k), S_{si}(k))^T$$

$$r'_i = (Q_{ai-1}(k), T_{i-1}(k), F_{ci}(k))^T$$

$$A'_{si} = \begin{Bmatrix} 0 & 1 & 0 \\ -a_{1i} & -a_{2i} & \\ 0 & c_{si} & j_{si} \end{Bmatrix}$$

$$B'_{si} = \begin{Bmatrix} 0 & 0 & 0 & 0 & 0 & 0 \\ b_{ai} & b_{ti} & b_{oi} & b_{ci} & b_{si} & 0 \\ 0 & 0 & 0 & 0 & 0 & l_{si} \end{Bmatrix}$$

$$C'_{si} = \begin{Bmatrix} 0 & c_{ai} & 0 \\ c & -_{ti} & \\ 0 & 0 & 1 \end{Bmatrix} \quad : \quad D_i = \begin{Bmatrix} d_{a1i} & d_{a2i} & d_{a3i} \\ d_{t1i} & d_{t2i} & d_{t3i} \\ 0 & 0 & 0 \end{Bmatrix}$$

4.7 SUMMARY

All the necessary equations have been obtained relating inputs to outputs. These relationships have been defined in terms of parameters to which no values have been attached. It is the purpose of Chapter 5 to try and make use of these relationships to identify the model parameters given the maximum likelihood model (Equations (4.24) and (4.25)). The steady-state analysis of SECTION 4.4 enables the validity of the cell transfer function and state-space models to be tested under steady-state conditions. Before continuing to Chapter 5 the reader is reminded that not all burners or mills are in operation at any time. These account for the transfer functions in equations (4.24) and (4.25) that are not available. Depending on which levels are inoperative certain solving techniques are ruled out while others are significantly complicated (SECTION 6.4.1).

CHAPTER 5 REALIZATION OF THE MODEL PARAMETERS

5.1 INTRODUCTION

In order to determine the mathematical model for the boiler sufficient information had to be accumulated. Information relating to boiler practices and design aims led to the model suggested in Chapter 4. The availability of quantitative data enables the model parameters to be identified. The quantitative information is of two kinds. The first kind provides data about the physical processes and the physical constants. This information enables the steady-state equations of SECTION 4.4 to be defined for all cells. The second category provides the information necessary for the parameter identification techniques. Time sequences, of relevant measuring points, recorded from the plant under normal operating conditions, are necessary for these techniques. All the available quantitative information may then be manipulated and combined to produce information which can be used in the model identification process.

This Chapter looks at the steady-state equations derived in SECTION 4.4. Justification is provided for the choice of some of the required constants. The method for obtaining the cascaded cell transfer model is discussed. It is shown how individual cell transfer function models may be deduced. The Chapter is completed by describing how the state-space equivalent for the cell transfer function model may be obtained.

5.2 THE STEADY-STATE EQUATIONS

It is possible to obtain two different equations for the steady-state conditions of S_{di} and S_{si}. This section intends to show that, although each equation uses different inputs to derive its output, they are compatible. The section finishes by defining the steady-state parameters resulting from the steady-state analysis of SECTION 4.4.

Consider the steady-state equations in SECTION 4.4. H_{ri}, the energy available for absorbtion, is related to Q_{di} and Q_{si} by equations (4.13) and (4.14). These relationships may be fixed using equation (4.2).

$$Q_{di} = 0,286 \; H_{ri} \qquad (5.1)$$

$$Q_{si} = 0,714 \; H_{i} \qquad (5.2)$$

From equation (4.16) it can be .een that;

$$H_{ri} = f_{hi}(\hat{F}_{ci}, \hat{F}_{ci-1}, \cdots, \hat{F}_{ci}, \hat{F}_{oi}, A/f, \hat{T}_{s}, \hat{T}_{i-1}, \hat{T}_{i}) \qquad (5.3)$$

where f_{hi} is a function of the listed variables.

It follows from equations (5.1) and (5.2) that Q_{di} and Q_{si} must also be functions of these variables. The variables used in defining S_{di} and S_{si} (Equation 4.17 and 4.18) can also be found.

$$S_{di} = Q_{di} + S_{di-1} \qquad (5.4)$$

$$S_{si} = Q_{si} + S_{si-1} \qquad (5.5)$$

The only additional variable in each of these equations is the energy flow rate of the steam entering the i'th cell, namely S_{di-1} and S_{si-1}.

Consider now the transfer function cell models (Equations 4.35 and 4.36);

$$X_{di} = K_{di} X_{di-1} + H_{di} Y_{i} + F_{di} T_{s} \qquad (5.6)$$

$$X_{si} = K_{si} X_{si-1} + H_{si} Y_{i} + F_{di} T_{s} \qquad (5.7)$$

Consider the inputs, in these equations, that define S_{di} and S_{si}.

$$S_{di} = f_{di}(Q_{ai-1}, T_{i}, S_{di-1}, F_{oi}, F_{ci}, T_{s}) \qquad (5.8)$$

$$S_{si} = f_{si}(Q_{ai-1}, T_{i-1}, S_{si-1}, F_{oi}, F_{ci}, T_{s}) \qquad (5.9)$$

where f_{di} and f_{si} are functions of the listed variables.

A/f is not listed in equations (5.8) or (5.9). The transfer function model assumes that the air/fuel ratio is fixed. The ratio changes primarily as a result of fluctuations in the moisture content and the calorific content of the coal. It changes very slowly with respect to the system response times defined by equations (5.6) and (5.7) and since the maximum deviation from the normal is never very large A/f is omitted from the variable list in equations (5.8) and (5.9).

The major apparent difference in the variable list for S_{di} arising out of equations (5.6) and (5.8) is the use of Q_{ai-1} instead of F_{ci-1} ..... F_{c2} ($F_{c1} = 0$). The steady state equation (5.4) uses F_{ci-1} ... F_{c2}, in conjuction with T_{i-1}, to calculate Q_{ai-1}, the energy inflow to the i'th cell. From the transfer function model point of view this is a modelled output from the previous cell and hence F_{ci-1}.... F_{c2} are in fact considered in equation (5.8).

The same applies to T_i in equation (5.4). T_i can be derived from equation (5.6) in terms of the same variables as S_{di}. It follows that T_i is already included in equation (5.8). This may be represented by another function f_{di}' as follows:-

$$S_{di} = f_{di}'\ (\ Q_{ai-1},\ T_{i-1},\ S_{di-1},\ F_{oi},\ F_{ci},\ T_s,\ T_i\ ) \qquad (5.10)$$

The variables in (5.10) are now no longer linearily independant. The argument in the foregoing two paragraphs applies equally well to S_{si}.

The two different methods for determining the steady-state conditions for S_{di} and S_{si} are therefore compatible. Later it should be possible to show that the results obtained from the cell transfer function model do indeed match those resulting from the steady-state analysis of SECTION 4.4.

CHAPTER 5 REALIZATION OF THE MODEL PARAMETE

In order to define the parameters of equations (5.4) and (5.5) the following constant values are assumed.

c_c	=	18	MJ/kg
c_{co}	=	40	MJ/kg
ρ_a	=	0,95	kg/m^3
c_a	=	0,78	$kJ/kg \cdot K^{-1}$
ρ_c	=	1500	kg/m^3

The following Taylor expansion points are assumed.

$\dot{m}_{f_i}$: i = 2 to 7 : 9,15 kg/s ; This represents the half-load mass flow rate of each mill.

$\dot{m}_{co_i}$: i = 2 to 7 : 0,14 kg/s ; This represents the half-load mass flow rate at each burner level.

$\hat{A/f}$: : 7,6 m^3/kg ; The ratio of the air volume to to the mass of coal.
$\left\{\tilde{A/f} = \hat{A/f} / \rho_c\right\}$

T_s : ; 250 ^oC ; This temperature varies between 150^oC and 350^oC.

T_i : i = 1 to 7 : 150 (i+1) ^oC ; This attempts to model the temperature profile within the boiler.

T_o : : 250^oC

T_o : : 300^oC

S_{di}, S_{si} and H_{ri} then become:

$$S_{di} = S_{di\,1} + 0{,}286\ H_{ri} \qquad (5.10)$$

$$S_{si} = S_{si\,1} + 0{,}714\ H_{ri} \qquad (5.11)$$

$$H_{ri} = K_{1i}'' + K_{2i}'' \hat{F}_{ci} + K_{3i}'' \sum_{j=1}^{i-1} \hat{F}_{cj} + K_{4i}'' \hat{F}_{oi}$$

$$+ K_{5i}'' A\hat{f}' + K_{6i}'' \hat{T}_s + K_{7i}'' \hat{T}_{i-1} + K_{8i}'' \hat{T}_i \qquad (5.12)$$

The parameters K_{1i}'' to K_{8i}'' for cells 1 to 9 are given in TABLE 5.1.

TABLE 5.1 TABLE OF PARAMETER VALUES FOR ALL CELLS AS DEFINED BY EQUATION 4.16 IN SECTION 4.4

Cell No	K_{1i}''	K_{2i}''	K_{3i}''	K_{4i}''	K_{5i}''	K_{6i}''	K_{7i}''	K_{8i}''
1	0	17,7	-3,2	40	0	0	0	0
2	161	16,9	-0,85	40	-1,36	52	0	0
3	145	16,0	-0,85	40	-3,4	52	52	104
4	129	15,2	-0,85	40	-5,5	52	104	155
5	114	14,3	-0,85	40	-7,5	52	155	207
6	99	13,5	-0,85	40	-9,5	52	207	259
7	83	12.6	-0,85	40	-11,6	52	299	311
8	90	15,2	2,55	40	11,9	0	311	311
9	114	17,7	2,50	40	15,0	0	311	311
Units	MJ/s	MJ/kg	MJ/kg	MJ/kg	MJ/s	$kJ/s.K^{-1}$	$kJ/s.K^{-1}$	$kJ/s.K^{-1}$

5.3 THE TRANSFER FUNCTION MODEL

5.3.1 THE CASCADED CELL MODEL

The relevant inputs and outputs for the combined plant were shown in FIGURE 4.5. At an earlier stage in the project data of selected points was logged. The majority of the relevant points appeared in this logged data. Indeed only two inputs/outputs of importance do not appear in this data. Due to time constraints it was decided that this available data should suffice. The list of points that were used from the logged data, appears in Appendix C. The important omissions from this list are the division wall outlet water pressure and temperature. This

prevented the determination of S_{so} or S_{d9} from the steam tables (Keenan, 1978). The problem was circumvented by eliminating S_{so} from the cascaded cell model. In its simplest form the available inputs are related to the available outputs according to equation (4.37) and equation (4.38).

All the transfer functions in equations (4.24) and (4.25) are found using the IMSL (International Mathematics and Sciences Library). The package FTWENX (Appendix D) performs the required maximum likelihood parameter estimation on several multi-input single-output time sequences. This provides an auto-regressive moving average model from which the required 'z' transforms are easily determined (Equation 5.14).

Before the data could be entered onto the PDP 11/34 computer, on which the software was run, some pre-processing of the data was necessary. The enthalpy flow rate at the division wall input, S_{do}, and at the evaporator output, S_{so}, had to be obtained from temperature, pressure and flow rate measurements (Keenan, 1978). In a similar way the flue gas enthalpy flow rates per kilogram (Q'_{a7} and Q'_{a9}) were obtained from the gas tables (Keenan, 1983). The air pressure was assumed to be one atmosphere since the pressure within the furnace seldom falls more than 100Pa below atmospheric pressure. The flue gas enthalpy flow rates, Q_{a7} and Q_{a9}, were computed by manipulating entered data (SECTION 6.3). A list of all data available for processing by the parameter estimation package, as well as the files, and the columns the data appears in, is shown in Appendix E.

The parameters estimated by the package FTWENX were stored in a new data file. These parameters were then used to generate the output time series from the given inputs. In this way the output from the model

could be compared against the measured outputs.

The form of the time series model determined by FTWENX is

$$\begin{Bmatrix} Q_{a9}\ (k+1) \\ T_9\ (k+1) \\ S_{s9}\ (k+1) \\ Q_{a7}\ (k+1) \\ T_7\ (k+1) \\ S_{s7}\ (k+1) \end{Bmatrix} = \begin{Bmatrix} a_1 & 0 & 0 & 0 & 0 & 0 \\ 0 & a_2 & & & & 0 \\ 0 & & a_3 & & & 0 \\ 0 & & & a_4 & & 0 \\ 0 & & & & a_5 & 0 \\ 0 & 0 & 0 & 0 & 0 & a_6 \end{Bmatrix} \begin{Bmatrix} Q_{a9}\ (k) \\ T_9\ (k) \\ S_{s9}\ (k) \\ Q_{a7}\ (k) \\ T_7\ (k) \\ S_{s7}\ (k) \end{Bmatrix}$$

$$+ \begin{Bmatrix} b_{11} & \cdots & b_{113} & 0 \\ b_{21} & & b_{213} & 0 \\ b_{31} & & b_{313} & b_{314} \\ b_{41} & & b_{413} & 0 \\ b_{51} & & b_{513} & 0 \\ b_{61} & \cdots & b_{613} & b_{614} \end{Bmatrix} \begin{Bmatrix} F_{o2}\ (k) \\ F_{o7}\ (k) \\ F_{c2}\ (k) \\ F_{c7}\ (k) \\ T_s\ (k) \\ S_{do}\ (k) \end{Bmatrix} \qquad (5.13)$$

This represents 6 multi-input, single-output predictive 1st order models. Taking the 'z' transforms yields the transfer function relationship

$$\begin{Bmatrix} Q_{a9}(Z) \\ T_9\ (Z) \\ S_{s9}(Z) \\ Q_{a7}(Z) \\ T_7\ (Z) \\ S_{s7}(Z) \end{Bmatrix} = \begin{Bmatrix} \frac{b_{11}z^{-1}}{1-a_1z^{-1}} & \cdots & \frac{b_{113}z^{-1}}{1-a_1z^{-1}} & 0 \\ & & & 0 \\ & & & \frac{b_{314}z^{-1}}{1-a_3z^{-1}} \\ & & & 0 \\ & & & 0 \\ \frac{b_{61}z^{-1}}{1-a_6z^{-1}} & \cdots & \frac{b_{613}z^{-1}}{1-a_6z^{-1}} & \frac{b_{614}z^{-1}}{1-a_6z^{-1}} \end{Bmatrix} \begin{Bmatrix} F_{o2}\ (k) \\ F_{o7}\ (k) \\ F_{c2}\ (k) \\ F_{c7}\ (k) \\ T_s\ (k) \\ S_{do}\ (k) \end{Bmatrix} \qquad (5.14)$$

5.3.2 THE CELL TRANSFER FUNCTION MODEL

To obtain the parameters of the cell transfer function it is necessary to equate the two forms of

the cascaded cell model. Coefficients of the fitted moving average model, when equated with coefficients in the algebraic cascaded cell model (Equations 4.37 and 4.38), yield the individual cell transfer functions. Each of these useful relationships is considered below. (For definition of the variables $g'_{d9i}, g'_{s9i}, k_{d98}$ and k_{s98} see Appendix B.)

1) g'_{s96} and $g^{6}_{s76} g_{s16}$;

The relationship between S_{do} and X_{s9} in equation (4.24) and equation (4.37) is given by

$$(0 \; 0 \; G_{s14} \; (1 + G_{d14}))^T = K_{s98} \; K^{6}_{s7} \; N_{s1} \; k_{d98} \; K^{6}_{d7} \; N_{d1} \qquad (5.15)$$

The assumptions are made that

$$K_{d7} = K_{s7}, \; N_{di} = N_{si}, \; K_{d98} = K_{s98}$$

The basis for this assumption, is that the same tube work and metal has been used in the evaporator and division wall steam surfaces. The relative areas of the energy absorbing surfaces are taken into account by \ (SECTION 4.5.2). The transfer function K_{s7} is then only defined by the length and thickness of the tubes. This assumption, while not completely accurate, states that the energy absorbing properties of a length of evaporator and a length of division wall are identical.

Equation (5.15) then becomes

$$(0 \; 0 \; G_{s14}(1+G_{d14}))^T = K_{s98}(K^{6}_{s7} N_{s1}) \; k_{s98} \; (K^{6}_{s7} \; N_{s1}) \qquad (5.16)$$

K^{6}_{s7} has the form (Appendix F)

$$K^{6}_{s7} = \begin{Bmatrix} x & x & 0 \\ x & x & 0 \\ x & x & g^{6}_{s76} \end{Bmatrix} \quad \text{where x is any transfer function}$$

$$N_{s1} = \{ 0 \; 0 \; g_{s16} \}^T$$

Hence

$$K^{6}_{s7} \; N_{s1} = \{ 0 \; 0 \; g^{6}_{s76} \; g_{s16} \}^T \qquad (5.17)$$

$$K_{s98}\ K^{6}_{s7}\ N_{s1} = \begin{Bmatrix} x & x & 0 \\ x & x & 0 \\ x & x & g'_{s96} \end{Bmatrix} \begin{Bmatrix} 0 \\ 0 \\ g^{6}_{s76}\ g_{s16} \end{Bmatrix}$$

$$= \begin{pmatrix} 0 & 0 & g'_{s96}\ g^{6}_{s76}\ g_{s16} \end{pmatrix}^{T} \qquad (5.18)$$

and

$$k_{s98}\ K^{6}_{s7}\ N_{s1} = \begin{pmatrix} x & x & g'_{s96} \end{pmatrix} \begin{Bmatrix} 0 \\ 0 \\ g^{6}_{s7}\ g_{s16} \end{Bmatrix}$$

$$= g'_{s96}\ g^{6}_{s7}\ g_{s16} \qquad (5.19)$$

Substituting (5.18) and (5.19) into (5.16) gives

$$\begin{pmatrix} 0 & 0 & G_{s14}(1 + G_{d14}) \end{pmatrix}^{T} = \begin{Bmatrix} 0 & 0 & \begin{Bmatrix} g'_{s96}\ g^{6}_{s76}\ g_{s16} \end{Bmatrix}^{2} \end{Bmatrix}$$

As expected $S_{(.)}$ does not influence G_{a9} or T_9 since re-radiation has not been considered.

The transfer function relating output S_{s9} to input S_{d0} is then

$$G_{s14}\ (\ 1 + G_{d14}\ ) = (\ g'_{s96}\ g^{6}_{s76}\ g_{s16}\ )^{2} \qquad (5.20)$$

In a similar way the relationship between S_{s7} and S_{d0} can be determined

$$G'_{s14}\ (\ 1 + G_{d14}\ ) = g'_{s96}\ (\ g^{6}_{s76}\ g_{s16}\ )^{2} \qquad (5.21)$$

The L.H.S. of equations (5.20) and (5.21) are known (SECTION 5.3.1). The ratio of these equations gives

$$\frac{G_{s14}\ (\ 1 + G_{d14}\ )}{G'_{s14}\ (\ 1 + G_{d14}\ )} = g'_{s96} \qquad (5.22)$$

Once g'_{s96} has been found $g^{6}_{s76}\ g_{s16}$ can be determined from either of equations (5.20) or (5.21).

2) K_{s98};

With g'_{s96} known, K_{s98} can be identified by by considering the relationship between the inputs F_{07} and F_{c7}, and the outputs of cells 7 and 9, X_{s7} X_{s9}.

From equations (4.25) and (4.38) the relationship between F_{07}, F_{c7} and X_{s7} yields:

$$\begin{Bmatrix} G'_{a6} & G'_{a12} \\ G'_{t6} & G'_{t12} \\ (G'_{s6} + G'_{s14}\, G_{d6}) & (G'_{s12} + G'_{s14}\, G_{d12}) \end{Bmatrix} =$$

$$(K^{6}_{s7}\, N_{s1}\, k_{s98}\, H_d + H_s) \qquad (5.23)$$

Similarly, the relationship between F_{07}, F_{c7} and X_{s9} yields

$$\begin{Bmatrix} G_{a6} & G_{a12} \\ G_{t6} & G_{t12} \\ (G_{s6} + G_{s14}\, G_{d6}) & (G_{s12} + G_{s14}\, G_{d12}) \end{Bmatrix} =$$

$$K_{s98} (K^{6}_{s7}\, N_{s1}\, k_{s98}\, H_d + H_s) \qquad (5.24)$$

Substituting (5.23) into (5.24) yields

$$\begin{Bmatrix} G_{a6} & G_{a12} \\ G_{t6} & G_{t12} \\ (G_{s6} + G_{s14}\, G_{d6}) & (G_{s12} + G_{s14}\, G_{d12}) \end{Bmatrix} =$$

$$\begin{Bmatrix} g'_{a94} & g'_{a95} & 0 \\ g'_{t94} & g'_{t95} & 0 \\ g'_{s94} & g'_{s95} & g'_{s96} \end{Bmatrix} \begin{Bmatrix} G'_{a6} & G'_{a12} \\ G'_{t6} & G'_{t12} \\ (G'_{s6} + G'_{s14}\, G_{d6}) & (G'_{s12} + G'_{s14}\, G_{d12}) \end{Bmatrix} \qquad (5.25)$$

The only unknowns are the first two columnns of the matrix K_{s98}. Sufficient information is contained in equation (5.25) to allow K_{s98} to be determined (Appendix G).

2) K_{s98};

With g'_{s96} known, K_{s98} can be identified by by considering the relationship between the inputs F_{o7} and F_{c7}, and the outputs of cells 7 and 9, X_{s7} X_{s9}.

From equations (4.25) and (4.38) the relationship between F_{o7}, F_{c7} and X_{s7} yields:

$$\begin{Bmatrix} G'_{a6} & G'_{a12} \\ G'_{t6} & G'_{t12} \\ (G'_{s6} + G'_{s14}\, G_{d6}) & (G'_{s12} + G'_{s14}\, G_{d12}) \end{Bmatrix} = \left(F^{6}_{s7}\, N_{s1}\, k_{s98}\, H_d + H_s \right) \qquad (5.23)$$

Similarly, the relationship between F_{o7}, F_{c7} and X_{s9} yields

$$\begin{Bmatrix} G_{a6} & G_{a12} \\ G_{t6} & G_{t12} \\ (G_{s6} + G_{s14}\, G_{d6}) & (G_{s12} + G_{s14}\, G_{d12}) \end{Bmatrix} = K_{s98}\left(K^{6}_{s7}\, N_{s1}\, k_{s98}\, H_d + H_s \right) \qquad (5.24)$$

Substituting (5.23) into (5.24) yields

$$\begin{Bmatrix} G_{a6} & G_{a12} \\ G_{t6} & G_{t12} \\ (G_{s6} + G_{s14}\, G_{d6}) & (G_{s12} + G_{s14}\, G_{d12}) \end{Bmatrix} = \begin{Bmatrix} g'_{a94} & g'_{a95} & 0 \\ g'_{t94} & g'_{t95} & 0 \\ g'_{s94} & g'_{s95} & g'_{s96} \end{Bmatrix} \begin{Bmatrix} G'_{a6} & G'_{a12} \\ G'_{t6} & G'_{t12} \\ (G'_{s6} + G'_{s14}\, G_{d6}) & (G'_{s12} + G'_{s14}\, G_{d12}) \end{Bmatrix} \qquad (5.25)$$

The only unknowns are the first two columnns of the matrix K_{s98}. Sufficient information is contained in equation (5.25) to allow K_{s98} to be determined (Appendix G).

3) H_s;

It is now possible to find H_s from equation (5.23). k_{s98} is available from K_{s98} (Appendix G). $K_{s7}^{6}\ N_{s1}$ is available from equation (5.17).

$$K_{s7}^{6}\ N_{s1}\ k_{s98} =$$

$$\begin{Bmatrix} 0 & 0 & 0 \\ 0 & 0 & 0 \\ (g_{s76}^{6}\ g_{s16}\ g_{s94}') & (g_{s76}^{6}\ g_{s16}\ g_{s95}') & (g_{s76}^{6}\ g_{s16}\ g_{s96}') \end{Bmatrix} \qquad (5.26)$$

The only unknowns in equation (5.23) are H_d and H_s but from SECTION (4.5.1),

$$H_s = \begin{Bmatrix} g_{ai2}\ g_{ai3} \\ g_{ti2}\ g_{ti3} \\ g_{si2}\ g_{si3} \end{Bmatrix} \text{ and } H_d = \begin{Bmatrix} g_{ai2}\ g_{ai3} \\ g_{ti2}\ g_{ti3} \\ \lambda\ g_{si2}\ \lambda\ g_{si3} \end{Bmatrix} \qquad (5.27)$$

λ is known hence there are only six unknowns. Six equations are available from equation (5.23) and so H_s may be completely solved (Appendix H).

4) K_{s1};

In order to determine K_{s7}, K_{s1} must be available. This allows g_{s76} in K_{s7} to be fixed using equations (5.21) and (5.22). K_{s1} is best determined from the air temperature T_o and energy flow rate Q_{ao}, of the air at the bottom of the cell. These values are not available and are set to zero in the model. They would not be expected to change much and, due to low temperature and low heat transfer below the burners, do not contribute a significant amount of energy to the system. For this reason

$$g_{s16} = 1$$

or

$$K_{s1} = \begin{Bmatrix} 0 & 0 & 0 \\ 0 & 0 & 0 \\ 0 & 0 & 1 \end{Bmatrix} \qquad (5.28)$$

This has the effect of making cell 1 transparent. That is, it does not affect the water entering the side walls nor does it affect the air temperature or energy flow rates.

5) K_{s7}:

Sufficient information is now available to enable K_{s7} to be determined. This is achieved by considering firstly the effects of the inputs to cells 2 and 3 on the output X_{s7}. The relationship between F_{o3}, F_{c3} and X_{s7} is given by equation (5.29). The relationship between F_{o2}, F_{c2} and X_{s7} is given by equation (5.30).

$$\begin{Bmatrix} G'_{a2} & G'_{a8} \\ G'_{t2} & G'_{t8} \\ (G'_{s2} + G'_{s14}\,G_{d2}) & (G'_{s8} + G'_{s14}\,G_{d8}) \end{Bmatrix} = (K^6_{s7}\,N_{s1}\,k_{s98}\,K^4_{s7}\,H_d + K^4_{s7}\,H_s) \qquad (5.29)$$

$$\begin{Bmatrix} G'_{a1} & G'_{a7} \\ G'_{t1} & G'_{t7} \\ (G'_{s1} + G'_{s14}\,G_{d1}) & (G'_{s7} + G'_{s14}\,G_{d7}) \end{Bmatrix} = (K^6_{s7}\,N_{s1}\,k_{s98}\,K^5_{s7}\,H_d + K^5_{s7}\,H_s) \qquad (5.30)$$

Appendix I shows that if

$$K^4_{s7}\,H_s = \begin{Bmatrix} p_1 & p_2 \\ p_3 & p_4 \\ p_5 & p_6 \end{Bmatrix} \quad \text{and} \quad K^5_{s7}\,H_s = \begin{Bmatrix} q_1 & q_2 \\ q_3 & q_4 \\ q_5 & q_6 \end{Bmatrix}$$

then from equations (5.29) and (5.30)

$$\begin{Bmatrix} G'_{a2} & G'_{a8} \\ G'_{t2} & G'_{t8} \end{Bmatrix} = \begin{Bmatrix} p_1 & p_2 \\ p_3 & p_4 \end{Bmatrix} \quad \text{and} \quad \begin{Bmatrix} G'_{a1} & G'_{a7} \\ G'_{t1} & G'_{t7} \end{Bmatrix} = \begin{Bmatrix} q_1 & q_2 \\ q_3 & q_4 \end{Bmatrix}$$

but

$$\begin{Bmatrix} q_1 & q_2 \\ q_3 & q_4 \\ q_5 & q_6 \end{Bmatrix} = K_{s7} \begin{Bmatrix} p_1 & p_2 \\ p_3 & p_4 \\ p_5 & p_6 \end{Bmatrix}$$

$$= \begin{Bmatrix} g_{a74} & g_{a75} & 0 \\ g_{t74} & g_{t75} & 0 \\ g_{s74} & g_{s75} & g_{s66} \end{Bmatrix} \begin{Bmatrix} p_1 & p_2 \\ p_3 & p_4 \\ p_5 & p_6 \end{Bmatrix} \quad \text{(5.31)}$$

Equation (5.32) can be extracted from equation (5.31)

$$\begin{Bmatrix} q_1 & q_2 \\ q_3 & q_4 \end{Bmatrix} = \begin{Bmatrix} g_{a74} & g_{a75} \\ g_{t74} & g_{t75} \end{Bmatrix} \begin{Bmatrix} p_1 & p_2 \\ p_3 & p_4 \end{Bmatrix} \quad \text{(5.32)}$$

The top two rows of K_{s7} are then easily identified;

$$\begin{Bmatrix} g_{a74} & g_{a75} \\ g_{t74} & g_{t75} \end{Bmatrix} = \begin{Bmatrix} q_1 & q_2 \\ q_3 & q_4 \end{Bmatrix} \begin{Bmatrix} p_1 & p_2 \\ p_3 & p_4 \end{Bmatrix}^{-1} \quad \text{(5.23)}$$

There remain two transfer functions in K_{s7} that are undefined. These are g_{s74} and g_{s75}. These are solved using the remaining measured data in equations (5.29) and (5.30) (See Appendix I).

6) F_s;

The only remaining matrices that need to be solved for are F_d and F_s. The relationship between Y_s and X_{s7} is given by equations (4.35) and (4.38).

$$\begin{Bmatrix} G'_{a13} \\ G'_{t13} \\ (G'_{s13} + G'_{s14} G_{d13}) \end{Bmatrix} =$$

$$K_{s7}^{6} N_{s1} k_{s98} (I - K_{s7}^{5}) (I - K_{s7})^{-1} F_d +$$

$$(I - K_{s7}^{5}) (I - K_{s7})^{-1} F_s \quad \text{(5.34)}$$

The matrix $(I - K_{s7}^{5})(I - K_{s7})^{-1}$ can be determined.

K^{δ}_{s7} N_{s1} k_{s98} is already known (Equation 5.25). F_s and F_d are the only unknowns and are related as follows:-

$$F_d = \begin{Bmatrix} \vartheta_{a1} \\ \vartheta_{t1} \\ \vartheta_{s1} \end{Bmatrix} \qquad F_s = \begin{Bmatrix} \vartheta_{a1} \\ \vartheta_{t1} \\ \vartheta_{s1} \end{Bmatrix}$$

The method for determining F_d and F_s appears in Appendix J.

It has been shown that all the matrices making up the division wall and the evaporator cascaded cell models can be identified from the available data. It is now possible to identify the state-space models from their equivalent transfer function models.

5.4 THE STATE-SPACE MODEL

The transfer function models of equations (4.32) and (4.33) can be written as

The division wall cell transfer function model:

$$\begin{Bmatrix} Q_{ai} \\ T_i \\ S_{di} \end{Bmatrix} = \begin{Bmatrix} \vartheta_{ai1} & \vartheta_{ai2} & \vartheta_{ai3} & \vartheta_{ai4} & \vartheta_{ai5} & 0 \\ \vartheta_{ti1} & \vartheta_{ti2} & \vartheta_{ti3} & \vartheta_{ti4} & \vartheta_{ti5} & 0 \\ \vartheta_{di1} & \vartheta_{di2} & \vartheta_{di3} & \vartheta_{di4} & \vartheta_{di5} & \vartheta_{di6} \end{Bmatrix} \begin{Bmatrix} T_{si} \\ F_{oi} \\ F_{ci} \\ Q_{ai-1} \\ T_{i-1} \\ S_{di-1} \end{Bmatrix} \quad (5.35)$$

The evaporator cell transfer function model:

$$\begin{Bmatrix} Q_{ai} \\ T_i \\ S_{si} \end{Bmatrix} = \begin{Bmatrix} \vartheta_{ai1} & \vartheta_{ai2} & \vartheta_{ai3} & \vartheta_{ai4} & \vartheta_{ai5} & 0 \\ \vartheta_{ti1} & \vartheta_{ti2} & \vartheta_{ti3} & \vartheta_{ti4} & \vartheta_{ti5} & 0 \\ \vartheta_{si1} & \vartheta_{si2} & \vartheta_{si3} & \vartheta_{si4} & \vartheta_{si5} & \vartheta_{si6} \end{Bmatrix} \begin{Bmatrix} T_{si} \\ F_{oi} \\ F_{ci} \\ Q_{ai-1} \\ T_i \\ S_{si-1} \end{Bmatrix} \quad (5.36)$$

All the g's represent 1st order transfer functions in the 'z' plane.

Similar equations can be derived from the state-space model definition of SECTION 4.6. For any model of the form:

$$x(k+1) = A\,x(k) + B\,u(k)$$
$$y(k) = C\,x(k) + D\,u(k)$$

The transfer function equivalent G(z) is obtained as follows (Owens, 1983) :-

$$G(z) = C\,(zI - A)^{-1}\,B + D \qquad (5.37)$$

The A, B, C and D matrices defined in SECTION 4.6.3 by equations (4.44) and (4.45) should give similar transfer function matrices to those in equations (5.35) and (5.36).

Consider first a transfer function matrix $K'_{si}(z)$ derived from the state-space model for the evaporator (Equation 4.45) using equation (5.37).

$$K'_{si}(z) = \begin{Bmatrix} 0 & c_{ai} & 0 \\ 0 & c_{ti} & 0 \\ 0 & 0 & 1 \end{Bmatrix} \begin{Bmatrix} z & -1 & 0 \\ a_{1i} & z+a_{2i} & 0 \\ 0 & -c_{si}m_{si} & z-j_{si} \end{Bmatrix} \begin{Bmatrix} 0 & 0 & 0 & 0 & 0 & 0 \\ b_{si} & b_{oi} & b_{ci} & b_{ai} & b_{ti} & 0 \\ 0 & 0 & 0 & 0 & 0 & l_{si} \end{Bmatrix}$$
$$+ \begin{Bmatrix} 0 & 0 & d_{a3i} & d_{a1i} & d_{a2i} & 0 \\ 0 & 0 & d_{t3i} & d_{t1i} & d_{t2i} & 0 \\ 0 & 0 & 0 & 0 & 0 & 0 \end{Bmatrix} \qquad (5.38)$$

$$(zI - A'_{si})^{-1} = \begin{Bmatrix} f_{1i} & f_{2i} & 0 \\ f_{3i} & f_{4i} & 0 \\ f_{5i} & f_{6i} & f_{7i} \end{Bmatrix} \qquad (5.39)$$

where

$f_{1i} = (z + a_{2i})(z - j_{si}) / p_{ol}$

$f_{2i} = (z - j_{si}) / p_{ol}$

$f_{3i} = -a_{1i}(z - j_{si}) / p_{ol}$

$f_{4i} = z(z - j_{si}) / p_{ol}$

$f_{5i} = -a_{1i}\,c_{si}\,m_{si} / p_{ol}$

$f_{6i} = z\,c_{si}\,m_{si} / p_{ol}$

$$f_{7i} = ((z + a_{2i}) z + a_{1i}) / p_{ol}$$

$$p_{ol} = (z (z + a_{2i}) + a_{1i}) (z - j_{si})$$

Substituting equation (5.39) into equation (5.38) and multiplying out gives:-

$$K_{si}(z) = \begin{Bmatrix} f_{4i} c_{ai} b_{si} & f_{4i} c_{ai} b_{oi} & f_{4i} c_{ai} b_{ci} + d_{a3i} \\ f_{4i} c_{ti} b_{si} & f_{4i} c_{ti} b_{oi} & f_{4i} c_{ti} b_{ci} + d_{t3i} \\ f_{6i} b_{si} & f_{6i} b_{oi} & f_{6i} b_{si} \end{Bmatrix}$$

$$\begin{Bmatrix} f_{4i} c_{ai} b_{ai} + d_{a1i} & f_{4i} c_{ai} b_{ti} + d_{a2i} & 0 \\ f_{4i} c_{ti} b_{ai} + d_{t1i} & f_{4i} c_{ti} b_{ti} + d_{t2i} & 0 \\ f_{6i} b_{ai} & f_{6i} b_{ti} & f_{7i} l_{si} \end{Bmatrix} \quad \text{(5.40)}$$

The state-space cell model for the evaporator can now be related to the transfer function cell model for the evaporator (Equation 5.36) which was developed in the previous section.

Consideration of the steady-state form for the tube surfaces (SECTION 4.6.2) yields a value for l_{si}, m_{si} and r_{si}. This information simplifies the task of determining the model parameters. Equation (4.43) reduces to equation (5.41) under steady-state conditions;

$$S_{si} = \frac{1}{1 - j_{si}} (l_{si} S_{si-1} + m_{si} H_s) \quad \text{(5.41)}$$

where

$$W_{si} = r_{si} H_{ri} \quad \text{(5.42)}$$

Equating the coefficients of equation (4.17), which arises out of the steady-state analysis of SECTION 4.4, with the coefficients of equation (5.41) gives

$$l_{si} = 1 - j_{si}$$

$$m_{si} = 1 - j_{si}$$

or $$l_{si} = m_{si} = 1 - j_{si} \quad \text{(5.43)}$$

Finally from equation (5.2) it can be deduced that

$$c_{si} = 0.714$$

The transfer function matrices of equations (5.40) and (5.36) may now be used to determine the state-space parameters of equation (4.45)

1) l_{si} and j_{si};

$$g_{si6} = f_{7i}\ l_{si}$$

$$= \frac{l_{si}}{z - j_{si}} \qquad (5.44)$$

This gives l_{si} and j_{si} directly from the best fit 1st order transfer function for g_{si6}

2) a_{1i}, a_{2i}, b_{si}, b_{oi}, b_{ci}, b_{ai} and b_{ti};

$$g_{si1} = f_{6i}\ b_{si}$$

$$= \frac{z\ c_{si}\ l_{si}\ b_{si}}{(z - j_{si})(z(z + a_{2i}) + a_{1i})}$$

$$= b$$

or $$\frac{z\ b_{si}}{(z + a_{2i})\ z + a_{1i}} = \frac{g_{si1}}{g_{si6} c_{si}} \qquad (5.45)$$

Again b_{si}, a_{2i} and a_{1i} can be determined to give a best fit in equation (5.45).

Similar equations can be derived for g_{si2} to g_{si5}. These have the form:

$$\frac{z\ X_j}{(z + a_{2i})\ z + a_{1i}} = \frac{g_{sij}}{g_{si6} c_{si}} \qquad (5.46)$$

where $j = 1$ to 5

and

$$(X_2\ X_3\ X_4\ X_5) = (b_{oi}, b_{ci}, b_{ti}, b_{ai})$$

These five equations may then be scaled and a best fit curve obtained for all five equations. Once a_{2i} and a_{1i} have been defined b_{si} to b_{ti} follow directly.

3) c_{ai} and c_{ti};

$$g_{ai1} = \frac{z \; c_{ai} \; b_{si}}{(z (z + a_{2i}) + a_{1i}} \qquad (5.47)$$

The only unknown is c_{ai} which must be chosen to provide the best fit. c_{ti} is obtained in a similar manner from equation (5.48).

$$g_{ti1} = \frac{z \; c_{ai} \; b_{si}}{z (z + a_{1i}) + a_{1i}} \qquad (5.48)$$

4) d_{ai1}, d_{ai2}, d_{ai3}, d_{ti1}, d_{ti2} and d_{ti3};

$$g_{ai3} = f_{4i} \; c_{ai} \; b_{ci} + d_{ai3}$$

or

$$d_{ai3} = g_{ai3} - c_{ai} \; b_{ci} \; f_{4i} \qquad (5.48)$$

where d_{ai3} is the only unknown and must be chosen accordingly. The same technique may be used to determine the remaining d parameters.

Having found all the parameters in the evaporator state-space model the majority of the parameters in the division wall state-space model are already known. The only unknown parameters are c_{di}, m_{di} and l_{di}.

As for the evaporator, a steady-state equation for the division wall tube surfaces may also be obtained from equation (4.42).

$$S_{di} = \frac{1}{1 - j_{di}} \; (l_{di} \; S_{si-1} + m_{di} \; H_{ri}) \qquad (5.49)$$

where

$$W_{di} = c_{di} \; H_{ri}$$

These equations yield

$$l_{di} = m_{di} = 1 - j_{di} \text{ from equation (4.19)}$$

and

$$c_{di} = 0{,}284 \text{ from equation (5.1)}$$

The assumption was made earlier that the tube surfaces of the division wall and evaporator have identical heat transfer properties. If this condition is applied to equations (5.41) and (5.49) then

$$j_{di} = j_{si} = j_i \qquad (5.51)$$

and

$$l_{di} = m_{di} = l_{si} = m_{si} = 1 - j_i \qquad (5.52)$$

Therefore all the paramaters in the evaporator and division wall state-space models can be identified from their respective transfer fuction models using the techniques described in this section.

5.5 SUMMARY

This chapter has provided a method for determining the parameters of the models suggested in Chapter 4. In doing so, some involved transfer function manipulation was necessary. This was particularly evident in the method for identifying K_{s7}. The technique for obtaining the cell transfer function model from the maximum likelihood model, and later, the cell state-space model from the cell transfer functon model, was expected to be accompanied by reduced model accuracy. The maximum likelihood parameter estimation model places the restriction of first order transfer functions relating inputs to outputs. The mathematics involved in determining the cell transfer function matrices theoretically allows each of these transfer function matrices to be exactly solved, given the maximum likelihood model. In practice further inaccuracies are introduced since the transfer functions are complex and are best simplified to first order transfer functions. These simplified transfer functions then define the cell transfer function model. Further inaccuracies, through simplification, occur when the cell state-space model is obtained, since extensive use is made of best fit techniques.

The motivation for moving right down to the state-space model level must be considered against this expected decrease in model accuracy. The state-space model contains the fewest unknown parameters. 90 parameters are required in the maximum likelihood model definition, 46 in the cell transfer function model definition and

only 18 parameters are required in the state-space model definition. This version then requires the least computation in predicting the attemporater steam condition. This is desirable should the ideas proposed in Chapter 2 be considered at a later date.

CHAPTER 6 A CRITICAL APPRAISAL OF THE ADOPTED APPROACH

6.1 INTRODUCTION

Chapter 5 described how the models developed in Chapter 4 could be realized. It showed that the mathematical techniques existed to identify these models from the logged data. It remains to actually use this method on a suitable set of data to verify the theory.

During the course of the investigation, culminating in the suggested method of Chapter 5, other modelling techniques were considered. Other methods for model identification were investigated before the presented approach was adopted. This chapter discusses the alternative modelling processes as well as some other methods for determining the model parameters. It continues by discussing aspects of the chosen model and reviewing the major assumptions made while developing the chosen model. The technique for determining the model parameters suggested in Chapter 5 is considered and comments are made concerning the attempts to identify the model parameters from the plant data.

6.2 THE EARLIER MODELLING ATTEMPTS

6.2.1 THE PHYSICAL MODEL

One approach for modelling the boiler is to describe its operation with suitable differential equations. These differential equations, with their known parameters, could be linked together to form a suitable system of equations.

A model of this nature requires a fairly extensive knowledge of thermodynamics and heat transfer. The traditional heat equation is well defined but applies to the process of heat conduction. Similar time varying equations for convection and radiation heat transfers are not as well understood. Unfortunately, convection and radiation effects are the major forms of heat

transfer within the boiler.

The process of energy transfer within the boiler is now considered.

The energy of the steam is represented by enthalpy and is obtained from steam tables and the Mollier diagram. Pressure and temperature measurements allow the enthalpy per kilogram of steam to be found. The flow rate of the steam in kg/s allows the enthalpy flow rate to be calculated (MJ/s).

The energy sources available to transfer heat to the steam are described in detail in SECTION 4.3.1. The major source of energy is the pulverised coal. The quality of the coal is continually fluctuating (SECTION 3.3.2). The moisture content, the calorofic content and the volatility of the coal change on a daily basis. This information is available via a "p.oximate" coal analysis performed each day by the station chemist.

The energy available within the furnace can be related to the steam energy using a model for the flame conditions within the furnace. This model enables the temperature of combustion as well as the distance from the flame to the side walls to be calculated. Both of these factors determine how much energy is radiated to the steam surfaces. The nature of fire makes it impossible to assume a constant flame envelope. The method of mixing fuel and air, with swirl vanes, ensures turbulent flow conditions within the furnace. The flame shape and size is therefore constantly in a state of flux. It follows that the rate of energy transfer is also constantly changing. The method best suited for describing these flame conditions assumes a point source providing the same heat transfer characteristics as the flame. The point source has a temperature associated with it which would produce

the same radiation effects as the flame. This temperature, at the flame centre, must be higher than the actual measured temperature to try to compensate for the inverse square law for radiation.

A disadvantage of this model is that convection air flow is dependant on the "upstream" air temperature which has been artificially inflated by the point source model. The point source flame model can still be justified by considering that 80% of heat transfer in the boiler is a result of radiation. The convection effects are therefore of secondary importance.

A model of this form is dependant on a method for determining the combustion temperature of the coal. Any error in this temperature is magnified many times since radiaion is a function of the fourth power of temperature. The combustion temperature could be measured if suitable instrumentation were available. It could then be related to the effective radiation temperature of the point source model.

The heat radiated from the furnace is conducted from the flue gas surface to the steam surface of the steam tubes. This process is modelled by the heat conduction equation. Information about the materials used is required if the tube conduction model is to be identified. The thickness, heat conductivity, absorbtion coefficient, and areas of all the tube surfaces are necessary to enable the rate of heat transfer across the tube boundary and the total amount of energy absorbed to be determined.

Modelling the physical processes taking place within the boiler is not too complex until the effects of combustion are considered. The modelling of heat transfer from a flame or a point source is complex and was considered beyond the scope of this work.

6.2.2 SYSTEM IDENTIFICATION

An alternative method for identifying a model for the boiler plant is to assume no knowledge of the plant , and to attempt to fit a model to input and output data measured from the plant. This then becomes a parameter estimation problem.

A review of some available parameter estimation techniques was made. The paper by Astrom, (1971) gives an excellent survey on model classification and model identification. The off-line nature of the identification problem allowes more freedom in the choice of modelling techniques. The majority of identification algorithms revolve around the least-squared error algorithm. The technique used to solve for the parameters in a discrete time input/output system is similar to the technique used to solve for the parameters in a state-space discrete time model. Both use variations on the least-squared error algorithm (Graupe, 1972 and Eykhoff, 1974). A parametric model for input/output sequences has the limitation that only the completely controllable and completely observable modes of the system can be identified. Access to state-space variable measurements ensures the complete definition of a state-space system, including its unobservable and uncontrollable modes.

Consider a state-space model for the boiler; two classes of variables may be used as state-space variables, namely temperature measurements or energy flow measurements. The cycle of interest in the boiler is primarily an energy cycle, so the choice of temperature or energy flow measurements must enable the radiation and convection energy transfers to be measured. Temperature measurements of the steam, flue gases and temperatures of combustion are representative of the energy distributed around the system. Unfortunately, a system using temperatures as its state variables

incorporates many non-linearities. The two most striking are the relationship between temperature and radiated energy, and the relationship between steam temperature and steam enthalpy. Radiation is a function of the fourth power of temperature and enthalpy is a non-linear function of pressure and temperature. These non-linearities can be avoided if energy flow measurements are used as the state variables.

The model suggested in SECTION 4.3 divides the boiler along its height. Reasonable state variables are steam and flue gas enthalpy flow measurements at various levels within the furnace. (SECTION 6.2.1). These values could be obtained if the required instrumentation at all levels was available. This instrumentation is not available and so direct or indirect measurements of the proposed state variable were not possible. A state-space model was therefore not feasible.

The alternative approach is to fit a transfer function model involving only input and output data streams. The model takes the form of several 'Z' plane transfer functions representing auto-regressive moving average models. A variation of the least squared error technique (a maximum likelihood parameter estimation method) is used to determine the model of equation (5.14)

6.2.3 A COMBINATION OF THE PHYSICAL INSIGHT AND SYSTEM IDENTIFICATION TECHNIQUES

A model of the form suggested by equation (5.14) is sufficient for use as a simulation model for the fast-time predictor instrument, if all the burner inputs are related to the model outputs. That is, there are no undetermined transfer functions in equation (5.14).

CHAPTER 6 A CRITICAL APPRAISAL OF THE ADOPTED APPROACH

It is normal procedure to use only 4 burners at full load. Some undetermined transfer functions will exist under these conditions. It is then not possible to determine the relationships between the unused burners and the outputs.

Data logged at a later date may include these transfer functions relating the previously unused mills to the outputs. The second data log could occur under different conditions to those prevailing at the time of the original logged data. Differences in conditions, resulting from inputs not considered, could bias the obtained model The unavailable transfer functions are required if the effect of any burner on the output is to be predicted.

Further motivation for continuing the modelling process down to a cell model level is the additional information that would be available from the cell model outputs. These could provide valuable information on excessive metal stresses elsewhere in the furnace. Irregularities indicated by the model could be tested for by the introduction of additional instrumentation. The effect would be a more accurate simulation and fast-time model, and hence a more accurate predictor instrument.

As discussed in SECTION 4.5.1, the boiler is divided into nine cells. The most significant assumption about these cells is that cells two to seven are assumed identical. Each of the nine cells can be modelled by either a state-space model or by a transfer function model. No measurements of the outputs to each cell are available. The outputs for the i'th cell are Q_{ai}, T_i, S_{si} and S_{di}. The models must then be determined by algebraic manipulation so that the parameters of the chosen cell models can be related to the maximum likelihood parameter model (Equation 5.14).

CHAPTER 6 A CRITICAL APPRAISAL OF THE ADOPTED APPROACH

The initial approach was to cascade the nine state-space cell models, and from the cascaded state-space model to determine its transfer function equivalent using equation (5.37). An approach of this nature initially gave a state-space model with fifty-four state variables. At this early stage a high order model was used to model the furnace dynamics. It was initially believed that the system had a few poles at the origin in the 'S' plane. These poles are part of fast furnace dynamics. Later simplification resulted in a simpler twenty-seven order system. The size of the state-space system prompted a brief investigation into model reduction techniques (Graupe, 1968). The algebraic form for the cascaded state-space model produces a near diagonal system matrix. The matrix contained predominantly zero elements. The diagonal matrix results from the uniformity of each cell and the chosen form of the cell state-space model. (Equations 4.44 and 4.45). A downfall of model reduction techniques, in this application, is that the more the order of the model is decreased, the stiffer the system matrix becomes. The lower order matrices are therefore more complex than the predominantly zero original matrices. A second problem is that model reduction techniques are based on rejecting all but the dominant eigenvalues. In this case the eigenvalues appear in algebraic form and so the dominant eigenvalues cannot be determined.

The procedure for solving for the state-space cell model parameters in the cascaded state-space model is complex. An iterative procedure must be used to relate the parameters in the cascaded state-space model to parameters in the maximum likelihood model. The iteration procedure is complete when chosen parameters in all the cell state-space models give a good approximation to the maximum likelihood model.

A simpler method for identifying a model for each cell is to fit a transfer function model to each cell. The cell transfer function models, when cascaded, give the equations (4.37) and (4.38). The method for determining the cell transfer function models is considerably more direct than the method for obtaining parameters in the large state-space system. A large amount of transfer function polynomial manipulation is required. This simpler approach was the method adopted for obtaining cell models from the maximum likelihood model.

6.3 THE CHOSEN MODEL

The method for obtaining a suitable cell model for predicting the effect of any burner on the outputs may be summarized as follows. A maximum likelihood parameter estimation technique is used to relate available inputs to outputs of interest. This information is used to determine parameters in the cell transfer function models. The parameters are obtained by equating transfer functions in equations (4.37) , (4.38) and (5.14). Finally a state-space model is determined that best fits the cell transfer function model.

The modelling process could have been considered complete after the cell transfer function model had been found. The process was however continued to include a method for determining a cell state-space model. The motivation for continuing to a state-space cell model is twofold. The cell state-space model is simpler to implement as a predictor algorithm. The discrete form for a state-space model is a one-step-ahead-state-variable predictor. Secondly it contains fewer variables (SECTION 5.5) and so requires fewer calculations to implement than the cell transfer function model. The simplicity or high number of zero terms in the cell state-space model matrices (Equations 4.44 and 4.45) is a result of the chosen canonical form as well as the insight provided by the steady-state analysis of SECTION 4.4.

CHAPTER 6 A CRITICAL APPRAISAL OF THE ADOPTED APPROACH

A simpler method for identifying a model for each cell is to fit a transfer function model to each cell. The cell transfer function models, when cascaded, give the equations (4.37) and (4.38). The method for determining the cell transfer function models is considerably more direct than the method for obtaining parameters in the large state-space system. A large amount of transfer function polynomial manipulation is required. This simpler approach was the method adopted for obtaining cell models from the maximum likelihood model.

6.3 THE CHOSEN MODEL

The method for obtaining a suitable cell model for predicting the effect of any burner on the outputs may be summarized as follows. A maximum likelihood parameter estimation technique is used to relate available inputs to outputs of interest. This information is used to determine parameters in the cell transfer function models. The parameters are obtained by equating transfer functions in equations (4.37) , (4.38) and (5.14). Finally a state-space model is determined that best fits the cell transfer function model.

The modelling process could have been considered complete after the cell transfer function model had been found. The process was however continued to include a method for determining a cell state-space model. The motivation for continuing to a state-space cell model is twofold. The cell state-space model is simpler to implement as a predictor algorithm. The discrete form for a state-space model is a one-step-ahead-state-variable predictor. Secondly it contains fewer variables (SECTION 5.5) and so requires fewer calculations to implement than the cell transfer function model. The simplicity or high number of zero terms in the cell state-space model matrices (Equations 4.44 and 4.45) is a result of the chosen canonical form as well as the insight provided by the steady-state analysis of SECTION 4.4.

CHAPTER 6 A CRITICAL APPRAISAL OF THE ADOPTED APPROACH

The accuracy of the cell transfer function and state-space models depends on whether sufficient inputs have been considered for the assumed linear model to be identified. (SECTION 6.2). A single linear model is assumed to be sufficient over the whole range of inputs and outputs. The choice of variables was made to try and eliminate any non-linearities. An alternative approach would be to form a piecewise linear model should the non-linearities be shown to be significant.

During the course of this report many assumptions are made concerning variables omitted from the chosen model. It is possible that these are sufficiently important to warrant their inclusion in the models. A list of these assumptions appears below. A reference to other sections of this report is included whenever the assumptions have been previously justified.

1) The air required to burn the oil to completion was ignored (SECTION 4.3.2.1).

2) The primary air flow was ignored (SECTION 4.3.1.1).

3) Re-radiation effects were ignored (SECTION 4.3.1.1).

4) The differences in the materials used in the division wall and evaporator were ignored (SECTION 4.3, Equation 4.11). The materials are different as evidenced by the different heat absorbtion rates quoted in SECTION 4.3.2.1 and SECTION 4.3.2.2.

5) The effects of mill biasing were ignored (SECTION 4.3.1.1).

6) The left and right halves of the boiler were assumed to behave identically. The coal flow rates and the air flow rates in each half may differ slightly. This is due to the action of independant damper controllers which control the air and pulverised fuel flow at each of the 24 burners.

   Excessive differences in each half of the boiler are not desirable since these differences may cause

pressure differential and temperature gradients across the division wall which could cause stress failures.

7) The temperature and enthalpy of the air at the base of the furnace was ignored. These were omitted from the model because the error in the energy balance resulting from this assumption was believed to be small. This was never verified. Suitable measurements were not available.

8) The air/fuel ratio was assumed constant. Over a long period of time changes in coal quality require accompanying changes of oxygen to ensure that the coal burns to completion. This variable was omitted from the models. It was assumed that over the time-span of the measured data this parameter remained constant. Measurements of the air/fuel ratio were not available; therefore this assumption was not verified. In the long term the model parameters would have to be tuned to cater for fluctuations in the air/fuel ratio.

9) The argument above can be extended to involve variations in the "proximate" analysis. Changes in volatility and calorific content of the coal upset the heat balance equation. Model parameters would require tuning to cater for the variations in the coal quality.

10) The effect of the economiser on the first steam attemporator outlet was ignored. Heat from the flue gases is transferred to the economiser pre-warming the division wall inlet water. Very early attempts at finding a model included the economiser. The economiser tubes were modelled as a simple single pass heat exchanger (Nicholson, 1980). At a later stage it was decided that the energy transferred to the economiser was not significant. Only 20% of the available energy rises into the convection zone of the furnace. Only a fraction of this passes over

the economiser tubes. The flue gas temperature drop across the economiser at full load is typically 100°C.

This list justifies the chosen model variables of FIGURES 4.4 and 4.5. The form of the transfer function model requires no further discussion other than to mention that since re-radiation effects are ignored Q_{a9}, T_9, Q_{a7} and T_7 are independant of S_{do} (Equations 4.19 and 4.20).

The form for the state-space model was discussed in SECTION 4.6. The assumption of a second order furnace model was based on the simplest transfer function capable of producing an overshoot (to indicate marginal flame stability). A controllable canonical form for the furnace was chosen because it suited the steady-state analysis of SECTION 4.4. Finally the outputs Q_{ai} and T_i were assumed to have negligible time constants. That is the gas dynamics for the state-space model are assumed to be identical.

Having found satisfactory cell models, the technique for determining the model parameters may be discussed.

6.4 THE METHOD FOR DETERMINING THE MODEL PARAMETERS

6.4.1 THE MAXIMUM LIKELIHOOD MODEL

It was necessary to fit a transfer function model to the input and output data obtained from the plant (Appendix K). The maximum likelihood estimation package was chosen from the IMSL. This best suited the requirements for obtaining a transfer function model. The technique takes into account correlations between various inputs and therefore produces a less biased parameter estimation than would be obtained from a simple least squared approach. The package enables the number of inputs to be easily changed. The order of the model may easily be changed to obtain a better fit. In this case, only a first order fit was attempted

(Equation 5.13). Techniques do exist for determining at which stage minimal model improvement has resulted from an increase in order (Strejc, 1980).

Available packages were used, rather than self-written packages, since the IMSL packages are well tried and tested. They provide warning codes or terminal error codes if they are unable to perform the given task. Re-writing available software is time consuming and not as reliable. The calling programme written to use the IMSL packages is fairly compact. Its modular form was simple to debug given the reliability of the IMSL packages.

In SECTION 5.3 it was mentioned how some pre-processing of data was required to condition it for use in the parameter estimation algorithm. The majority of the time-sequences require little or no pre-processing, however there are some exceptions. These parameters are listed along with assumptions made in determining their respective time sequences.

1) The steam enthalpy flow rate at the inlet to the division wall, S_{do}, was assumed to be a function of temperature, pressure and flow rate. Pressure and temperature measurements of superheated steam are sufficient to define the enthalpy of the steam. The conditions at the division wall inlet are such that there is a mixture of phases. The percentage moisture content at the division wall inlet was not available. This is essential to accurately determine the enthalpy/kg. A volumetric flow rate measurement at this point, as well as the mass flow rate, would give an indication of the percentage of water that has been converted to steam thus enabling a more accurate value for the enthalpy/kg to be obtained.

   As the load on the boiler unit increases the moisture content at the division wall inlet

increases until it is 100% water. The point at which the flow is made up of only water is well defined on the Mollier diagram. The initial state, at the division wall inlet, of the measured data is that of superheated steam (This is possible because in the early stages of the start-up the flow rate is very low). Interpolation between these two unique points is used to determine the enthaply/kg at a given pressure and temperature, but at an unknown moisture content. The enthalpy flow rate in MJ/s is then obtained by multiplication of the enthalpy with the mass flow rate.

2) The enthalpy flow rate at the evaporator outlet, S_{s9}, is obtained without the problems associated with S_{do}. At nearly all times the temperature and pressure measurements at the evaporator outlet define unique points on the Mollier diagram. Deviations into saturated steam regions are few in number. The enthalpy flow rate is obtained by making use of the mass flow rate as described above.

The data collected from the plant did not include temperature and pressure measurements at the evaporator outlet but included temperature and pressure measurements at the attemperator outlet. The steam enthalpy flow rate at the outlet of the first attemperator was used. The quantity of attemperating water added to the steam flow is small. Its effect on the enthalpy flow rate is minimal.

3) The enthalpy flow rate at the outlet of the 7th cell, S_{s7}, was obtained as a function of S_{do} and S_{s9} (Appendix E). Temperature and pressure measurements of the steam condition at the outlet of the 7th cell do not exist. The assumption was made that by the time the steam reached the output of cell 7 it had absorbed 80% of the

available energy. This is justified by considering that 80% of energy is transferred due to radiation effects in the combustion zone (S_{s7} is the enthalpy flow rate just above the 'A' level burners).

4) The temperature of the flue gases at the outlet of the 9th cell was measureable. This is representative of the energy left in the flue gases after passing through the 9th cell. This is after energy has been extracted by all the tube banks in the convection zone of the boiler. The model chosen does not consider this energy loss. These tube banks were ignored. For this reason the flue gas temperature just below the economiser is used. For the purposes of the chosen model this is a better indication of the flue gas energy at the outlet of the 9th cell. It is a compromise resulting from not considering the tube banks and allows the conservation of energy to apply within the framework of the chosen model.

5) The flue gas enthalpy flow rates Q_{a9} and Q_{a7} were assumed to be functions of temperature, air/fuel ratio and coal flow rate. Pressure has been assumed to be 1 atmosphere. The deviation from this seldom exceeds 100Pa. The enthalpy/kg is then obtained as a function of temperature from the gas tables. The mass flow rate of the air is obtained from A/f and the total coal flow rate. The product of the enthalpy/kg and the air mass flow rate yields the enthalpy flow rate in MJ/s.

The quality of the data used in the maximum likelihood parameter estimation technique has been discussed in this section. The effectiveness of the modelling technique using the available non-ideal data is discussed below.

CHAPTER 6 A CRITICAL APPRAISAL OF THE ADOPTED APPROACH

It was not possible to obtain a satisfactory identification of the model described by equation (5.14). Results, from the parameter estimation calling programme were transferred to a comparison utility. This enabled the output time series to be predicted from the input data. All attempts at re-organising data, ignoring selected inputs and reducing the size of the data set failed to produce an acceptable model.

The reconstructed output time sequences for the steam enthalpy flow rates $\$_{s7}$ and $\$_{s9}$ were the only time sequences that were of the same order as the measured output data. The other model outputs T_9, T_7, $\$_{a9}$ and $\$_{a7}$ gave totally unacceptable output time sequences. The importance of this observation is that the steam conditions change at a relatively slow rate when compared with the flue gas dynamics. This probably indicates that the failure of the suggested method may be attributed to a violation of the Nyquist sampling theorem. The logged data was sampled once every five minutes. In retrospect the speed of response of the flue gas dynamics is considerably faster than this. Even the dynamics of the steam tubes are probably many times faster than the sampling rate of once every five minutes suggests.

The decision had been made at an earlier stage not to collect additional data from the plant. The data already available was to be used. This original data was not ideally suited to the task. As discussed earlier in this section and in SECTION 3, not all the relevant data points were logged. The omission of certain data was overcome as illustrated in Chapter 5. After having attempted to identify the maximum likelihood model a further inadequacy of the data has been highlighted: that is, the probable violation of the Nyquist sampling theorem.

No attempt at actually obtaining model parameters

progressed beyond this point. The steady-state analysis of SECTIONS (4.4) and (5.2) was never used, as intended, to test the validity of the identified models. The steady-state analysis did serve a valuable purpose in determining the state-space model as well as providing additional insight into the modelling problem.

6.4.2 THE CELL TRANSFER FUNCTION MODELS

In order to obtain a cell transfer function model of the form shown in equations (4.30) and (4.31) it was necessary to equate transfer functions in the cascaded cell model (Equations 4.37 and 4.38) with those in the maximum likelihood model (Equation 4.14). Some complicated expressions resulted in solving transfer function matrices from the division wall and evaporater models. Assumptions were made in SECTION 5.3.2 aimed at simplifying the process of equating coefficients to a level from which results could be obtained. This complexity arose as a direct result of not having available the steam enthalpy flow rate, S_{so}. Much simpler mathematics could have been used to determine the cell transfer function models of equations (4.30) and (4.31) had S_{so} been available. The necessary data points exist but did not appear on the logged data.

If S_{so} had been available it would not have been necessary to relate K_{s7} to K_{d7}, F_s to F_d or H_s to H_d. These could have been identified in their own right. The obtained model would have been expected to be more accurate, more robust and more reliable.

6.4.3 THE STATE-SPACE MODELS

The method for obtaining the cell state-space model from the cell transfer function model could be improved upon if measurements of some of the state-

variables were possible. The outlet of each cell S_{s1} could theoretically be measured as could the energy available at the centre of the cell. These measurements are not available.

The form of the model was never tested. It has the attraction that it involves relatively few parameters when compared with the maximum likelihood model and the cell transfer function model (SECTION 5.5). Its sparse nature and convenient predictive form are ideal for the intended fast-time model. It is not known whether the decrease in the number of parameters and increase in the model simplicity is compromised by a degradation of the simulation performance.

6.5 SUMMARY

This chapter is aimed at providing some insight into the thoughts behind the adopted model. It attempted to show how the model evolved within the limitations of the available data. The methods for obtaining the model parameters were discussed. The sampling rate is suggested as a possible reason for the failure of the maximum likelihood parameter estimator to yield a satisfactory model identification. This was believed to be too slow to capture the fast dynamics of the steam tubes and of the flue gases. Methods for improving the chances of obtaining a model, using the maximum likelihood parameter estimator, were discussed. The final chapter of this dissertation considers future work and major conclusions.

CHAPTER 7 CONCLUSION AND RECOMMENDATIONS

The final chapter in this dissertation is divided into two sections. The approach adopted to the problem described in Chapter 1 is outlined in the conclusion along with important conclusions resulting from this study. Areas for future work, to extend on this investigation, are recommended.

7.1 CONCLUSION

A fast time predictor instrument for supplying the operator with additional information was suggested in Chapter 2. This was tested against other methods for boiler control in Chapter 3. A simulation model, enabling a fast time predictor instrument to be tested and developed, was discussed in Chapter 4. A technique for identifying model parameters was suggested in Chapter 5. Only half hour of data collected at an early stage of this work. It was decided to try to obtain the model parameters from this data although it was not suitable for the task (SECTION 6.4.1). Assumptions were made in SECTION 5.7.2 enabling the inadequacies of the input data to be overcome. The technique failed to produce a satisfactory identification of the model parameters. This was attributed to non-ideal data as well as violation of the Nyquist sampling theorem.

This study has indicated that the plant investigated is complex. It has however been shown that it is still possible to model the boiler processes. It is believed that the advantages of successfully implementing a fast-time predictor instrument are enormous. This investigation would be worth continuing if the problem of parameter estimation can be overcome.

7.2 RECOMMENDATIONS

The data obtained from the plant was in the form of a tabular computer print out. The process of entering this data onto another computer is time consuming and error prone. If the investigation is to be continued,

then the data could be logged directly to a mass storage device. The data is available from the analogue signal marshalling racks in the unit control rooms. These voltages may be sampled by a seperate data acquisition system.

2) The technique used, in Chapter 5 to try to obtain parameters for the models in Chapter 4, could be simplified if more appropriate data points were collected in a new data log (SECTION 6.4.1). Because the system response times were faster than anticipated the new data should be logged at a faster rate one sample every 30s).

3) The assumptions listed in SECTION 6.3 require verification. If it is still not possible to identify a model after recommendation 2) has been considered, then this may indicate that these assumptions (SECTION 6.3) are false.

4) Once a model for the cells is obtained and the modelling process completed, it will be possible to test the performance of the simulation when the cell transfer function models and the cell state-space models are used in the simulation. An indication will then be available on the degrading of the simulation performance at different stages of the modelling process. This must be viewed against the corresponding reduction in the model complexity.

5) Extra instrumentation could be added to the boiler enabling more information about temperature and pressure profiles of the water/steam and flue gases to be collected. This would enable a more accurate simulation model to be obtained since additional cell model inputs and outputs would be available. . This would remove the necessity for having to resort to the transfer function manipulation of SECTION 4.5.

6) In the longer term, some work is required on the man-machine interfaces. That is, how best to

implement a fast time predictor instrument and how to present the information to the operator. Once a satisfactory simulation model has been found, it would then be possible to design and test the predictor instrument in a relatively short time.

REFERENCES

1. ASTROM, K.J ; EYKHOFF, P. (1979) "System Identification - A Survey." Automatica, Volume 7 pp 123 - 162: Great Britain: Pergamon Press.

2. ASTROM, K.J; WITTENMARK, B. (1973) "On Self-Tuning Regulations" Automation, Vol.9, pp 123 - 162: Great Britain: Pergamon Press.

3. ASTROM, K.J; BORISSON, U; LJUNG, L; WITTENMARK, B (1977) "Theory and Application of Self-Tuning Regulations." Automatica, Vol 13, No 5, pp 457 - 476: Great Britain: Pergamon Press.

4. BABCOCK AND WILCOX COMPANY. (1955) Steam - Its Generation and Use: 37th Ed. New York: Babcock and Wilcox.

5. CENTRAL ELECTRICITY GENERATING BOARD. (1971) Modern Power Station Practice , Volume 2: 2nd Ed. Oxford: Pergamon Press.

6. DORF, R.C. (1980) Modern Control Systems: 3rd Ed. Reading: Addison-Wesley.

7. DUDA, R.O ; GASCHNIG, J.G. (1981) "Knowledge Based Expert Systems Come of Age." Byte, September 1981: New York: Byte Publications, McGraw-Hill.

8. ELGERD, O.I. (1967) Control Systems Theory. Electronic and Electrical Engineering Series: Kogakusha: McGraw-Hill.

9. ESCOM. Notes on Basic Power Station Operation: Training Centre, Johannesburg: Electricity Supply Commission.

10. ESCOM. Visitors Information Brochure - Duvha Power Station: Witbank: Electricity Supply Commission.

11. EYKHOFF, P (1974) System Identification: Great Britain: John Wiley & Sons.

12. GRAUPE, D. (1972) Identification of Systems: New York: Von Nostrand Reinhold Company.

13. GRAUPE, D ; SWANICK, B.H ; CASSIR, G.R. (1968) " Reduction and Identification of Multi-variable Processes Using Regression Analysis." IEEE Transactions on Automatic Control, October 1978: New York: IEEE Press.

14. HOLMAN, J.P. (1980: Thermodynamics: 3rd Ed. Tokyo: McGraw-Hill.

15. HOLLIS, P.C. (1982) Guide to Boiler Optimisation: Duvha, Witbank: Electricity Supply Commission.

16. KEENAN, J.H ; KEYES, F.G ; HILL, P.G ; MOORE, J.G. (1978) Steam Tables (SI - Units): New York: John Wiley & Sons.

17. KEENAN, J.H ; CHAO, J ; KAYE, J. (1983) Gas Tables - International Version: New York: John Wiley & Sons.

18. KELLEY, C.R. (1958) "A Predictor Instrument for Manual Control." 8th Annual Office of Naval Research, Human Engineering Conference, Ann Arbor, Michigan: September 25.

19. KELLEY, C.R. (1962) "Predictor Instruments Look into the Future. Control Engineering: March 1962.

20. McCORMICK, E.J. (1964) Human Factors Engineering: New York: McGraw-Hill.

21. MERRY, M. (1983) "An Expert System Shell for Fault Diagnosis." The GEC Journal of Research. Volume 1. No 1 pp 39 - 47.

22. NICHOLSON, H. (1980). Modelling of Dynamic Systems, Volume 1: Exeter: Peter Peregrinus LTD.

23. OWENS, D.H. (1978) Feedback and Multivariable Systems: 1st Ed. Stevenage: Peter Peregrinus.

24. OWENS, D.H. (1981) Multivariable and Optimal Systems: New York: Academic Press.

25. PITTS, D.R ; SISSOM, L.E. (1977) Heat Transfer. Schaum Outline Series: New York: McGraw-Hill.

26. RIEPE, J. (1983) "The Design of an On-Board Look-Ahead - Simulation for Approach." Simulation In Engineering Sciences: Elsevier Science Publishers, IMACS.

27. SCHWEPPE, F.C. (1973) Uncertain Dynamic Systems. Electrical Engineering Series: New Jersey: Prentice Hall.

28. SHERIDAN, T.B.; FERREL, W.R. (1974) Man - Machine Systems: Cambridge, Massachusetts: MIT Press.

29. STREJC, C (1980) "Least Squares Parameter Estimation." Automatica, Volume 16, pp 535 - 550: Great Britain: Pergamon Press.

APPENDIX A TWO METHODS FOR LINEARIZATION OF THE HEAT RADIATION EQUATION

METHOD ONE: TAYLOR'S LINEARIZATION

Linearization is required about the point T_s which has lies between the upper and lower temperature limits T_2 and T_1.
The equation is:-

$$Q = A\sigma T^4$$

The Taylor expansion is

$$Q = A\sigma T_s^4 + 4 A\sigma T_s^3 (T - T_s)$$

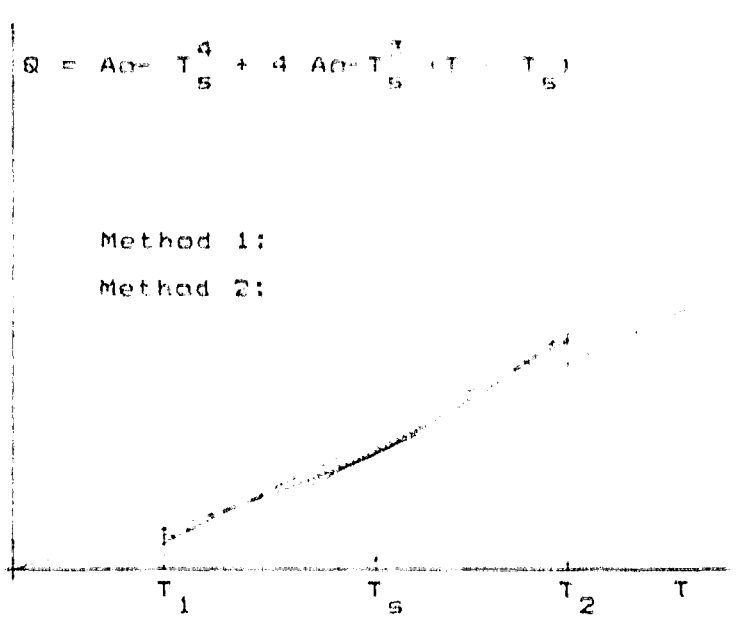


FIGURE A.1: LINEARIZATION OF THE HEAT RADIATION EQUATION

The greater the distance of T from T_s the greater the error. This is an acceptable technique when T_s is the steady state temperature and T always returns to T_s. An alternative technique to always keep the error to a minimum for any temperature within T_1 to T_2 follows:-

METHOD TWO: THE LEAST SQUARED ERROR

This is based on minimising the mean squared error over the interval T_1 to T_2

$$E = \int_{T_1}^{T_2} (A\sigma T^4 - A\sigma (mT + C))^2 \, dT$$

Require $dE/dm = 0$ and $dE/dc = 0$

for the error to be minimised

$$E = (T_2^6 - T_1^6)/6 - 2m(T_2^5 - T_1^5)/5 + (mT_2 + c)^3/3m - (mT_1 + c)^3/3m \quad \text{(A.1)}$$

$$\frac{dE}{dm} = -(T_2^6 - T_1^6)/3 + (mT_2 + c)^2 T_2/m - (mT_1 + c)^2 T_1/m = 0 \quad \text{(A.2)}$$

$$\frac{dE}{dc} = -2(T_2^5 - T_1^5)/5 + (mT_2 + c)^2/m - (mT_1 + c)^2/m = 0 \quad \text{(A.3)}$$

Equations (A.2) and (A.3) are two equations in two unknowns. The variables m and c can be solved for in terms of T_2 and T_1.

∴ The linearized version of the heat radiation equation is then

$$Q = A\sigma\varepsilon(mT + c)$$

APPENDIX B DERIVATION OF THE CASCADED CELL MODEL FROM THE SINGLE CELL MODEL

The cell equations for the division wall and the screw wall are:-

$$X_{d1} = K_{d1}\, X_{d1-1} + H_{d1}\, Y_1 + F_{d1}\, T_S \qquad \text{(B.1)}$$

$$X_{s1} = K_{s1}\, X_{s1-1} + H_{s1}\, Y_1 + F_{s1}\, T_S \qquad \text{(B.2)}$$

The cascaded cell models for the division wall and the screw wall are:

$$X_{d9} = K_{d9}\, K_{d8} \left\{ K_{d7}^{6}\, K_{d1}\, X_{d0} + \sum_{i=5}^{0} K_{d7}^{i}\, H_d\, Y_{7-i} \right.$$

$$\left. = \left(I - K_{d7}^{5} \right) \left(I - K_{d7} \right)^{-1} F_d\, T_S \right\} \qquad \text{(B.3)}$$

$$X_{s9} = K_{s9}\, K_{s8} \left\{ K_{s7}^{6}\, K_{s1}\, X_{s0} + \sum_{i=5}^{0} K_{s7}^{i}\, H_s\, Y_{7-i} \right.$$

$$\left. + \left(I - K_{s7}^{5} \right) \left(I - K_{s7} \right)^{-1} F_s\, T_S \right\} \qquad \text{(B.4)}$$

S_{s0} which equals S_{d9} must be eliminated in equations (B.3) and (B.4)

Let $K_{d1} = \left(M_{d1}\ N_{d1} \right)$ $\qquad$ $K_{s1} = \left(M_{s1}\ N_{s1} \right)$

$$K_{d9}\, K_{d8} = K_{d98} = \begin{Bmatrix} k_{a98} \\ k_{t98} \\ k_{d98} \end{Bmatrix} \quad ; \quad K_{s9}\, K_{s8} = K_{s98} = \begin{Bmatrix} k_{a98} \\ k_{t98} \\ k_{s98} \end{Bmatrix}$$

$$\text{where } M_{d1} = \begin{Bmatrix} g_{a14} & g_{a15} \\ g_{t14} & g_{t15} \\ g_{d14} & g_{d15} \end{Bmatrix} \quad ; \quad M_{s1} = \begin{Bmatrix} g_{a14} & g_{a15} \\ g_{t14} & g_{t15} \\ g_{s14} & g_{s15} \end{Bmatrix}$$

$$N_{d1} = \left(0\ 0\ g_{d16} \right)^T \quad ; \quad N_{s1} = \left(0\ 0\ g_{s16} \right)^T$$

Also $\qquad X_{s0} = \left(Q_{a0}\ T_0\ S_{s0} \right)$ $\qquad$ $\left(\ldots_{d0}\ T_0\ S_{d9} \right)^T$

$$k_{a98} = \left(g'_{a94}\ g'_{a95}\ 0 \right) \qquad k_{t98} = \left(g'_{t94}\ g'_{t95}\ 0 \right)$$

$$k_{d98} = \left(g'_{d94}\ g'_{d95}\ g'_{d96} \right) \qquad k_{s98} = \left(g'_{s94}\ g'_{s95}\ g'_{s96} \right)$$

Then

$$X_{s9} = K_{s98} \left(K^{6}_{s7} M_{s1} \begin{Bmatrix} Q \\ T_0 \end{Bmatrix}_{ao} + K^{6}_{s7} N_{s1} S_{d9} + \sum_{i=5}^{0} K^{1}_{s7} H_s Y_{7-1} + \left(I - K^{5}_{s7} \right) \left(I - K_{s7} \right)^{-1} F_s T_s \right) \quad \text{(B.5)}$$

$$S_{d9} = k_{d98} \left(K^{6}_{d7} M_{d1} \begin{Bmatrix} Q \\ T_0 \end{Bmatrix}_{ao} + K^{6}_{d7} N_{d1} S_{do} + \sum_{i=5}^{0} K^{1}_{d7} H_d Y_{7-1} + \left(I - K^{5}_{d7} \right) \left(I - K_{d7} \right)^{-1} F_d T_s \right) \quad \text{(B.6)}$$

Substituting equation (B.6) into equation (B.5) yields :-

$$\begin{aligned} \dashrightarrow \quad X_{s9} = k_{s98} \Bigg\{ & K^{6}_{s7} \left(M_{s1} + N_{s1} k_{d98} K^{6}_{d7} M_{d1} \right) \begin{Bmatrix} Q \\ T_0 \end{Bmatrix}_{ao} \\ & + K^{6}_{s7} N_{s1} k_{d98} K^{6}_{d7} N_{d1} S_{do} \\ & + \left(K^{6}_{s7} N_{s1} k_{d98} \sum_{i=3}^{0} K^{1}_{d7} H_d + \sum_{i=5}^{0} K^{1}_{s7} H_s \right) Y_{7-1} \\ & + \left(K^{6}_{s7} N_{s1} k_{d98} \left(I - K^{5}_{d7} \right) \left(I - K_{d7} \right)^{-1} F_d \right. \\ & \left. + \left(I - K^{5}_{s7} \right) \left(I - K_{s7} \right)^{-1} F_s \right) T_s \Bigg\} \end{aligned} \quad \text{(B.7)}$$

APPENDIX C THE LIST OF POINTS USED FROM THE LOGGED DATA

Point No	Point Description	Purpose	Required by Variable
NA10F002	Division wall flow rate (mass)	Obtain enthalpy flow rate	S_{do}
NA10T004	Division wall inlet temperature	Look up enthalpy in steam tables	S_{do}
NA10P002	Division wall inlet pressure	Look up enthalpy in steam tables	S_{do}
NA10F002	Evaporator flow rate (mass)	Obtain enthalpy flow rate	S_{s9}
NA21T007	Evaporator outlet temperature	Look up enthalpy in steam tables	S_{s9}
NA21P004	Evaporator outlet pressure	Look up enthalpy in steam tables	S_{s9}
NS01T001	Secondary air temperature	-	T_5
NR11T001	Screw wall outlet/ upper part inlet flue gas temperature	Flue gas enthalpy flow rate & temp	T_7, Q_{a7}
NR11T007	Flue gas upper part outlet temperature	Flue gas enthalpy flow rate	T_9, Q_{a9}
NM10FC01	Mill A feeder flow rate	-	F_{c7}
NM20FC01	Mill B feeder flow rate	-	F_{c3}
NM30FC01	Mill C feeder flow rate	-	F_{c5}
NM40FC01	Mill D feeder flow rate	-	F_{c6}
NM50FC01	Mill E feeder flow rate	-	F_{c2}
NM60FC01	Mill F feeder flow rate	-	F_{c4}
Hand Logged	Level A oil flow rate rate	-	F_{o7}
Hand Logged	Level B oil flow rate rate	-	F_{o3}

Point No	Point Description	Purpose	Required by Variable
Hand Logged	Level C oil flow rate rate	-	F_{o5}
Hand Logged	Level D oil flow rate rate	-	F_{o6}
Hand Logged	Level E oil flow rate rate	-	F_{o2}
Hand Logged	Level F oil flow rate rate	-	F_{o4}

APPENDIX D THE IMSL ROUTINES

The Fortran programme written, to determine the transfer function model of equation (3.14), has the task of transferring the correct data to and from the library routine FTWENX. The programme specification for FTWENX is included in this appendix Many other library routines are required to enable FTWENX to run. These are considered to be of secondary importance and hence no programme specification is supplied.

IMSL ROUTINE NAME - FTWENX

PURPOSE - MAXIMUM LIKELIHOOD PARAMETER ESTIMATES FOR A MULTICHANNEL, SINGLE OUTPUT TIME SERIES MODEL

USAGE - CALL FTWENX (X,IX,NS,LS,IP,LAG,ID,R,IR,T,PMAC, WK,IER)

ARGUMENTS

X - INPUT MATRIX OF DIMENSION LS BY NS CONTAINING NS TIME SERIES, OF WHICH X(*,1) IS THE BASE TIME SERIES OR OUTPUT CHANNEL.

IX - INPUT ROW DIMENSION OF THE MATRIX X EXACTLY AS SPECIFIED IN THE DIMENSION STATEMENT IN THE CALLING PROGRAM.

NS - INPUT NUMBER OF TIME SERIES. NS MUST BE GREATER THAN OR EQUAL TO ONE.

LS - INPUT LENGTH OF EACH TIME SERIES. LS MUST BE GREATER THAN OR EQUAL TO ONE.

IP - INPUT VECTOR OF LENGTH NS. IP(I) CONTAINS THE NUMBER OF REGRESSIVE PARAMETERS (IN THE DIFFERENCED FORM OF THE MODEL) ASSOCIATED WITH TIME SERIES I, I=1,2,...,NS. IP(I) MUST BE GREATER THAN OR EQUAL TO ZERO FOR I=1,2,...,NS.

LAG - INPUT VECTOR OF LENGTH NS. LAG(I) CONTAINS THE LAG OF TIME SERIES I WITH RESPECT TO THE BASE TIME SERIES. LAG(I) MUST BE GREATER THAN ZERO FOR I=1,2,...,NS.
NOTE THAT LS MUST BE GREATER THAN OR EQUAL TO THE MAXIMUM OF (LAG(I)+IP(I)) FOR I=1,2,...,NS.

ID - INPUT VECTOR OF LENGTH NS. IF ID(I) = 0, THE TIME SERIES I IS TO BE TRANSFORMED BY REMOVING THE MEAN. IF ID(I) IS POSITIVE, TIME SERIES I IS DIFFERENCED ID(I) TIMES. NO TRANSFORMATION IS APPLIED IF ID(I) IS NEGATIVE. I=1,2,...,NS.

R - WORK AREA MATRIX OF DIMENSION L BY L WHERE L EQUALS THE SUM OF IP(I), I=1,...,NS.

IR - INPUT ROW DIMENSION OF THE MATRIX R EXACTLY AS SPECIFIED IN THE DIMENSION STATEMENT IN IN THE CALLING PROGRAM.

T - OUTPUT VECTOR OF LENGTH N CONTAINING PARAMETER ESTIMATES OF THE UNDIFFERENCED MODEL FORM, WHERE N EQUALS THE SUM OF IP(I) AND THE MAXIMUM OF (0,ID(I)), FOR I=1,...,NS.
THE PARAMETER ESTIMATES FOR THE FIRST TIME SERIES ARE CONTAINED IN T(1),T(2),..., T(IP(1)+MAX(0,ID(1))). THE PARAMETER ESTIMATES FOR THE SECOND TIME SERIES ARE CONTAINED IN T(I+1),T(I+2),..., T(I+IP(2)+MAX(0,ID(2))), WHERE I=IP(1)+MAX(0,ID(1)).

THE PARAMETER ESTIMATES FOR TIME SERIES NS
ARE CONTAINED IN T(J+1),T(J+2),...,
T(J+IP(NS)+MAX(0,ID(NS))), WHERE
J=IP(NS-1)+MAX(0,ID(NS-1)).

PMAC - OUTPUT MOVING AVERAGE CONSTANT IN THE UNDIFFERENCED MODEL.

WK - WORK AREA VECTOR OF LENGTH NS+L,WHERE L EQUALS THE SUM OF IP(I),I=1,...,NS.

IER - ERROR PARAMETER. (OUTPUT)
TERMINAL ERROR
IER=129 INDICATES AN ERROR OCCURRED IN IMSL ROUTINE LEQT1F.
IER=130 INDICATES THAT ONE OF IP(I),LAG(I), IX,NS, OR LS WAS OUT OF RANGE.

PRECISION/HARDWARE - SINGLE AND DOUBLE/H32
- SINGLE/H36,H48,H60

REQD. IMSL ROUTINES - FTCRXY,LEQT1F,LUDATF,LUELMF,UERTST,UGETIO

NOTATION - INFORMATION ON SPECIAL NOTATIC AND CONVENTIONS IS AVAILABLE IN THE MANUAL INTRODUCTION OR THROUGH IMSL ROUTINE UHELP

REMARKS 1. IN PICKING SIGNIFICANT LAGS, CROSS-VARIANCE STUDIES AVAILABLE FROM IMSL ROUTINES FTCROS AND FTFREQ MIGHT BE USED.

2. NOTE THAT THE STRUCTURE OF FTWENX APPARENTLY ALLOWS ONLY PARAMETER ESTIMATION AT LAGS BY EACH OTHER. THIS MAY BE EXTENDED AS IN THE FOLLOWING EXAMPLE; SUPPOSE THAT TWO PARAMETERS ARE DESIRED WITH SERIES Z AT LAGS 5 AND 10. TIME SERIES Z SHOULD BE INCLUDED TWICE IN MATRIX X. FIRST IN COLUMN ONE OF MATRIX X WITH IP(1)=1 AND LAG(1)=5 AND AGAIN IN COLUMN 2 WITH IP(2)=1 AND LAG(2)=10.

Algorithm

This routine calculates the maximum likelihood estimates of the regressive parameters in a multi-input, single output time series model.

First each time series is transformed as indicated in vector ID to make each series stationary. Next, the normal equations are formed and solved. Finally, PMAC is calculated, and parameter estimates corresponding to series where ID(M) is positive are undifferenced.

The case NS=3 is used to illustrate the form of the model and parameter usage.

Let

$W = X(*,1)$ $P_w = IP(1)$ $L_w = LAG(1)$ $D_w = MAX(0,ID(1))$

$Y = X(*,2)$ $P_y = IP(2)$ $L_y = LAG(2)$ $D_y = MAX(0,ID(2))$

$Z = X(*,3)$ $P_z = IP(3)$ $L_z = LAG(3)$ $D_z = MAX(0,ID(3))$

hen the undifferenced predictive form of the model is:

$$W_t = PMAC + \sum_{i=1}^{P_w+D_w} \phi_i \, W_{t-L_w+1-i}$$

$$+ \sum_{i=1}^{P_y+D_y} \theta_i \, Y_{t-L_y+1-i}$$

$$+ \sum_{i=1}^{P_z+D_z} \psi_i \, Z_{t-L_z+1-i}$$

where $(\phi_1,\ldots,\phi_{P_w+D_w},\theta_1,\ldots,\theta_{P_y+D_y},\psi_1,\ldots,\psi_{P_z+D_z})$ is output vector T.

This may be easily extended to any case for general NS. Note that $P_w=0$ is available.

See references:

1. Box, G. E. P. and Jenkins, G. M., Time Series Analysis; Forecasting and Control, Holden-Day, San Francisco, 1970.

2. Robinson, E. A., Multichannel Time Series Analysis With Digital Computer Programs, Holden-Day, San Francisco, 1967.

Example

Given a multi-input, single output time series model, we want to calculate the maximum likelihood estimates of the regressive parameters. We can proceed as follows:

Input:

```
INTEGER   IX,NS,LS,IP(2),LAG(2),ID(2),IR,IER
REAL      X(10,2),R(3,3),T(3),PMAC,WK(5)
```

$$X = \begin{bmatrix} 3. & 0. \\ 1. & 1. \\ 0. & 2. \\ 0. & 4. \\ 3. & 5. \\ 5. & 3. \\ 4. & 2. \\ 2. & 0. \\ 1. & 2. \\ 0. & 2. \end{bmatrix}$$

IX = 10
NS = 2
LS = 10
IP = (2,1)

Then the undifferenced predictive form of the model is:

$$W_t = PMAC + \sum_{i=1}^{P_w+D_w} \phi_i \, W_{t-L_w+1-i}$$

$$+ \sum_{i=1}^{P_y+D_y} \theta_i \, Y_{t-L_y+1-i}$$

$$+ \sum_{i=1}^{P_z+D_z} \psi_i \, Z_{t-L_z+1-i}$$

where $(\phi_1,\ldots,\phi_{P_w+D_w},\theta_1,\ldots,\theta_{P_y+D_y},\psi_1,\ldots,\psi_{P_z+D_z})$ is output vector T.

This may be easily extended to any case for general NS. Note that $P_w=0$ is available.

See references:

1. Box, G. E. P. and Jenkins, G. M., Time Series Analysis; Forecasting and Control, Holden-Day, San Francisco, 1970.

2. Robinson, E. A., Multichannel Time Series Analysis With Digital Computer Programs, Holden-Day, San [illegible]o, 1967.

Example

Given a multi-input, single output time series model, we want to calculate the maximum likelihood estimates of the regressive parameters. We can proceed as follows:

Input:

```
INTEGER   IX,NS,LS,IP(2),LAG(2),ID(2),IR,IER
REAL      X(10,2),R(3,3),T(3),PMAC,WK(5)
```

$$X = \begin{bmatrix} 3. & 0. \\ 1. & 1. \\ 0. & 2. \\ 0. & 4. \\ 3. & 5. \\ 5. & 3. \\ 4. & 2. \\ 2. & 0. \\ 1. & 2. \\ 0. & 2. \end{bmatrix}$$

```
IX  =  10
NS  =  2
LS  =  10
IP  =  (2,1)
```

```
LAG   = (1,2)
ID    = (0,0)
IR    =  3
CALL FTWENX (X,IX,NS,LS,IP,LAG,ID,R,IR,T,PMAC,WK,IER)
   :
   :
END
```

Output:

```
T     = (-2.7324,0.99036,3.7066)
PMAC  =  -2.5741
IER   =   0
```

Then the fitted model is

$$w_t = -2.5741 - 2.7324w_{t-1} + 0.99036w_{t-2} + 3.7066y_{t-2}$$

where w and y correspond to X(*,1) and X(*,2), respectively.

APPENDIX E THE DATA FILES AND THEIR CONTENTS

NAME	COLUMN	VARIABLE	HOW DERIVED
DATUS1.DAT	1	t	Time reference
	2	S_{do}	Entered
	3	S_{s9}	Entered
	4	S_{s7}	$S_{do}+0,8*(S_{s9}-S_{do})$
	5	T_7	Entered
	6	Q_{a7}'	Entered
	7	T_9	Entered
	8	Q_{a9}'	Entered
	9	T_s	Entered
	10	Q_{a7}	$Q_{a9}'.F_{c234567}*7,6$
	11	Q_{a9}	$Q_{a7}'.F_{c234567}*7,6$
DATUS2.DAT	1	t	Time reference
	2	F_{c2}	Entered / 3.6
	3	F_{c3}	Entered / 3.6
	4	F_{c4}	Entered / 3.6
	5	F_{c5}	Entered / 3.6
	6	F_{c6}	Entered / 3.6
	7	F_{c7}	Entered / 3.6
	8	F_{c23}	$F_{c2} + F_{c3}$
	9	F_{c45}	$F_{c4} + F_{c5}$
	10	F_{c67}	$F_{c6} + F_{c7}$
	11	F_{c234}	$F_{c2} + F_{c3} + F_{c4}$
	12	F_{c567}	$F_{c5} + F_{c6} + F_{c7}$
	13	$F_{c1234567}$	$F_{c234} + F_{c567}$

NAME	COLUMN	VARIABLE	HOW DERIVED
DATUS3.DAT	1	t	Time
	2	F_{o2}	Entered * 0,2833
	3	F_{o3}	Entered * 0,2833
	4	F_{o4}	Entered * 0,2833
	5	F_{o5}	Entered * 0,2833
	6	F_{o6}	Entered * 0,2833
	7	F_{o7}	Entered * 0,2833
	8	F_{o23}	$F_{o2} + F_{o3}$
	9	F_{o45}	$F_{o4} + F_{o5}$
	10	F_{o67}	$F_{o6} + F_{o7}$
	11	F_{o234}	$F_{o2} + F_{o3} + F_{o4}$
	12	F_{o567}	$F_{o5} + F_{o6} + F_{o7}$
	13	$F_{o234567}$	$F_{o234} + F_{o567}$

APPENDIX F THE MULTIPLICATION OF SPECIFIC MATRIX FORMS

THEOREM: Any two matrices of the form

$$A = \begin{Bmatrix} x & x & 0 \\ x & x & 0 \\ x & x & x \end{Bmatrix}$$ when multiplied

together yield a matarix of the same form.

PROOF:

Let $A = \begin{Bmatrix} B & C \\ D & E \end{Bmatrix}$

where

$$B = \begin{Bmatrix} b_1 & b_2 \\ b_3 & b_4 \end{Bmatrix} \qquad C = \begin{Bmatrix} 0 \\ 0 \end{Bmatrix}$$

$$D = \begin{Bmatrix} d_1 & d_2 \end{Bmatrix} \qquad E = \begin{Bmatrix} e \end{Bmatrix}$$

Then

$$A_1 \; A_2 = \begin{Bmatrix} B_1 & C_1 \\ D_1 & E_1 \end{Bmatrix} \begin{Bmatrix} B_2 & C_2 \\ D_2 & E_2 \end{Bmatrix}$$

$$= \begin{Bmatrix} B_1B_2 + C_1D_2 & B_1C_2 + C_1E_2 \\ D_1B_2 + E_1D_2 & D_1C_2 + E_1E_2 \end{Bmatrix}$$

But $C_1 = C_2 = \begin{pmatrix} 0 & 0 \end{pmatrix}^T$

therefore

$$A_1 \; A_2 = \begin{Bmatrix} B_1 \; B_2 & 0 \\ D_1B_2 + E_1D_2 & E_1 \; E_2 \end{Bmatrix}$$

APPENDIX G DETERMINING THE MATRIX K_{s98}

It is necessary to solve a system of the form

$$A = K B \qquad \text{(G.1)}$$

where

$$A = \begin{Bmatrix} a_1 & a_2 \\ a_3 & a_4 \\ a_5 & a_6 \end{Bmatrix} \qquad B = \begin{Bmatrix} b_1 & b_2 \\ b_2 & b_3 \\ b_5 & b_6 \end{Bmatrix}$$

$$K = \begin{Bmatrix} k_1 & k_2 & 0 \\ k_3 & k_4 & 0 \\ k_5 & k_6 & k_7 \end{Bmatrix}$$

Only k_1 to k_6 are unknown. The equation (G.1) may be divided into the following equations

$$\begin{Bmatrix} a_1 & a_2 \\ a_3 & a_4 \end{Bmatrix} = \begin{Bmatrix} k_1 & k_2 \\ k_3 & k_4 \end{Bmatrix} \begin{Bmatrix} b_1 & b_2 \\ b_3 & b_4 \end{Bmatrix} \qquad \text{(G.2)}$$

$$\begin{Bmatrix} a_5 & a_6 \end{Bmatrix} = \begin{Bmatrix} k_5 & k_6 \end{Bmatrix} \begin{Bmatrix} b_1 & b_2 \\ b_3 & b_4 \end{Bmatrix} + k_7 \begin{Bmatrix} b_5 & b_6 \end{Bmatrix} \qquad \text{(G.3)}$$

Both these equations may be rearranged as shown;

$$\begin{Bmatrix} k_1 & k_2 \\ k_3 & k_4 \end{Bmatrix} = \begin{Bmatrix} a_1 & a_2 \\ a_3 & a_4 \end{Bmatrix} \begin{Bmatrix} b_1 & b_2 \\ b_3 & b_4 \end{Bmatrix}^{-1} \qquad \text{(G.4)}$$

$$\begin{Bmatrix} k_5 & k_6 \end{Bmatrix} = \begin{Bmatrix} a_1 - k_7 b_5 & a_6 - k_7 b_6 \end{Bmatrix} \begin{Bmatrix} b_1 & b_2 \\ b_2 & b_4 \end{Bmatrix}^{-1} \qquad \text{(G.5)}$$

The LHS of equations (G.4) and (G.5) yield the unknown terms of K.

APPENDIX H DETERMINING THE MATRIX H_s

It is necessary to solve the equation (H.1) where H_d and H_s are unknown but related as given below.

$$G = K H_d + H_s \qquad \text{(H.1)}$$

where

$$G = \begin{Bmatrix} g_1 & g_2 \\ g_3 & g_4 \\ g_5 & g_6 \end{Bmatrix} \qquad K = \begin{Bmatrix} 0 & 0 & 0 \\ 0 & 0 & 0 \\ k_1 & k_2 & k_3 \end{Bmatrix}$$

$$H_d = \begin{Bmatrix} h_1 & h_2 \\ h_3 & h_4 \\ \lambda h_5 & \lambda h_6 \end{Bmatrix} \qquad H_s = \begin{Bmatrix} h_1 & h_2 \\ h_3 & h_4 \\ h_5 & h_6 \end{Bmatrix}$$

$$\lambda = 0{,}4$$

$K H_d$ may be written as

$$K H_d = \begin{Bmatrix} 0 & 0 \\ 0 & 0 \\ k_1' & k_2' \end{Bmatrix} \qquad \text{(H.2)}$$

where

$$(k_1' \; k_2') = (k_1 \; k_2) \begin{Bmatrix} h_1 & h_2 \\ h_3 & h_4 \end{Bmatrix} + k_3 \lambda (h_5 \; h_6)$$

Equation (H.1) may be written as

$$\begin{Bmatrix} g_1 & g_2 \\ g_3 & g_4 \\ g_5 & g_6 \end{Bmatrix} = \begin{Bmatrix} h_1 & h_2 \\ h_3 & h_4 \\ k_1' + h_5 & k_2' + h_6 \end{Bmatrix} \qquad \text{(H.3)}$$

Equation (H.3) allows h_1 to h_4 to be determined directly. Only h_5 and h_6 remain undetermined. Consider again equations (H.2) and (H.3).

$$(g_5 \; g_6) = ((k_1 + h_5') \quad (h_2 + h_6'))$$

$$= (k_1 \; k_2) \begin{Bmatrix} h_1 & h_2 \\ h_3 & h_4 \end{Bmatrix} + k_3 \lambda (h_5 \; h_6) + (h_5 \; h_6)$$

or

$$(h_5 \; h_6) = \frac{1}{(1 + k_3 \lambda)} (g_5 \; g_6) - (k_1 \; k_2) \begin{Bmatrix} h_1 & h_2 \\ h_3 & h_4 \end{Bmatrix} \qquad \text{(H.4)}$$

APPENDIX I DETERMINING THE MATRIX K_{s7}

The matrix K_{s7} has to be determined from two equations of the form

$$M_1 = X\ K_{s7}^{5}\ H_d + K_{s7}^{5}\ H_s \qquad \text{(I.1)}$$

$$N_1 = X\ K_{s7}^{4}\ H_d + K_{s7}^{4}\ H_s \qquad \text{(I.2)}$$

where

$$M_1 = \begin{Bmatrix} m_1 & m_2 \\ m_3 & m_4 \\ m_5 & m_6 \end{Bmatrix} \qquad N_1 = \begin{Bmatrix} n_1 & n_2 \\ n_3 & n_4 \\ n_5 & n_6 \end{Bmatrix}$$

$$X = \begin{Bmatrix} 0 & 0 & 0 \\ 0 & 0 & 0 \\ x_1 & x_2 & x_3 \end{Bmatrix} \qquad K_{s7} = \begin{Bmatrix} g_1 & g_2 & 0 \\ g_3 & g_4 & 0 \\ g_5 & g_6 & g_7 \end{Bmatrix}$$

$$H_d = \begin{Bmatrix} h_1 & h_2 \\ h_3 & h_4 \\ \lambda h_5 & \lambda h_6 \end{Bmatrix} \qquad H_s = \begin{Bmatrix} h_1 & h_2 \\ h_3 & h_4 \\ h_5 & h_6 \end{Bmatrix}$$

The matrices $X\ K_{s7}^{4}$ and $X\ K_{s7}^{5}$ have the form

$$X\ K_{s7}^{n} = \begin{Bmatrix} 0 & 0 & 0 \\ 0 & 0 & 0 \\ Z & Z & Z \end{Bmatrix} \qquad \text{where Z is any transfer function} \qquad \text{(I.3)}$$

Let $K_{s7}^{5}\ H_s$ and $K_{s7}^{4}\ H_s$ have the following forms

$$K_{s7}^{5} H_s = Q = \begin{Bmatrix} q_1 & q_2 \\ q_3 & q_4 \\ q_5 & q_6 \end{Bmatrix} \qquad K_{s7}^{4} H_s = P = \begin{Bmatrix} p_1 & p_2 \\ p_3 & p_4 \\ p_4 & p_5 \end{Bmatrix} \qquad \text{(I.4)}$$

Consideration of (I.1) to (I.4) gives

$$\begin{Bmatrix} m_1 & m_2 \\ m_3 & m_4 \end{Bmatrix} = \begin{Bmatrix} q_1 & q_2 \\ q_3 & q_4 \end{Bmatrix} \text{ and } \begin{Bmatrix} n_1 & n_2 \\ n_3 & n_4 \end{Bmatrix} = \begin{Bmatrix} p_1 & p_2 \\ p_3 & p_4 \end{Bmatrix}$$

This arises out of the mostly zero matrix of equation (I.3).

It also follows that

$$Q = K_{s7}\ P$$

or

$$\begin{Bmatrix} q_1 & q_2 \\ q_3 & q_4 \\ q_5 & q_6 \end{Bmatrix} = \begin{Bmatrix} g_1 & g_2 & 0 \\ g_3 & g_4 & 0 \\ g_5 & g_6 & g_7 \end{Bmatrix} \begin{Bmatrix} p_1 & p_2 \\ p_3 & p_4 \\ p_5 & p_6 \end{Bmatrix} \qquad \text{(I.4)}$$

Extracting g_1 to g_4 from equation (I.5) gives

$$\begin{Bmatrix} g_1 & g_2 \\ g_3 & g_4 \end{Bmatrix} = \begin{Bmatrix} q_1 & q_2 \\ q_3 & q_4 \end{Bmatrix} \begin{Bmatrix} p_1 & p_2 \\ p_3 & p_4 \end{Bmatrix}^{-1} \qquad \text{(I.6)}$$

g_7 in K_{s7} is already known. It only remains to find g_5 and g_6.

Let

$$K_{s7}^4 \; H_d = R = \begin{Bmatrix} r_1 & r_2 \\ r_3 & r_4 \\ r_5 & r_6 \end{Bmatrix} \qquad \text{(I.7)}$$

Since the form of K_{s7}^4 is the same as that for K_{s7}^5 and since H_d is similar to H_s it can be shown that

$$\begin{Bmatrix} r_1 & r_2 \\ r_3 & r_4 \end{Bmatrix} = \begin{Bmatrix} p_1 & p_2 \\ p_3 & p_4 \end{Bmatrix} \qquad \text{(I.8)}$$

Substituting R and P into (I.1) and (I.2) gives

$$M_1 = X K_{s7} R + K_{s7} P \qquad \text{(I.9)}$$

and

$$N_1 = X R + P \qquad \text{(I.10)}$$

Consider m_5 and m_6 in equation (I.9).

$$\begin{aligned} \begin{pmatrix} m_5 & m_6 \end{pmatrix} = {} & \begin{pmatrix} x_1 & x_2 \end{pmatrix} \begin{Bmatrix} g_1 & g_2 \\ g_3 & g_4 \end{Bmatrix} \begin{Bmatrix} p_1 & p_2 \\ p_3 & p_4 \end{Bmatrix} \\ & + x_3 \begin{pmatrix} g_5 & g_6 \end{pmatrix} \begin{Bmatrix} p_1 & p_2 \\ p_3 & p_4 \end{Bmatrix} + x_3 g_7 \begin{pmatrix} r_5 & r_6 \end{pmatrix} \\ & + \begin{pmatrix} g_5 & g_6 \end{pmatrix} \begin{Bmatrix} p_1 & p_2 \\ p_3 & p_4 \end{Bmatrix} + g_7 \begin{pmatrix} p_5 & p_6 \end{pmatrix} \end{aligned}$$

$$= \begin{pmatrix} x_1 & x_2 \end{pmatrix} \begin{Bmatrix} g_1 & g_2 \\ g_3 & g_4 \end{Bmatrix} \begin{Bmatrix} p_1 & p_2 \\ p_3 & p_4 \end{Bmatrix}$$

$$+ g_7 \left\{ x_3 \begin{pmatrix} r_5 & r_6 \end{pmatrix} + \begin{pmatrix} p_5 & p_6 \end{pmatrix} \right\}$$

$$+ \begin{pmatrix} g_5 & g_6 \end{pmatrix} \begin{pmatrix} x_3 + 1 \end{pmatrix} \begin{Bmatrix} p_1 & p_2 \\ p_3 & p_4 \end{Bmatrix} \qquad \text{(I.11)}$$

Similarly for equation (I.10)

$$\begin{pmatrix} n_5 & n_6 \end{pmatrix} = \begin{pmatrix} x_1 & x_2 \end{pmatrix} \begin{Bmatrix} p_1 & p_2 \\ p_3 & p_4 \end{Bmatrix}$$

$$+ x_3 \begin{pmatrix} r_5 & r_6 \end{pmatrix} + \begin{pmatrix} p_5 & p_6 \end{pmatrix} \qquad \text{(I.12)}$$

Re-arranging equations (I.11) and (I.12) gives

$$\begin{pmatrix} g_5 & g_6 \end{pmatrix} = \left\{ \begin{pmatrix} m_5 & m_6 \end{pmatrix} - \begin{pmatrix} x_1 & x_2 \end{pmatrix} \begin{Bmatrix} g_1 & g_2 \\ g_3 & g_4 \end{Bmatrix} \begin{Bmatrix} p_1 & p_2 \\ p_3 & p_4 \end{Bmatrix} \right.$$

$$\left. - g_7 \left(x_3 \begin{pmatrix} r_5 & r_6 \end{pmatrix} + \begin{pmatrix} p_5 & p_6 \end{pmatrix} \right) \right\} \frac{1}{\begin{pmatrix} x_3 + 1 \end{pmatrix}} \begin{Bmatrix} p_1 & p_2 \\ p_3 & p_4 \end{Bmatrix}^{-1} \qquad \text{(I.13)}$$

and

$$x_3 \begin{pmatrix} r_5 & r_6 \end{pmatrix} + \begin{pmatrix} p_5 & p_6 \end{pmatrix} = \begin{pmatrix} n_5 & n_6 \end{pmatrix} - \begin{pmatrix} x_1 & x_2 \end{pmatrix} \begin{Bmatrix} p_1 & p_2 \\ p_3 & p_4 \end{Bmatrix} \qquad \text{(I.14)}$$

Substituting equation (I.14) into equation (I.13) gives

$$\begin{pmatrix} g_5 & g_6 \end{pmatrix} = \left\{ \begin{pmatrix} m_5 & m_6 \end{pmatrix} - \begin{pmatrix} x_1 & x_2 \end{pmatrix} \begin{Bmatrix} g_1 & g_3 \\ g_3 & g_4 \end{Bmatrix} \begin{Bmatrix} p_1 & p_2 \\ p_3 & p_4 \end{Bmatrix} \right.$$

$$\left. - g_7 \left\{ \begin{pmatrix} n_5 & n_6 \end{pmatrix} - \begin{pmatrix} x_1 & x_2 \end{pmatrix} \begin{Bmatrix} p_1 & p_2 \\ p_3 & p_4 \end{Bmatrix} \right\} \right\} \frac{1}{\begin{pmatrix} x_3 + 1 \end{pmatrix}} \begin{Bmatrix} p_1 & p_2 \\ p_3 & p_4 \end{Bmatrix}^{-1} \qquad \text{(I.15)}$$

APPENDIX J DETERMINING THE MATRIX F_s

The equation to be solved has the form

$$M = X K F_d + K F_s \qquad \text{(J.1)}$$

where

$$M = \begin{Bmatrix} m_1 \\ m_2 \\ m_3 \end{Bmatrix} \qquad X = \begin{Bmatrix} 0 & 0 & 0 \\ 0 & 0 & 0 \\ x_1 & x_2 & x_3 \end{Bmatrix}$$

$$K = \begin{Bmatrix} k_1 & k_2 & 0 \\ k_3 & k_4 & 0 \\ k_5 & k_6 & k_7 \end{Bmatrix}$$

$$F_d = \begin{Bmatrix} f_1 \\ f_2 \\ \lambda f_3 \end{Bmatrix} \qquad F_s = \begin{Bmatrix} f_1 \\ f_2 \\ f_3 \end{Bmatrix} \qquad \lambda = 0,4$$

The unknowns are f_1 f_2 and f_3.

Consider m_1 and m_2 in equation (J.1)

$$\begin{Bmatrix} m_1 \\ m_2 \end{Bmatrix} = \begin{Bmatrix} k_1 & k_2 \\ k_3 & k_4 \end{Bmatrix} \begin{Bmatrix} f_1 \\ f_2 \end{Bmatrix}$$

or

$$\begin{Bmatrix} f_1 \\ f_2 \end{Bmatrix} = \begin{Bmatrix} 1 & k_2 \\ k_3 & k_4 \end{Bmatrix}^{-1} \begin{Bmatrix} m_1 \\ m_2 \end{Bmatrix} \qquad \text{(J.2)}$$

Similarly

$$m_3 = \begin{pmatrix} x_1 & x_2 & x_3 \end{pmatrix} K F_d + \begin{pmatrix} k_5 & k_6 & k_7 \end{pmatrix} F_s$$

$$= \begin{pmatrix} x_1 & x_2 \end{pmatrix} \begin{Bmatrix} k_1 & k_2 \\ k_3 & k_3 \end{Bmatrix} \begin{Bmatrix} f_1 \\ f_2 \end{Bmatrix} + x_3 \begin{pmatrix} k_5 & k_6 & k_7 \end{pmatrix} F_d$$

$$+ \begin{pmatrix} k_5 & k_6 & k_7 \end{pmatrix} F_s$$

$$= \begin{pmatrix} x_1 & x_2 \end{pmatrix} \begin{Bmatrix} k_1 & k_2 \\ k_3 & k_4 \end{Bmatrix} \begin{Bmatrix} f_1 \\ f_2 \end{Bmatrix}$$

$$+ \begin{pmatrix} k_5 & k_6 \end{pmatrix} \begin{Bmatrix} f_1 \\ f_2 \end{Bmatrix} \begin{pmatrix} x_3 + 1 \end{pmatrix} \qquad \text{(J.3)}$$

$$+ \begin{pmatrix} k_7 \begin{pmatrix} x_3 \lambda f_3 + f_3 \end{pmatrix}$$

Re-arranging

$$f_3 = \frac{1}{k_7 (x_3 \lambda + 1)} \left\{ m_3 - (x_1 \; x_2) \begin{Bmatrix} k_1 & k_2 \\ k_3 & k_4 \end{Bmatrix} \begin{Bmatrix} f_1 \\ f_2 \end{Bmatrix} - (k_5 \; k_6) \begin{Bmatrix} f_1 \\ f_2 \end{Bmatrix} (x_3 + 1) \right\} \quad \text{(J.3)}$$

APPENDIX K GRAPHS OF THE INPUTS AND OUTPUTS CONSIDERED IN SECTION 5.3.1

The list of graphs appearing in this Appendix is given below. The inputs F_{c4} and F_{c6} were zero throughout the time period of interest and are not included. (The variables plotted in each graph appear in brackets.)

GRAPH 1: OIL FLOW RATES FOR EACH BURNER LEVEL
(F_{o2}, F_{o3}, F_{o4}, F_{o5}, F_{o6}, F_{o7})

GRAPH 2: COAL FLOW RATE FOR MILL E
(F_{c2})

GRAPH 3: COAL FLOW RATE FOR MILL B
(F_{c3})

GRAPH 4: COAL FLOW RATE FOR MILL C
(F_{c5})

GRAPH 5: COAL FLOW RATE FOR MILL A
(F_{c7})

GRAPH 6: SECONDARY AIR TEMPERATURE
(T_s)

GRAPH 7: STEAM ENTHALPY FLOW RATE AT THE DIVISION WALL INLET
(S_{do})

GRAPH 8: FLUE GAS ENTHALPY FLOW RATE AT THE EXIT OF THE 9TH CELL
(Q_{a9})

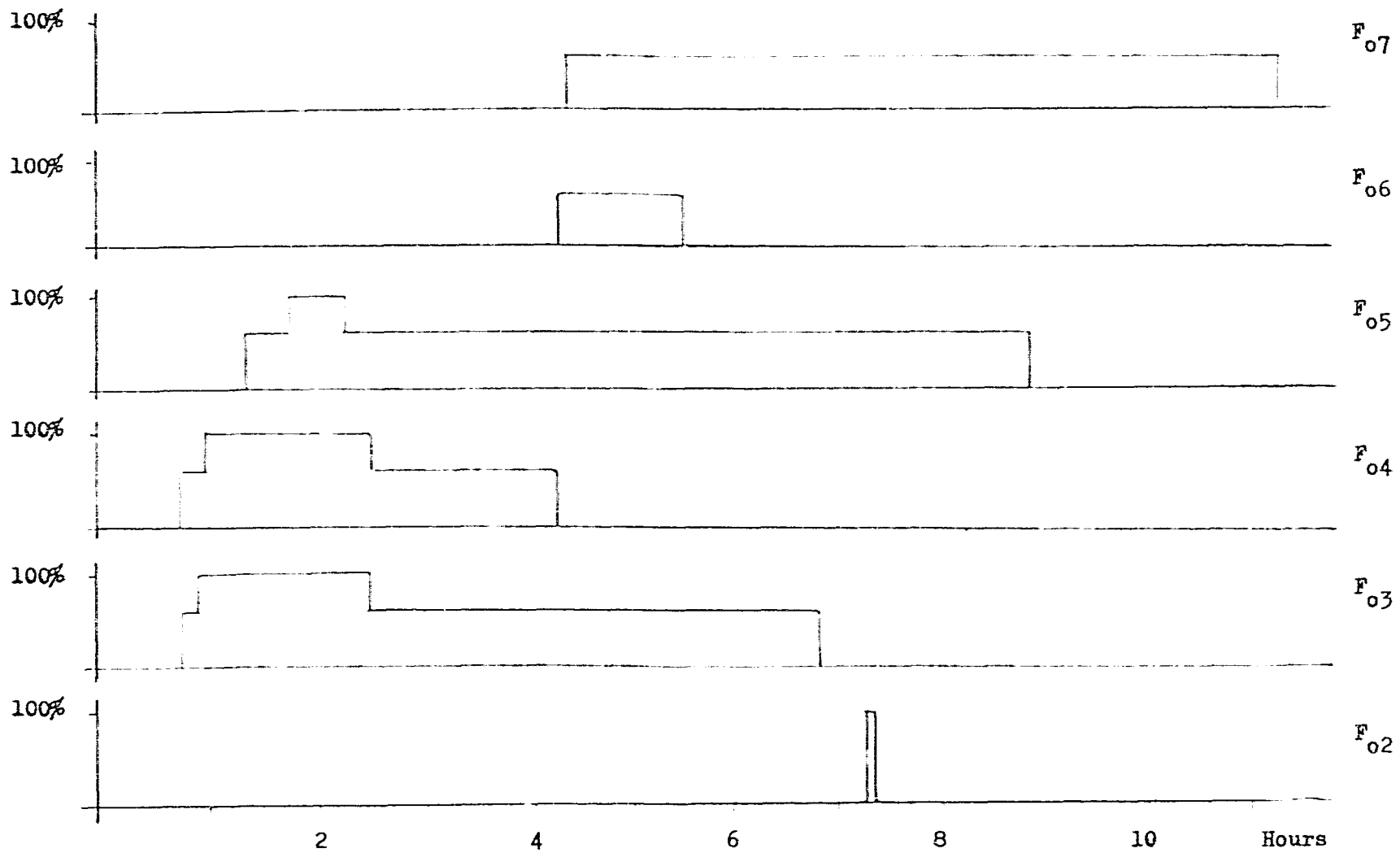
GRAPH 9: FLUE GAS ENTHALPY FLOW RATE AT THE EXIT OF THE 7TH CELL
(Q_{a7})

GRAPH 10: FLUE GAS TEMPERATURE AT THE EXIT OF THE 9TH CELL
(T_9)

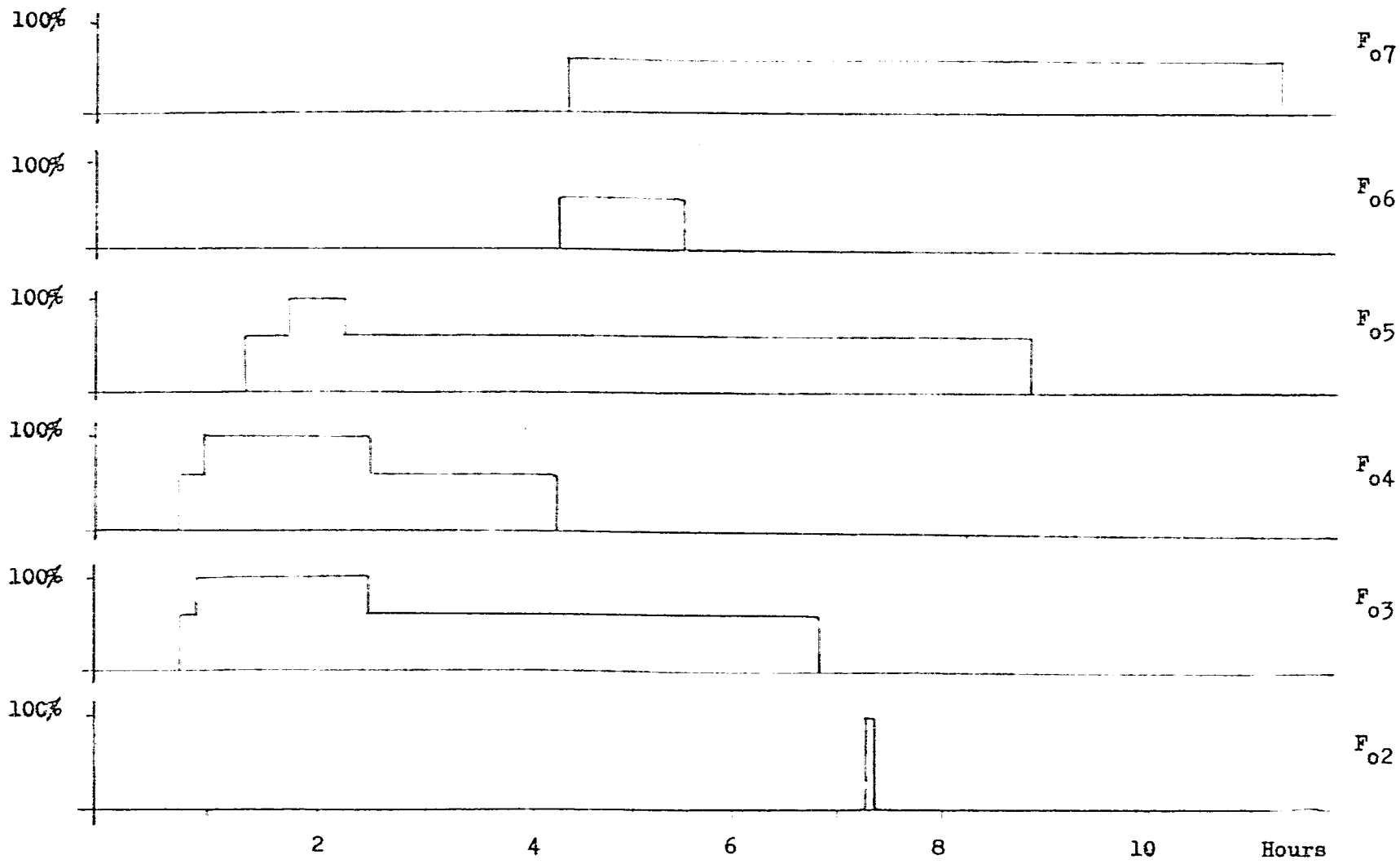
GRAPH 11: FLUE GAS TEMPERATURE AT THE EXIT OF THE 7TH CELL
(T_7)

GRAPH 12: STEAM ENTHALPY FLOW RATE AT THE EVAPORATOR EXIT
(S_{s9})

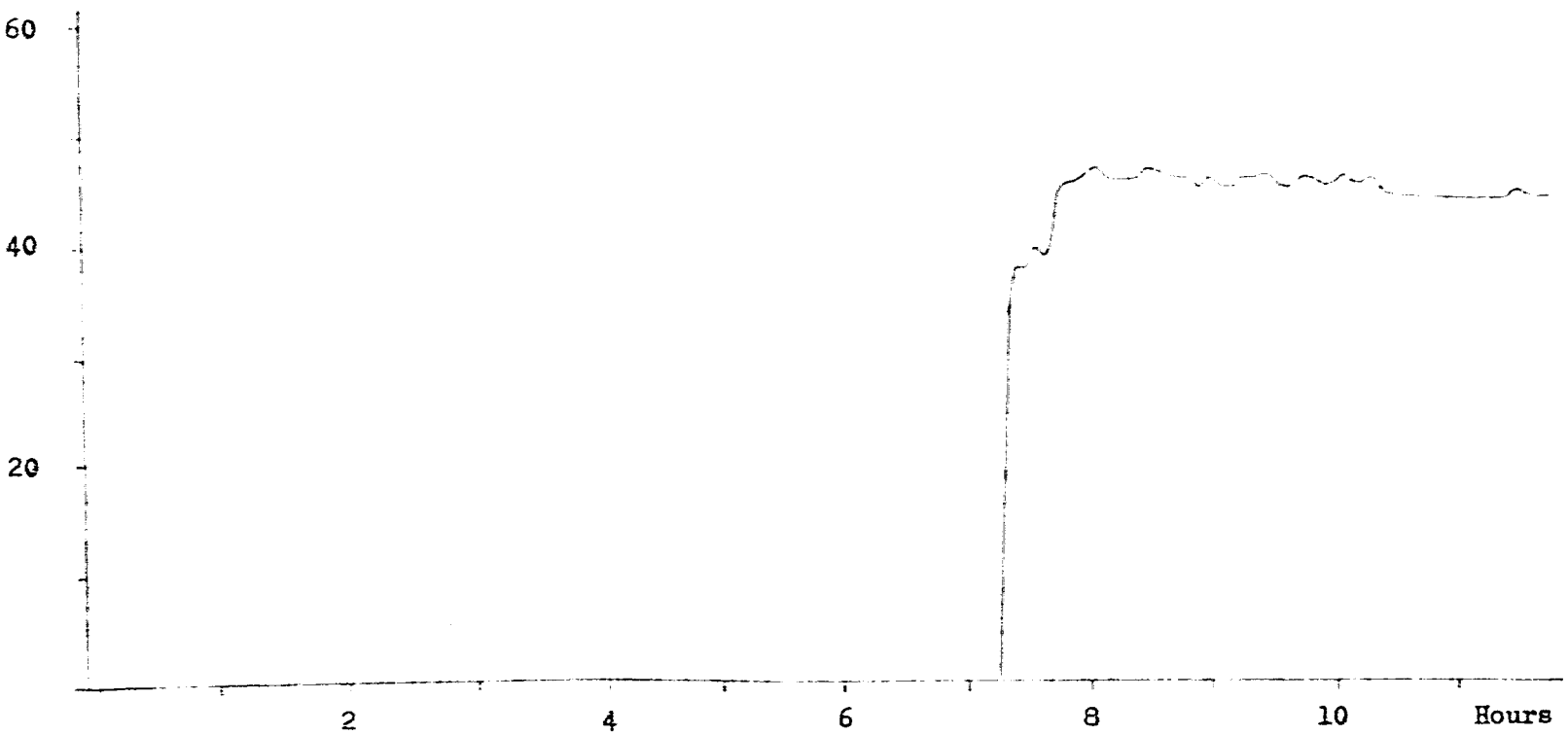
GRAPH 13: STEAM ENTHALPY FLOW RATE AT THE EXIT OF THE 7TH CELL
(S_{s7})



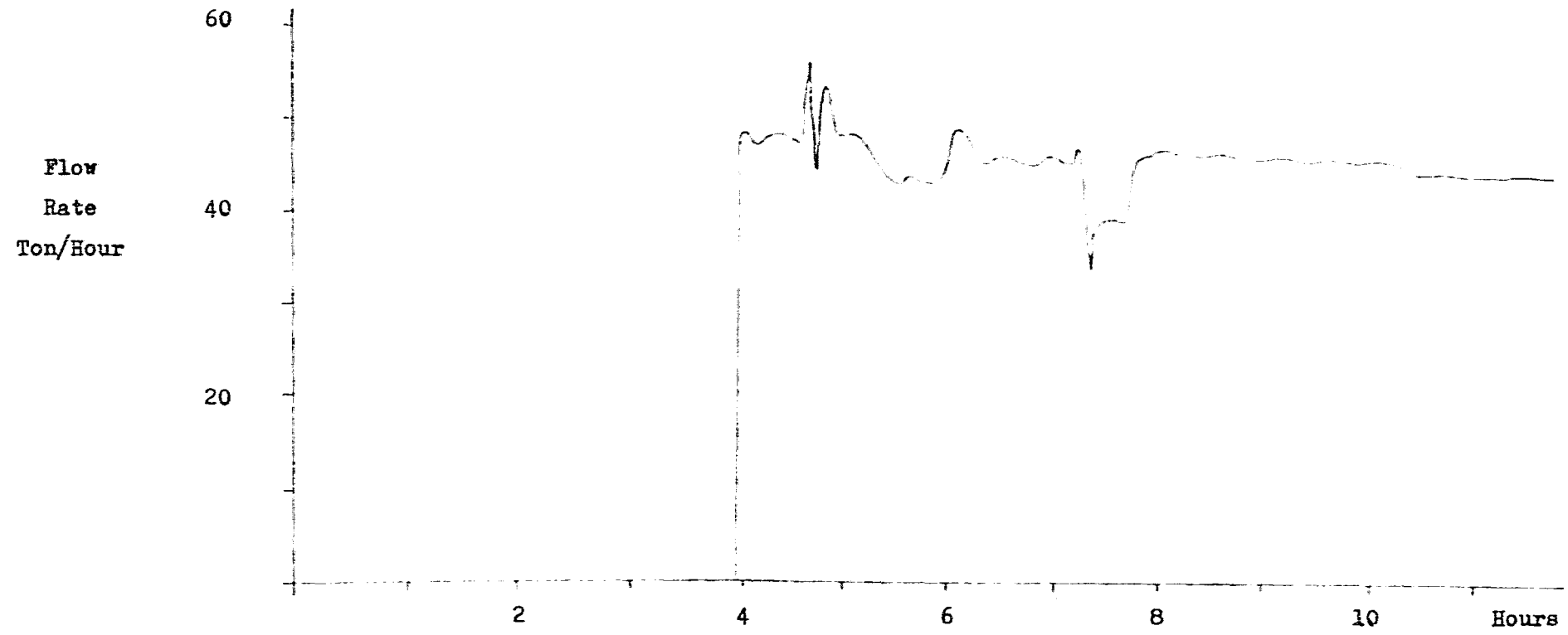
GRAPH 1: OIL FLOW RATES FOR EACH BURNER LEVEL



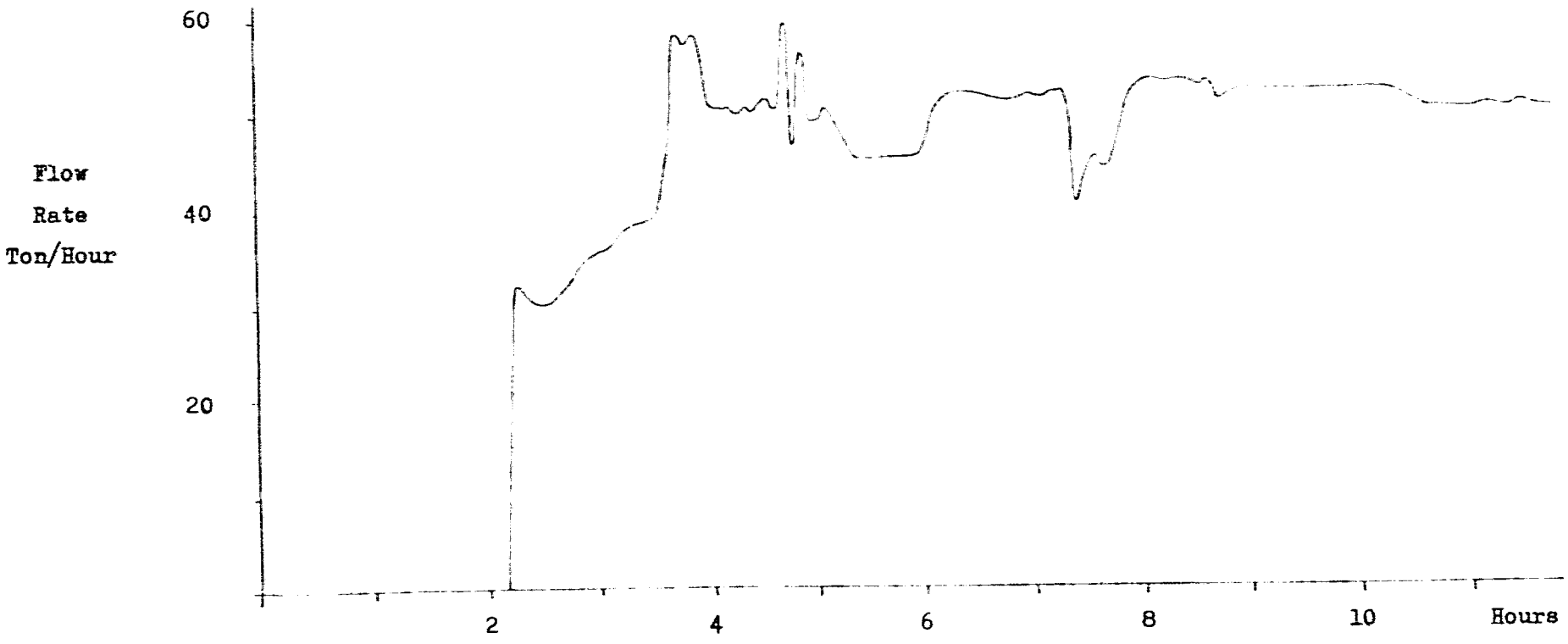
GRAPH 1: OIL FLOW RATES FOR EACH BURNER LEVEL



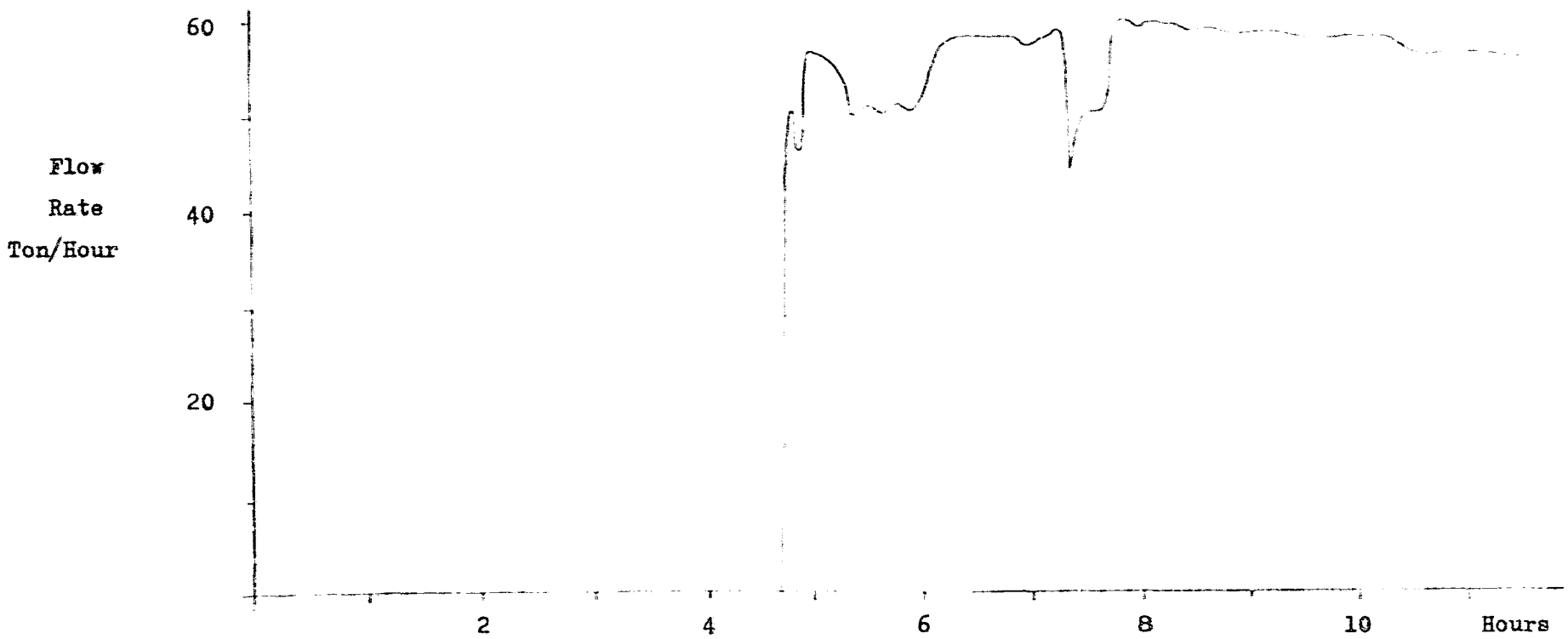
GRAPH 2: COAL FLOW RATE FOR MILL E



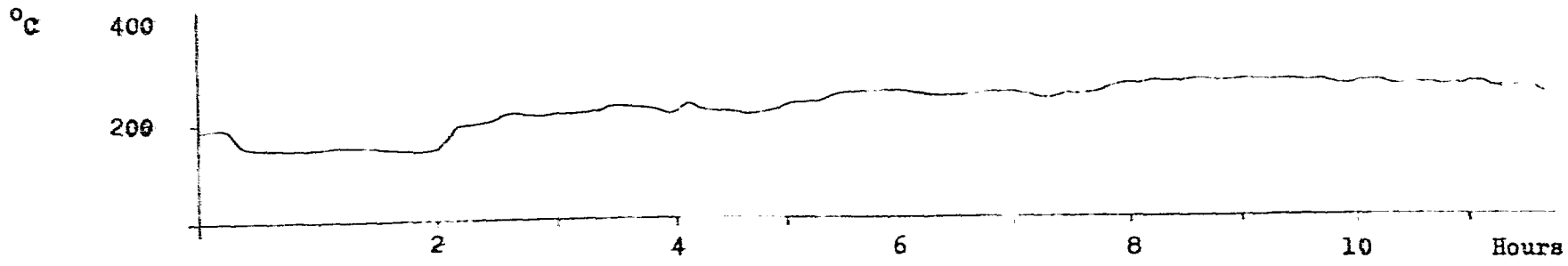
GRAPH 3: COAL FLOW RATE FOR MILL B



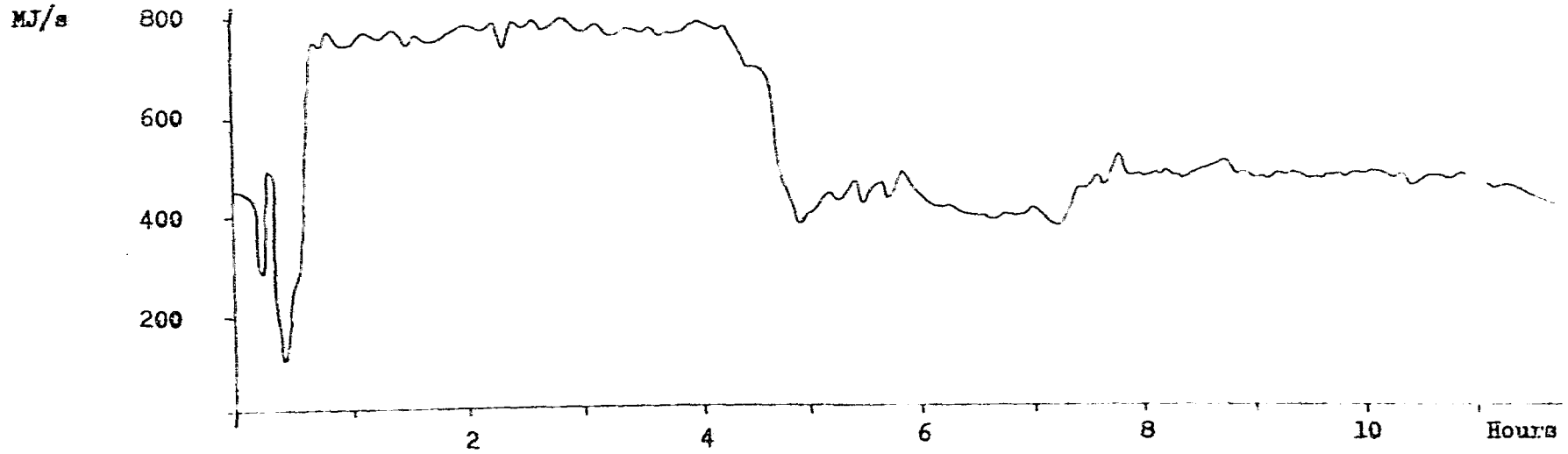
GRAPH 4: COAL FLOW RATE FOR MILL C



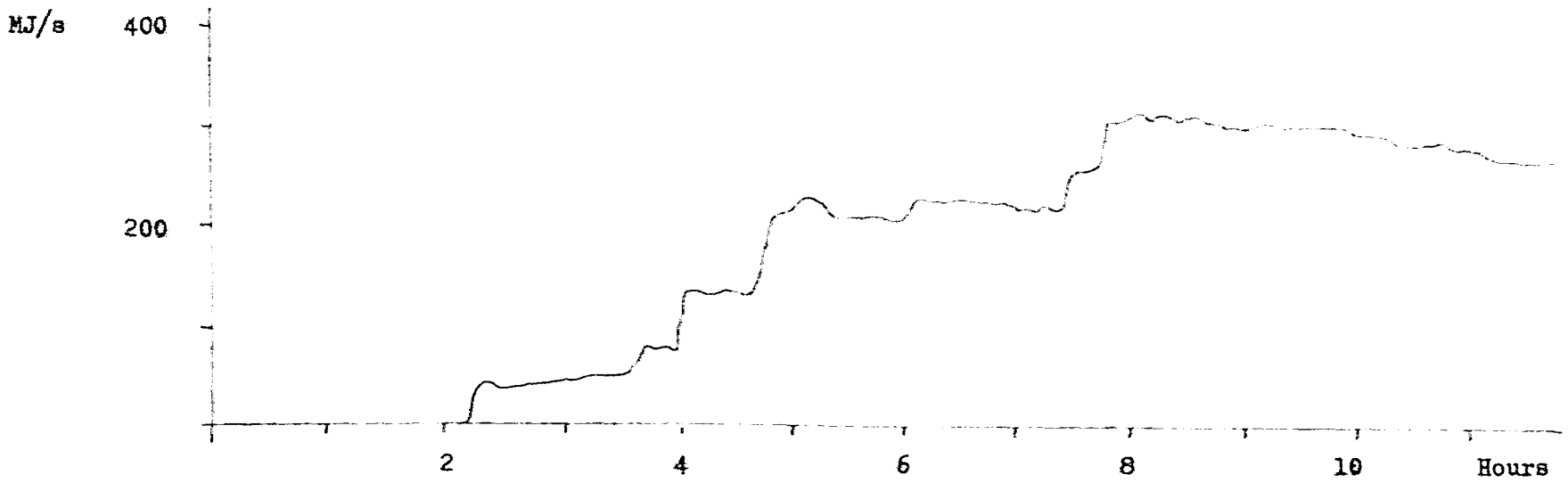
GRAPH 5: COAL FLOW RATE FOR MILL A



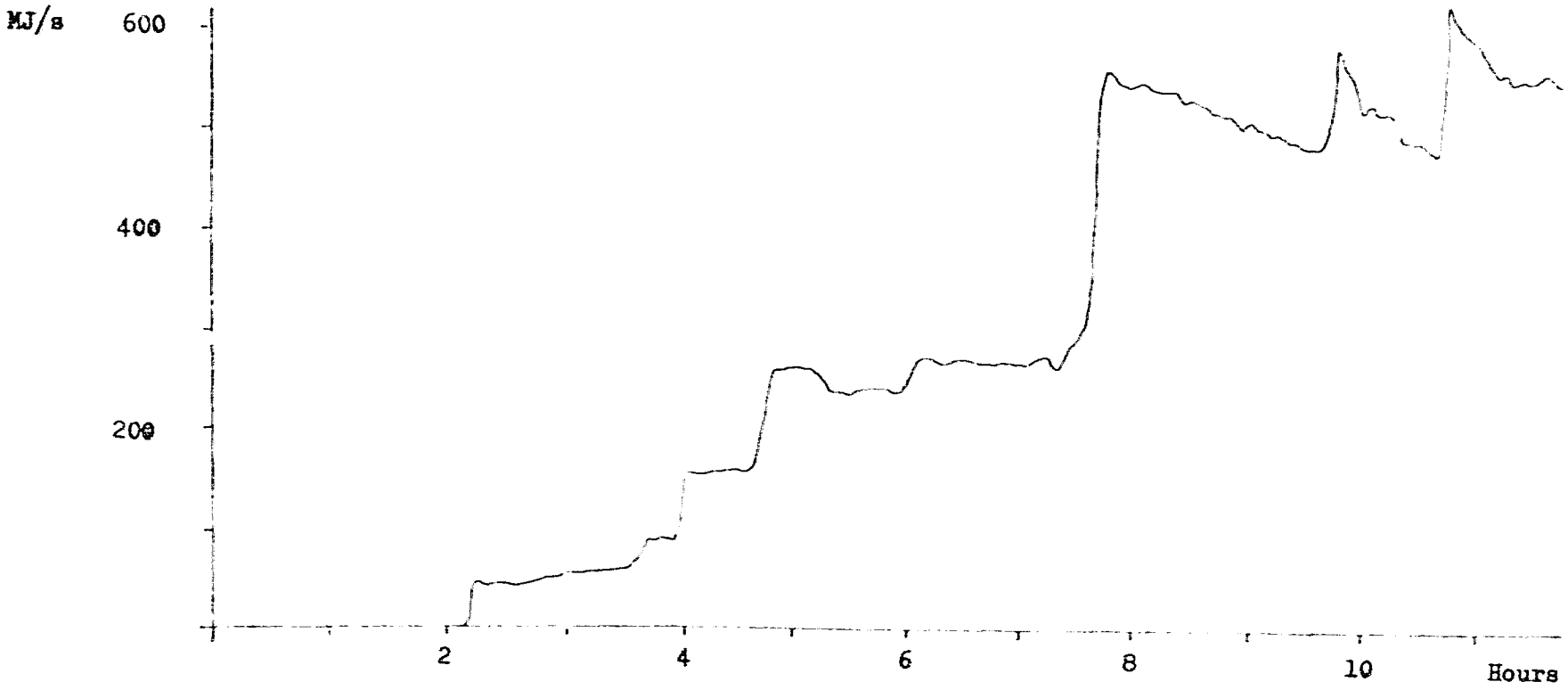
GRAPH 6: SECONDARY AIR TEMPERATURE



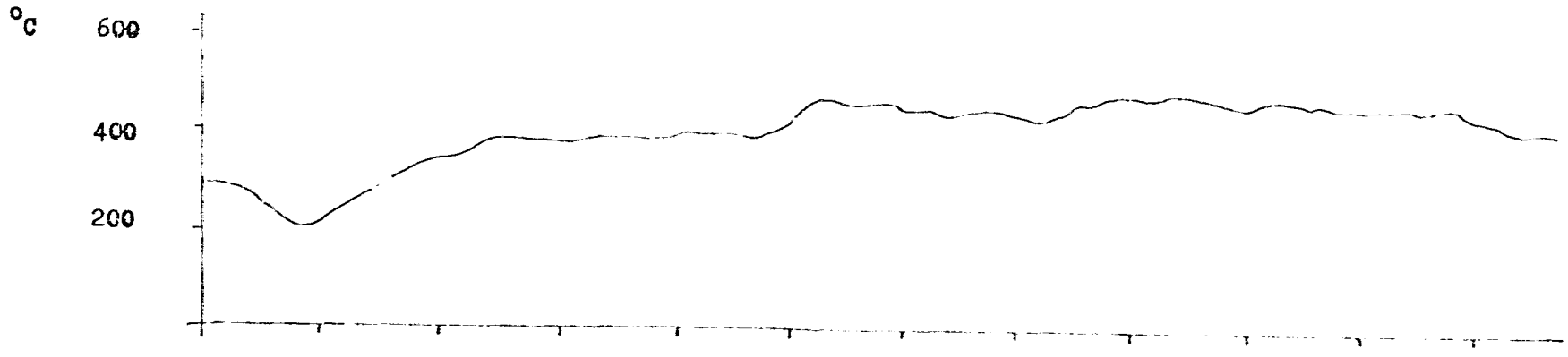
GRAPH 7: STEAM ENTHALPY FLOW RATE AT THE DIVISION WALL INLET



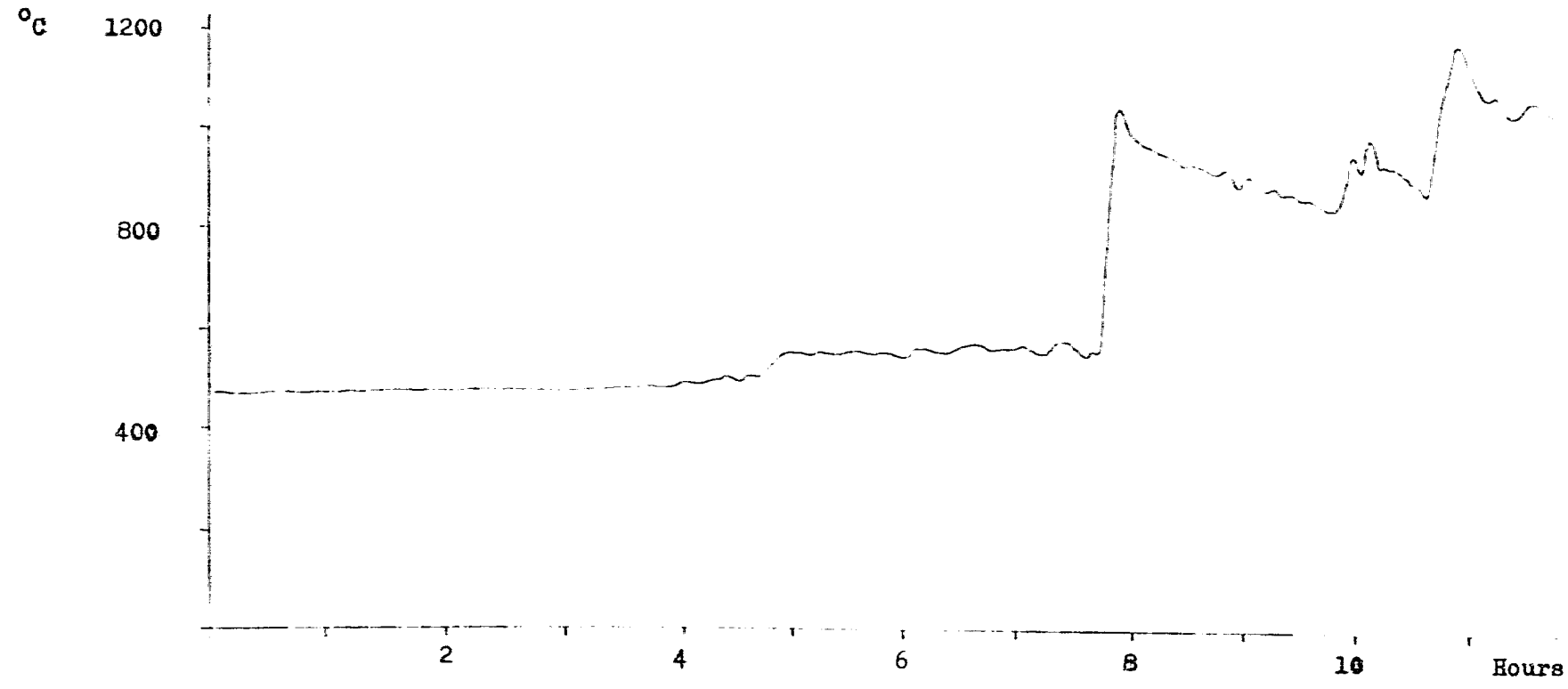
GRAPH 8: FLUE GAS ENTHALPY FLOW RATE AT THE EXIT OF THE 9TH CELL



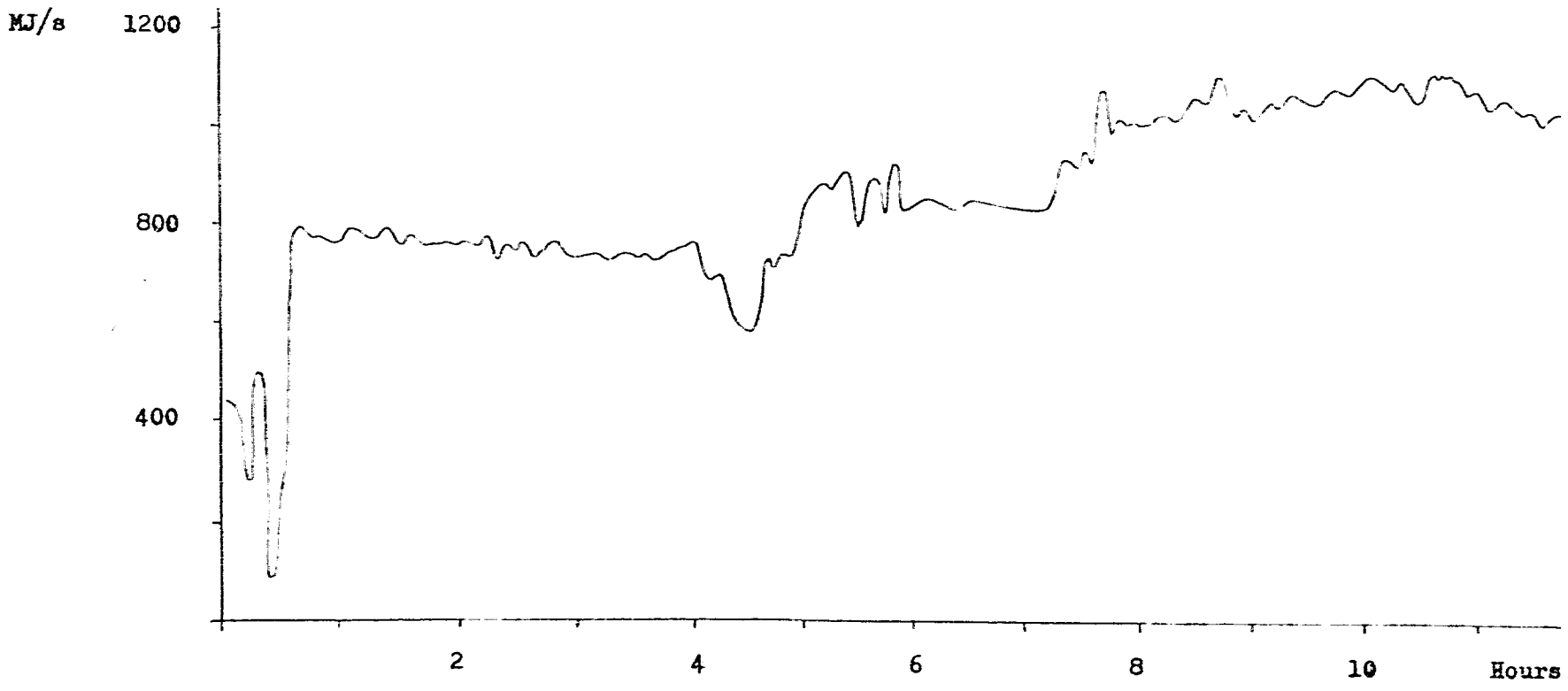
GRAPH 9: FLUE GAS ENTHALPY FLOW RATE AT THE EXIT OF THE 7TH CELL



GRAPH 10: FLUE GAS TEMPERATURE AT THE EXIT OF THE 9TH CELL

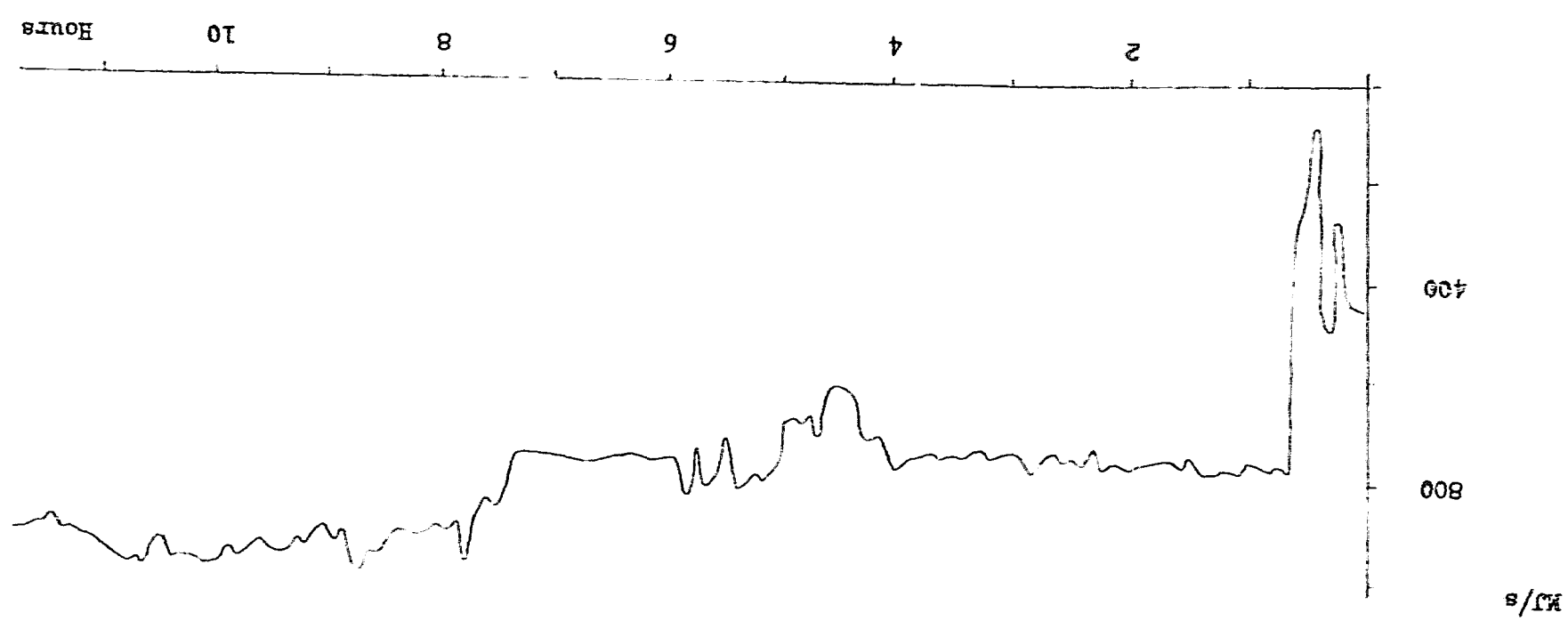


GRAPH 11: FLUE GAS TEMPERATURE AT THE EXIT OF THE 7TH CELL



GRAPH 12: STEAM ENTHALPY FLOW RATE AT THE EVAPORATOR EXIT

GRAPH 13: STEAM ENTHALPY FLOW RATE AT THE EXIT OF TES 7TH CELL



Author Bradford David George
Name of thesis A Simulation Model For Use In Testing A Fast-time Predictor Instrument For Benson Boiler Steam Temperature Control. 1985

PUBLISHER:
University of the Witwatersrand, Johannesburg
©2013

LEGAL NOTICES:

Copyright Notice: All materials on the University of the Witwatersrand, Johannesburg Library website are protected by South African copyright law and may not be distributed, transmitted, displayed, or otherwise published in any format, without the prior written permission of the copyright owner.

Disclaimer and Terms of Use: Provided that you maintain all copyright and other notices contained therein, you may download material (one machine readable copy and one print copy per page) for your personal and/or educational non-commercial use only.

The University of the Witwatersrand, Johannesburg, is not responsible for any errors or omissions and excludes any and all liability for any errors in or omissions from the information on the Library website.